ISSN: 2458-8156

Journal Home page : http://dergipark.ulakbim.gov.tr/ejens * E-mail : editor@cnrgroup.eu

hosted by Turkish JournalPark ACADEMIC

EJENS

European Journal of Engineering and Natural Sciences CODEN: EJENS

Analysis Of Laminated Composite Plates Using Element-Free Galerkin Method

Omer Yavuz Bozkurt[1]*, Ozkan Ozbek[2]

[1]*Gaziantep University, Mechanical Engineering Department, 27310, Şehitkamil/Gaziantep, Turkey.*

[2]*Gaziantep University, Mechanical Engineering Department, 27310, Şehitkamil/Gaziantep, Turkey.*

**Corresponding Author email: oybozkurt@gantep.edu.tr*

Publication Info

Paper received:
10 December 2015

Revised received:
15 December 2015

Accepted:
18 December 2015

Abstract

The desire to use materials with high strength/weight or stiffness/weight ratio is increased the importance of composite materials nowadays. Due to this, much attention has been devoted to the numerical analysis of composite plates. The performance of well-known numerical methods, Finite Element Method (FEM) and Boundary Element Method (BEM), are based on the quality mesh structures. Meshfree methods are free from the meshes and the drawbacks of mesh-based interpolation techniques. Because of its high convergence rate, Element-Free Galerkin Method (EFGM) is one of the most widely used meshfree method in solid body mechanics and it is a promising candidate for the analysis of composite materials. In this study; deflection analysis of laminated composite plates are studied using EFGM. Several laminated composite plate problems are solved using EFGM and the displacement results of EFGM solutions are compared with the results of exact and FEM solutions at the critical points.

Key words

Laminate, composite plate, element-free Galerkin method, meshfree methods

1. INTRODUCTION

Nowadays, composite materials have played an important role in the engineering applications that require high strength/weight or stiffness/weight ratios. Because of that, analysis of composite materials have gained great significance. Several plate theories are present for the bending analysis of composite plates in the literature such as are Classical Plate Theory (CLPT) [1], First Order Shear Deformation Theory (FSDT) [1], Higher Order Shear Deformation Theory (HSDT) [1] etc. The FSDT, also known as Mindlin-Reissner plate theory, is widely used since it includes transverse shear effects and its simplicity.

Due to the complex structure of composite materials, several numerical methods, such as FEM, BEM and meshfree methods, have been used for the analyses of composite laminates in the literature. Sheikh et al. [2] used FEM on the solution of composite plates having different shapes. Moments and stresses using BEM were examined by Albuquerque and his friends [3]. Haddad et al. [4] applied to Finite Difference Method (FDM) for free vibration analysis of composite plates.

The performances of FEM and BEM depend on mesh quality of the problem model. Meshfree methods have been developed to overcome this limitation. Element-Free Galerkin Method (EFGM), which was originally developed by Belytschko [5], is one of the most widely used meshfree method in solid mechanics due to its simplicity and high convergence rate. Also, many scientists propose that EFGM has good solution accuracy in solid mechanics [6]. The EFGM is seen as a promising candidate for the analysis of composite materials. It was used by Belinha and Dinis for the analysis of anisotropic plates and laminates [7]. Also, EFGM has been preferred for the various analysis of

composite plates such as buckling problems [8], vibration problems [9], bending problems [7], crack analysis [10], fracture analysis [11], etc.

In this study, EFGM and FEM programs, based on FSDT, have been written on MATLAB programming environment for the deflection analysis of laminated composite plates. Several numerical examples are solved using particular number of nodes in the problem domain. The displacement results of EFGM are presented and compared with the results of FEM and exact solution in terms of accuracy.

2. FIRST SHEAR DEFORMATION THEORY (FSDT) FOR THE LAMINATED COMPOSITE PLATES

A typical Mindlin-Reissner plate with mid-plane lying in the x-y plane of Cartesian coordinate system is depicted in Fig 1. The displacement field of a point at a distance z to the mid-plane can be written as

$$\mathbf{u} = \begin{Bmatrix} u \\ v \\ w \end{Bmatrix} = \begin{Bmatrix} -z\theta_x(x,y) \\ -z\theta_y(x,y) \\ w(x,y) \end{Bmatrix} \tag{1}$$

where (u, v, w) are the displacements of the plate in the x, y, z directions. θ_x and θ_y are the rotations of cross-section of the plate about y and x axes, respectively. The linear strains in the Mindlin-Reissner plate are the strains resulting from bending are obtained in terms of the rotations, θ_x, θ_y and of the mid-surface displacement, w, as

$$\boldsymbol{\varepsilon} = \begin{Bmatrix} \varepsilon_{xx} \\ \varepsilon_{yy} \\ \gamma_{xy} \\ \gamma_{yz} \\ \gamma_{xz} \end{Bmatrix} = \begin{Bmatrix} -z\frac{\partial\theta_x(x,y)}{\partial x} \\ -z\frac{\partial\theta_y(x,y)}{\partial y} \\ -z\frac{\partial\theta_x(x,y)}{\partial y} - z\frac{\partial\theta_y(x,y)}{\partial x} \\ -\theta_y(x,y) + \frac{\partial w(x,y)}{\partial y} \\ -\theta_x(x,y) + \frac{\partial w(x,y)}{\partial x} \end{Bmatrix} \tag{2}$$

Using the generalized Hooke's law for orthotropic linear elastic materials, the stresses for the i^{th} layer is given as,

$$\boldsymbol{\sigma}^i = \bar{\mathbf{c}}^i\boldsymbol{\varepsilon} \tag{3}$$

where

$$\boldsymbol{\sigma}^i = \{\sigma_{xx} \quad \sigma_{yy} \quad \tau_{xy} \quad \tau_{yz} \quad \tau_{xz}\}^T \tag{4}$$

$$\bar{\mathbf{c}}^i = \mathbf{T}^T\mathbf{c}^i\mathbf{T} \tag{5}$$

where $\mathbf{c}^i$ is the material matrix of the i^{th} layer. It includes six independent material properties that are E_1, E_2, ϑ_{12}, G_{12}, G_{13} and G_{23},. The material matrix of the orthotropic materials can be written as

$$\mathbf{c}^i = \begin{bmatrix} \frac{E_1}{1-\nu_{12}\nu_{21}} & \frac{E_1\nu_{21}}{1-\nu_{12}\nu_{21}} & 0 & 0 & 0 \\ \frac{E_1\nu_{12}}{1-\nu_{12}\nu_{21}} & \frac{E_2}{1-\nu_{12}\nu_{21}} & 0 & 0 & 0 \\ 0 & 0 & G_{12} & 0 & 0 \\ 0 & 0 & 0 & G_{23} & 0 \\ 0 & 0 & 0 & 0 & G_{31} \end{bmatrix} \tag{6}$$

and $\mathbf{T}$ is the transformation matrix, which has lay-up of the laminae, can be given as

$$\mathbf{T} = \begin{bmatrix} \cos^2\theta & \sin^2\theta & -\sin 2\theta & 0 & 0 \\ \sin^2\theta & \cos^2\theta & \sin 2\theta & 0 & 0 \\ \sin\theta\cos\theta & -\sin\theta\cos\theta & \cos^2\theta - \sin^2\theta & 0 & 0 \\ 0 & 0 & 0 & \cos\theta & -\sin\theta \\ 0 & 0 & 0 & \sin\theta & \cos\theta \end{bmatrix} \tag{7}$$

where the θ is the lay-up or orientation of fiber on the i^{th} lamina.

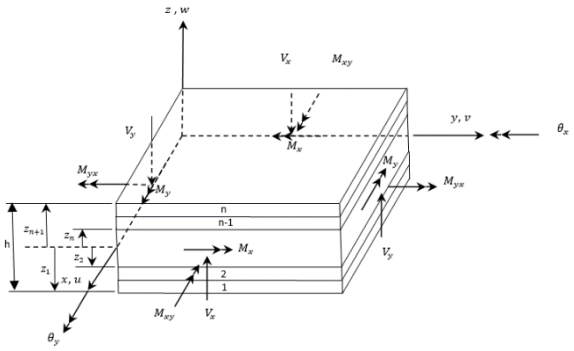

Figure 1. A typical laminate plate

Considering the $\{\varepsilon_{xx}\ \ \varepsilon_{yy}\ \ \gamma_{xy}\} = z\,\{\bar{\varepsilon}_{xx}\ \ \bar{\varepsilon}_{yy}\ \ \bar{\gamma}_{xy}\}$ the stresses on the top face of layer (i) are

$$\begin{aligned}
\sigma_{xx}^{z_i+1} &= z_{i+1}\left[\bar{c}_{11}{}^{i}\,\bar{\varepsilon}_{xx} + \bar{c}_{12}{}^{i}\,\bar{\varepsilon}_{yy} + \bar{c}_{13}{}^{i}\,\bar{\gamma}_{xy}\right]\\
\sigma_{yy}^{z_i+1} &= z_{i+1}\left[\bar{c}_{12}{}^{i}\,\bar{\varepsilon}_{xx} + \bar{c}_{22}{}^{i}\,\bar{\varepsilon}_{yy} + \bar{c}_{23}{}^{i}\,\bar{\gamma}_{xy}\right]\\
\tau_{xy}^{z_i+1} &= z_{i+1}\left[\bar{c}_{13}{}^{i}\,\bar{\varepsilon}_{xx} + \bar{c}_{23}{}^{i}\,\bar{\varepsilon}_{yy} + \bar{c}_{33}{}^{i}\,\bar{\gamma}_{xy}\right]\\
\tau_{xz}^{z_i+1} &= \left[\bar{c}_{44}{}^{i}\,\gamma_{xz} + \bar{c}_{45}{}^{i}\,\gamma_{yz}\right]\\
\tau_{yz}^{z_i+1} &= \left[\bar{c}_{45}{}^{i}\,\gamma_{xz} + \bar{c}_{55}{}^{i}\,\gamma_{yz}\right]
\end{aligned} \tag{8}$$

The bending moments (M_{ij}) and the shear forces (V_{ij})are

$$\begin{aligned}
M_{xx} &= \sum_i^n \int_{z_i}^{z_i+1} z\,\sigma_{xx}^i dz\\
M_{yy} &= \sum_i^n \int_{z_i}^{z_i+1} z\,\sigma_{yy}^i dz\\
M_{xy} &= \sum_i^n \int_{z_i}^{z_i+1} z\,\tau_{xy}^i dz
\end{aligned} \tag{9}$$

and

$$\begin{aligned}
V_{xx} &= k_{sh}\sum_i^n \int_{z_i}^{z_i+1} \tau_{xz}^i dz\\
V_{yy} &= k_{sh}\sum_i^n \int_{z_i}^{z_i+1} \tau_{yz}^i dz
\end{aligned} \tag{10}$$

where k_{sh} is the shear correction factor. Substituting the stress values in Eqs. (8) into moment in Eqs. (9) and shear forces in Eqs. (10):

$$\begin{aligned}
M_{xx} &= \sum_i^n \left[\frac{z_{i+1}^3}{3} - \frac{z_i^3}{3}\right]\left[\bar{c}_{11}{}^{i}\,\bar{\varepsilon}_{xx} + \bar{c}_{12}{}^{i}\,\bar{\varepsilon}_{yy} + \bar{c}_{13}{}^{i}\,\bar{\gamma}_{xy}\right]\\
M_{yy} &= \sum_i^n \left[\frac{z_{i+1}^3}{3} - \frac{z_i^3}{3}\right]\left[\bar{c}_{12}{}^{i}\,\bar{\varepsilon}_{xx} + \bar{c}_{22}{}^{i}\,\bar{\varepsilon}_{yy} + \bar{c}_{23}{}^{i}\,\bar{\gamma}_{xy}\right]\\
M_{xy} &= \sum_i^n \left[\frac{z_{i+1}^3}{3} - \frac{z_i^3}{3}\right]\left[\bar{c}_{13}{}^{i}\,\bar{\varepsilon}_{xx} + \bar{c}_{12}{}^{i}\,\bar{\varepsilon}_{yy} + \bar{c}_{13}{}^{i}\,\bar{\gamma}_{xy}\right]\\
V_{xx} &= k_{sh}\sum_i^n [z_{i+1} - z_i]\left[\bar{c}_{44}{}^{i}\,\gamma_{xz} + \bar{c}_{45}{}^{i}\,\gamma_{yz}\right]\\
V_{yy} &= k_{sh}\sum_i^n [z_{i+1} - z_i]\left[\bar{c}_{45}{}^{i}\,\gamma_{xz} + \bar{c}_{55}{}^{i}\,\gamma_{yz}\right]
\end{aligned} \tag{11}$$

The Eqs. (11) can be arranged as in the following form:

$$\mathbf{M} = \begin{bmatrix} M_{xx} \\ M_{yy} \\ M_{xy} \end{bmatrix} = \sum_i^n \mathbf{D}^i \mathbf{L} \Phi \left(\frac{z_{i+1}^3}{3} - \frac{z_i^3}{3}\right) = \left[\sum_i^n \mathbf{D}^i \left(\frac{z_{i+1}^3}{3} - \frac{z_i^3}{3}\right)\right] \mathbf{L}\Phi$$

$$\mathbf{V} = \begin{bmatrix} V_{xx} \\ V_{yy} \end{bmatrix} = k_{sh}\sum_i^n [\mathbf{A}_{sh}^i(\nabla \mathbf{w} - \Phi)(z_{i+1} - z_i)] = k_{sh}\,[\sum_i^n \mathbf{A}_{sh}^i (z_{i+1} - z_i)](\nabla \mathbf{w} - \Phi) \tag{12}$$

where,

$$\mathbf{L} = \begin{bmatrix} -\frac{\partial}{\partial x} & 0 & -\frac{\partial}{\partial y} \\ 0 & -\frac{\partial}{\partial y} & -\frac{\partial}{\partial x} \end{bmatrix} \tag{13}$$

$$\Phi = \{\theta_x \quad \theta_y\}^T \tag{14}$$

$$\nabla = \left\{\frac{\partial}{\partial x} \quad \frac{\partial}{\partial y}\right\}^T \tag{15}$$

and $\mathbf{D}^i$and $\mathbf{A}_{sh}^i$are the material properties related with bending and shear effects. They can be written in the matrix forms, as follows:

$$\mathbf{D}^i = \begin{bmatrix} \bar{c}_{11}{}^i & \bar{c}_{12}{}^i & \bar{c}_{13}{}^i \\ \bar{c}_{12}{}^i & \bar{c}_{22}{}^i & \bar{c}_{23}{}^i \\ \bar{c}_{13}{}^i & \bar{c}_{23}{}^i & \bar{c}_{33}{}^i \end{bmatrix} \tag{16}$$

$$\mathbf{A}_{sh}^i = \begin{bmatrix} \bar{c}_{44}{}^i & \bar{c}_{45}{}^i \\ \bar{c}_{45}{}^i & \bar{c}_{55}{}^i \end{bmatrix} \tag{17}$$

In the absence of mass forces, the equilibrium equations obtained using the virtual work principle are given as,

$$\begin{aligned} \mathbf{L}^T\mathbf{M} - \mathbf{V} &= 0 \\ \nabla^T\mathbf{V} + \mathbf{b} &= 0 \end{aligned} \tag{18}$$

where $\mathbf{b}$ is the vector of applied external forces. EFGM is used for the solution of this system equations.

3. ELEMENT-FREE GALERKIN METHOD

3.1. Moving-Least Square (MLS) Approximation

The MLS approximation for the function of a field variable $u(\mathbf{x})$ in a local domain Ω is defined at a point $\mathbf{x}$ as

$$u^h(\mathbf{x}) = \sum_{i=1}^{m} p_i(\mathbf{x})a_i(\mathbf{x}) = \mathbf{p}^T(\mathbf{x})\mathbf{a}(\mathbf{x}) \tag{19}$$

where m is the number of basis terms, $\mathbf{p}^T(\mathbf{x}) = \{p_1(\mathbf{x}), p_2(\mathbf{x}), p_3(\mathbf{x}), \cdots, p_m(\mathbf{x})\}$ is the vector of monomial basis functions, $\mathbf{a}^T(\mathbf{x}) = \{a_1(\mathbf{x}), a_2(\mathbf{x}), a_3(\mathbf{x}), \cdots, a_m(\mathbf{x})\}$ is the vector of coefficients, and $\mathbf{x}^T = [x, y]$ is the position vector for 2D problems. The monomials are selected from the Pascal triangle with providing minimum completeness to build the basis function $\mathbf{p}^T(\mathbf{x})$. For example, the linear and quadratic basis functions in 2D problems can be given by

$$\mathbf{p}^T(\mathbf{x}) = [1, x, y], \qquad m = 3 \tag{20}$$

$$\mathbf{p}^T(\mathbf{x}) = [1, x, y, x^2, xy, y^2], \qquad m = 6 \tag{21}$$

The difference between the function $u(\mathbf{x})$ and its local approximation $u^h(\mathbf{x})$ must be minimized by weighted discrete L_2 norm to obtain the vector of coefficients $\mathbf{a}(\mathbf{x})$.

$$J = \sum_{i=1}^{n} w(\mathbf{x} - \mathbf{x}_i)[\mathbf{p}^T(x_i)\mathbf{a}(\mathbf{x}) - u_i]^2 \tag{22}$$

where n is the number of nodes in the support domain of point $\mathbf{x}$, u_i is the nodal value of u at $\mathbf{x} = x_i$, $w(\mathbf{x} - x_i)$ is the weight function associated with the influence domain of node i. From weight function properties, it must be greater than zero for all nodes in the support domain of point $\mathbf{x}$.

The minimization of weighted residual with respect to $\mathbf{a}(\mathbf{x})$ at any arbitrary point $\mathbf{x}$ gives

$$\frac{\partial J}{\partial \mathbf{a}} = 0 \tag{23}$$

which can be written as a set of linear equations.

$$\mathbf{A}(\mathbf{x})\mathbf{a}(\mathbf{x}) = \mathbf{B}(\mathbf{x})\mathbf{U}_s \tag{24}$$

where $\mathbf{U}_s = \{u_1, u_2, u_3, \cdots, u_n\}^T$ is the vector of nodal values of field function for the nodes of support domain. The matrices $\mathbf{A}$ and $\mathbf{B}$ have the following forms

$$\mathbf{A}(\mathbf{x}) = \sum_{i=1}^{n} w_i(\mathbf{x})p(x_i)p^T(x_i), \qquad w_i(\mathbf{x}) = w(\mathbf{x} - x_i) \tag{25}$$

$$\mathbf{B}(\mathbf{x}) = [w_1(\mathbf{x})p(x_1) \quad w_2(\mathbf{x})p(x_2) \quad \cdots \quad w_n(\mathbf{x})p(x_n)] \tag{26}$$

The matrix $\mathbf{A}$ is called as weighted moment matrix of MLS and if it is non-singular $\mathbf{a}(\mathbf{x})$ can be written as

$$\mathbf{a}(\mathbf{x}) = \mathbf{A}^{-1}(\mathbf{x})\mathbf{B}(\mathbf{x})\mathbf{U}_s \tag{27}$$

The local approximation $u^h(\mathbf{x})$ can be rewritten by substituting Eq. (19)

$$u^h(\mathbf{x}) = \sum_{i=1}^{n} \phi_i(\mathbf{x})u_i = \mathbf{\Phi}^T(\mathbf{x})\mathbf{U}_S \tag{28}$$

where $\mathbf{\Phi}^T$is the vector of MLS shape functions and it can be expressed as

$$\mathbf{\Phi}^T(x) = \{\phi_1(x) \quad \phi_2(x) \quad \cdots \quad \phi_n(x)\} = \mathbf{p}^T(x)\mathbf{A}^{-1}(x)\mathbf{B}(x) \tag{29}$$

The partial derivatives of shape function can be achieved by the following equation.

$$\Phi_{,i} = (\mathbf{p}^T\mathbf{A}^{-1}\mathbf{B})_{,i} = \mathbf{p}_{,i}^T\mathbf{A}^{-1}\mathbf{B} + \mathbf{p}^T\mathbf{A}_{,i}^{-1}\mathbf{B} + \mathbf{p}^T\mathbf{A}^{-1}\mathbf{B}_{,i} \tag{30}$$

where

$$\mathbf{A}_{,i}^{-1} = -\mathbf{A}^{-1}\mathbf{A}_{,i}\mathbf{A}^{-1} \tag{31}$$

The spatial derivative are designated with index i following a comma. The weight functions are one of the most important points for derivation of MLS shape functions. The continuity and locality features of the MLS approximation are mainly based on weight functions. The weight function must be positive inside the support domain by taking its maximum value at the centre of support domain and must be zero outside the support domain using a monotonically decrease. There are various weight functions in literature [6]. The cubic spline weight function is used in this work and is given by

$$w_i(\mathbf{x} - x_i) = w(\bar{r_i}) = \begin{cases} 2/3 - 4\bar{r_i}^2 + 4\bar{r_i}^3 & \bar{r_i} \le 0.5 \\ 4/3 - 4\bar{r_i} + 4\bar{r_i}^2 - 4/3\,\bar{r_i}^3 & 0.5 < \bar{r_i} \le 1 \\ 0 & \bar{r_i} > 1 \end{cases} \tag{32}$$

For rectangular influence domain in 2-D problems, weight functions can be obtained by

$$w(\bar{r_i}) = w(r_x)w(r_y) = w_x w_y \tag{33}$$

$$r_x = \frac{|x - x_i|}{r_{wx}} \quad \text{and} \quad r_y = \frac{|y - y_i|}{r_{wy}} \tag{34}$$

where r_{wx} and r_{wy} are the size of support domain in the x and y direction.

3.2. Galerkin Weak Form and Enforcement Boundary Conditions

The Galerkin weak form for Mindlin-Reissner plates can written as

$$\int_\Omega \delta(\mathbf{L}_d u)^T D L_d u d\Omega - \int_\Omega \delta(\mathbf{L}_u u)^T b d\Omega - \int_{\Gamma_t} \delta(\mathbf{L}_u u)^T t_\Gamma dS + \delta \int_{\Gamma_u} \frac{1}{2}(u_b - u_\Gamma)^T \alpha (u_b - u_\Gamma) d\Gamma = 0 \tag{35}$$

The discrete system equation can be written as

$$(\mathbf{K} + \mathbf{K}^\alpha)\mathbf{U} = (\mathbf{F} + \mathbf{F}^\alpha) \tag{36}$$

where **K** is the global stiffness matrix and is obtained by assembling the point stiffness matrices

$$K_{ij} = \int_\Omega \mathbf{B}_i^T \mathbf{D} \mathbf{B}_j d\Omega \tag{37}$$

in which

$$\mathbf{B}_i = \begin{bmatrix} 0 & 0 & 0 & \frac{\partial \phi_i}{\partial x} & \frac{\partial \phi_i}{\partial y} \\ \frac{\partial \phi_i}{\partial x} & 0 & \frac{\partial \phi_i}{\partial y} & \phi_i & 0 \\ 0 & \frac{\partial \phi_i}{\partial y} & \frac{\partial \phi_i}{\partial x} & 0 & \phi_i \end{bmatrix}^T \tag{38}$$

and the $\mathbf{K}^\alpha$is the matrix of penalty factors defined by

$$(\mathbf{K}^\alpha)_{ij} = \int_{\Gamma_u} \varphi_i^T \boldsymbol{\alpha} \varphi_j d\Gamma \tag{39}$$

where φ_i is a diagonal matrix. If the relevant DOF is free, the diagonal elements of φ_i are equal to 0, otherwise equal to 1.

The force vector **F** in Eq. (35) is the global force vector assembled using the nodal force vector of

$$F_i = \int_\Omega (\mathbf{L}_u \Phi_i)^T b d\Omega + \int_\Omega (\mathbf{L}_u \Phi_i)^T t_\Gamma dS \tag{40}$$

where Φ_i is a diagonal matrix of shape functions.

The $\mathbf{F}^{\alpha}$ vector shows the forces obtained by the implementation of essential boundary conditions and can be obtained as follows

$$F_i^{\alpha} = \int_{\Gamma_u} \varphi_i{}^T \alpha u_{\Gamma} d\Gamma \quad (41)$$

4. NUMERICAL RESULTS AND DISCUSSIONS

In this section, a few numerical examples have been performed to demonstrate the applicability and the accuracy of the EFGM. Plates with boundary conditions, thickness ratios, number of layers, fiber orientations and materials are studied. The results are provided in terms of normalized displacements for the convenience of comparison and validated by comparing them with analytical results taken from the literature and FEM results. The behaviour of all composite materials used is considered as linear elastic. The value of shear correction factor is constant and taken as $5/6$ for all examples. The properties of materials used in the examples are given in Table 1. The linear polynomial basis, cubic spline weight function, 2.5 for the dimensionless support domain size and 7×7 Gauss quadrature integration points are used in all EFGM solutions.

Table 1. Properties of laminated composite plates

	M1	**M2**	**M3**
$\boldsymbol{E1}, Pa$	250×10^9	40×10^6	300×10^9
$\boldsymbol{E2}, Pa$	10×10^9	1.0×10^6	12×10^9
$\boldsymbol{G_{12}}, Pa$	5×10^9	0.6×10^6	6×10^9
$\boldsymbol{G_{13}}, Pa$	5×10^9	0.6×10^6	6×10^9
$\boldsymbol{G_{23}}, Pa$	2×10^9	0.5×10^6	2.4×10^9
$\boldsymbol{v_{12}}$	0.25	0.25	0.25

4.1. Simply supported laminated composite plates under uniformly distributed load

The deformation of a simply supported square laminated plate subjected to a uniformly distributed transverse load $q = 100$ kN/m^2 is analysed using different lamination schemes with thickness/span ratios of $h/L = 0.1, h/L = 0.05$ and $h/L = 0.01$. The laminates used are orthotropic laminate with one layer of [0°] orientation, symmetric cross-plies with three, four, five and seven layers of [0°/90°/0°], [0°/90°/90°/0°], [0°/90°/0°90°/0°] and [0°/90°/90°/0°/90°/90°/0°] orientations, respectively. The material M1, presented in Table 1, is used in this example.

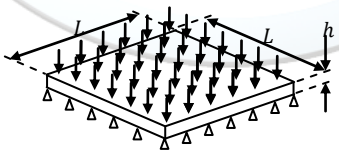

Figure 2. Simply supported laminated composite square plate

Due to the symmetry, only a quarter of plate is modelled using 441 nodes in the EFGM and FEM solutions. The dimensionless center deflection of plate is presented in Table 2. It can be seen that the accuracy of EFGM solution is near to the exact solution and is better than the FEM.

Table 2. Central deflections $100wE_2h^3/(qL^4)$ *under uniform transverse load*

h/L	Lay-up	FEM	EFGM	Exact [12]
0.01	0	0.662553	0.659729	0.6528
	0/90/0	0.680383	0.677547	0.6697
	0/90/90/0	0.694267	0.691600	0.6833
	0/90/0/90/0	0.698297	0.695732	0.6874
	0/90/90/0/90/90/0	0.701414	0.698928	0.6896
0.05	0	0.737233	0.734517	0.7262
	0/90/0	0.769471	0.766675	0.7572
	0/90/90/0	0.781553	0.778914	0.7694
	0/90/0/90/0	0.769781	0.767292	0.7581
	0/90/90/0/90/90/0	0.767333	0.764929	0.7575
0.1	0	0.966699	0.963153	0.9519
	0/90/0	1.038240	1.034393	1.0219
	0/90/90/0	1.040156	1.036504	1.0250
	0/90/0/90/0	0.986117	0.982779	0.9727
	0/90/90/0/90/90/0	0.969344	0.966131	0.9643

4.2. Simply supported angle-ply square plate under uniformly distributed load

The deformation of an angle-ply simply supported square plate subjected to a uniformly distributed transverse load $q = 1$ is examined using four layers $[\theta°/-\theta°/\theta°/-\theta°]$. The solutions are presented with a constant thickness-to-span ratio, h / L, of 0.1. The material M2 is used in this example.

Because of the asymmetry, the whole plate is modelled using 441 nodes in the EFGM and FEM solutions. Table 3 presents the dimensionless center deflection of plate. It is visible that the accuracy of EFGM solution is more accurate than the FEM. Also, it can be achieved to exact results by particular number of nodes used in the solution.

Table 3. Central deflections $100wE_2h^3/(qL^4)$ *under uniform transverse load*

Arrangement of layers $[\theta°/-\theta°/\theta°/-\theta°]$	FEM	EFGM	Exact [12]
-5/+5/-5/+5	6.922555	6.892311	6.741
-15/+15/-15/+15	6.205659	6.180749	6.086
-30/+30/-30/+30	4.841598	4.820746	4.825
-45/+45/-45/+45	4.430046	4.410081	4.426

4.3. Clamped laminated composite plates under uniformly distributed load

Clamped laminated square plate with four different aspect ratios of $h / L = 0.1, h / L = 0.05, h / L = 0.02$ and $h / L = 0.01$ are analyzed to determine deformations under the uniformly distributed transverse load $q = 1$. The unidirectional laminate of material M3 is used with four layer of $[0°/90°/90°/0°]$ orientation. Due to the symmetry, only a quarter of plate is modelled using 441 nodes in the EFGM and FEM solutions. The dimensionless center deflection of plate is presented in Table 4. A close agreement between the results of EFGM and exact solution is shown for all thickness ratios examined. Again the results of EFGM is better than the FEM ones.

Table 4. Central deflections $100wE_2h^3/(qL^4)$ *under uniform transverse load*

h/L	FEM	EFGM	Exact [13]
0.1	0.465766	0.46542	0.4651
0.05	0.234185	0.234522	0.2342
0.02	0.158636	0.159152	0.159
0.01	0.147079	0.147363	0.1475

5. CONCLUSIONS

In this study, the EFGM based on First Order Shear Deformation Theory is successfully implemented in the bending analyses of laminated composite plates. The results for the analyzed plates are in good agreement with the results of exact solutions. It is also shown that the accuracy of EFGM solutions are better than the FEM ones for the analyzed plates.

REFERENCES

[1]. J. N. Reddy, A. A. Khdeir, "Buckling of vibration of laminated composite plates using various plate theories," *AIAA Journal*, 27(12), 1808-1817, 1989.
[2]. A. H. Sheikh, S. Haldar, D. Sengupta, "A high precision shear deformable element for the analysis of laminated composite plates of different shapes," *Composite Structures*, 55(3), 329-336, 2002.
[3]. A. Reis, E. L. Albuquerque, F. L. Torsani, L. P. Junior, P. Sollero, "Computation of moments and stresses in laminated composite plates by the boundary element method," *Engineering Analysis with Boundary Elements*, 35, 105-113, 2010.
[4]. S. K. Numayr, R. H. Haddad, M. A. Haddad, "Free vibration of composite plates using the finite difference method," *Thin-Walled Structures*, 42, 399-414, 2004.
[5]. T. Belytschko, "Meshless methods an overview and recent developments," *International Journal for Numerical Methods in Engineering*, 38, 1655-1679, 1996.
[6]. G.R. Liu, *Mesh Free Methods Moving Beyond The Finite Element Method*, Taylor and Francis Group, (2003).
[7]. J. Belinha, L. M. J. S. Dinis, "Analysis of plates and laminates using the element-free Galerkin method," *Computers and Structures*, 84, 1547-1559, 2006.
[8]. A. G. Arani, Sh. Maghamikia, M. Mohammadimehr, A. Arefmanesh, "Buckling analysis of laminated composite rectangular plates reinforced by SWCNTs using analytical and finite element methods," *Journal of Mechanical Science and Technology*, 25(3), 809-820, 2011.
[9]. M. R. Aagaah, M. Mahinfalah, G. N. Jazar, "Natural frequencies of laminated composite plates using third order shear deformation theory," *Composite Structures*, 72, 273-279, 2006.
[10]. S. S. Ghorashi, S. R. Sabbagh-Yazdi, S. Mohammadi, "Element free Galerkin method for crack analysis of orthotropic plates," *Computational Methods in Civil Engineering*, 1, 1-13, 2010.
[11]. S. S. Ghorashi, S. Mohammadi, S. R. Sabbagh-Yazdi, "Orthotropic enriched element free Galerkin method for fracture analysis of composites," *Engineering Fracture Mechanics*, 78, 1906-1927, 2011.
[12]. J. N. Reddy, *Mechanics of laminated composite plates*, CRC Press, 1996.
[13]. P. Umasree, K. Bhaskar, "Accurate flexural analysis of clamped moderately thick cross-ply rectangular plates by superposition of exact untruncated infinite series solutions," *Journal of Reinforced Plastics Composite*, 24(16), 1723-1736, 2002.

ISSN: 2458-8156

Journal Home page : http://dergipark.ulakbim.gov.tr/ejens * E-mail : editor@cnrgroup.eu

hosted by Turkish JournalPark ACADEMIC

EJENS

European Journal of Engineering and Natural Sciences CODEN: EJENS

Identification of Waste Sources in Ready-Mixed Concrete Plants

Aynur Kazaz[1]*, Serdar Ulubeyli[2], Bayram Er[1], Ahmet Arslan[1], Murat Atici[1]

[1]*Akdeniz University, Department of Civil Engineering, 07058, Antalya, Turkey.*

[2]*Bulent Ecevit University, Department of Civil Engineering, 67100, Zonguldak, Turkey.*

**Corresponding Author email: akazaz@akdeniz.edu.tr*

Publication Info

Paper received:
10 December 2015

Revised received:
15 December 2015

Accepted:
18 December 2015

Abstract

In today's highly industrialized world, an enormous amount of wastes is originated from the construction industry. This type of wastes conversely affects both macro-economic conditions and environment of a country or a region. Therefore, waste management is an important aspect of project management. Although there is a wide variety of construction materials, concrete is still the mostly used one in the construction industry and thus has a big impact on the amount of construction-based wastes. Reducing such wastes is among the objectives of the waste management issue in construction projects. Accordingly, the determination of waste sources is the first step to deal with them. Based on these arguments, the current paper presents a study that aims to identify the sources of fresh concrete wastes in ready-mixed concrete (RMC) plants as a part of an on-going research project. Toward this aim, production and delivery processes of RMC were reported and discussed in a detailed manner from the perspective of waste management. As a result, four sources were identified for such wastes. It was also found out that only two types of these sources (i.e., over-order and residual RMC in the truck-mixer drum) are quantifiable.

Key words

Construction waste, Fresh concrete waste, Ready-mixed concrete, Waste sources

1. INTRODUCTION

Today, construction wastes constitute approximately 20–40% of the area occupied by wastes in a country ([16], [5], [10]). Construction wastes produced per year in England [8] and US [20] are estimated as 91 and 164 million tons, respectively. Especially in developing countries such as Turkey where the construction industry is in a rapid development process (Figure 1), the rate of construction wastes is expected to be higher [19]. Therefore, minimizing or recycling construction wastes is a crucial activity for using the limited natural resources efficiently for a long term.

Although there are different construction systems, reinforced-concrete structures are still common. Easy supply and low cost of raw materials, easy forming, and low know-how requirement in the production process are main reasons of using concrete in construction projects. In a concrete building, the cost of concrete may rise up to 10% of the total project cost [3]. In addition, according to Turkish Ready Mixed Concrete Association [18], Turkey has an annual ready-mixed concrete (RMC) production amount of 102 million m^3 (Figure 2).

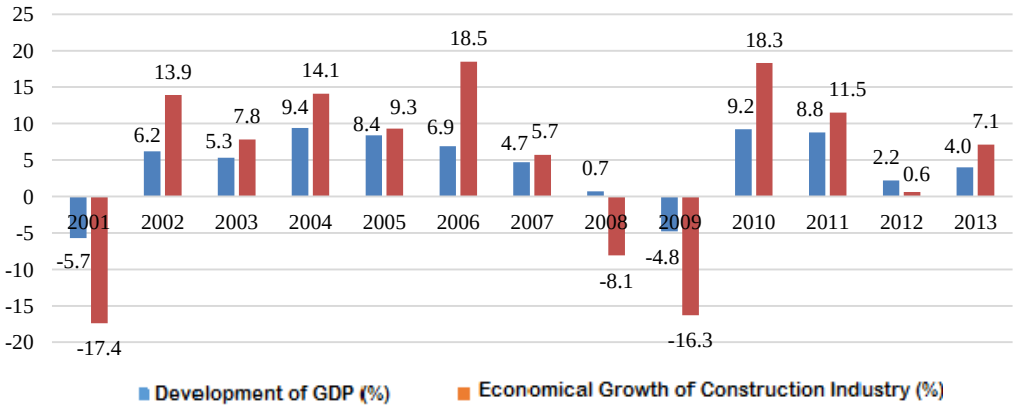

Figure 1. Comparison of the economic role of the construction industry with the development of GDP in Turkey

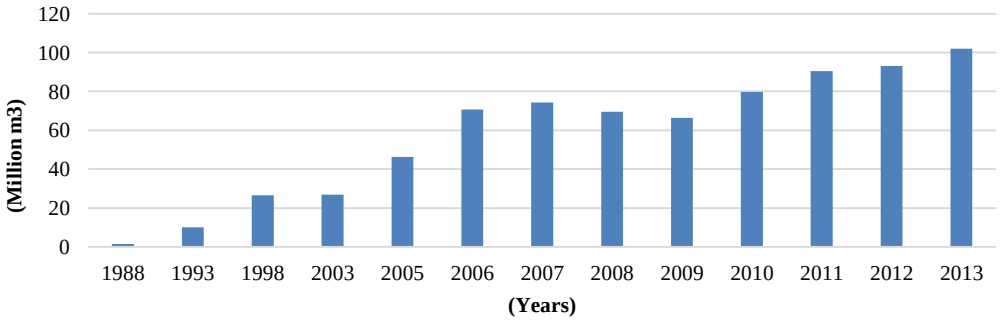

Figure 2. The annual production amount of RMC

This production amount places Turkey in the first rank in Europe and the third rank in the world (Table 1). Therefore, it can be argued that concrete wastes have a big impact on construction-based wastes, and reducing them will improve both macro-economic conditions and the built environment in Turkey.

Waste management encompasses preventing, collecting, transporting, and disposal of wastes. Main principles of waste management are reducing, reusing, and recycling of wastes. Therefore, for an effective waste management procedure in a construction site, it is important to determine which kinds of wastes can be reduced, reused, or recycled. Concrete wastes appear in two ways during the whole lifecycle of a construction project: (i) as the fresh concrete waste during the implementation phase and (ii) as the demolition waste during the destruction of the structure.

Demolition wastes are generated as hardened concrete after the building completes its economic life. Therefore, reducing demolition wastes or recycling them to their raw materials seems impossible in the current technological conditions. However, reusing crushed demolition wastes as filling materials or aggregate for fresh concrete are common practices in the construction industry ([1], [11], [14], [15], [21], [2], [6], [13]).

Fresh concrete wastes occur both in construction sites and in RMC plants at the start of the economic life of a project before concrete gets hardened. There are recycling facilities which separate the fresh concrete to its raw materials. Therefore, identifying the sources of fresh concrete wastes can be helpful both for determining preventive measures and for calculating the amount of this waste that can be recycled. In this context, the current paper presents a study that aims to identify the sources of fresh concrete wastes in RMC plants as a part of an on-going research project.

Table 1. The RMC production amount of ERMCO countries in 2013

Country	**Amount of Production (million m^3)**	**RMC per Person (m^3/person)**
Spain	16.3	0.3
İtaly	31.7	0.5
Turkey (2013)	*102*	*1.3*
Germany	45.6	0.6
France	38.6	0.6
England (UK)	19.6	0.3
Portugal	2.7	0.3
Belgium	12.5	1.1
Poland	18	0.5
İreland	2.4	0.5
Netherland	6.6	0.4
Norway	3.8	0.8
Sweden	3.3	0.3
Total of Europe	218.1	0.5
Russia	44	0.3
USA	230	0.8
Japan	99	0.8

2. LIFECYCLE OF THE FRESH CONCRETE

Concrete is mainly used to produce the bearing elements of a structure. Therefore, the quality of the fresh concrete has a big impact on the strength of a structure. This quality depends on the mixing ratios of raw materials used in the fresh concrete production. For example, an increase of 20% and 30% of the water content will decrease the strength of concrete by %30 and 50%, respectively [17]. Although the concrete quality is determined by internationally and nationally accepted standards, the fresh concrete produced in site by unskilled workers will likely have a high risk for quality. In addition, since the amount of concrete produced in site is limited, every production may also have different qualities. In order to overcome these problems, the fresh concrete is produced in RCM plants where the production is supported by automation systems and the product is transported by truck mixers to construction sites.

The production process in RMC plants starts with laboratory tests. In these tests, the quality of raw materials and their compatibilities are evaluated. In fact, these tests are conducted when new raw materials arrive to the batching plant. Therefore, each RMC plant has also a quality control department. After these tests are completed, for each concrete class a specific mixing ratio is determined and saved into the automation system.

In RMC plants, concrete is produced in two ways: (i) dry system and (ii) wet system (Figure 3). In the dry system, cement and aggregate are mixed in truck mixers without adding water and admixture. The water and admixture are added at the construction site before concrete is poured. Nevertheless, this system seems to be logical when the transport distance is too long. If the transport time exceeds two hours, there will be some quality problems. If the moisture content of the truck mixer is too high, the chemical reaction between cement and aggregate will start before the necessary water is added. In addition, admixtures and water may be added by unskilled workers in site and the necessary mixing for a homogenous concrete production may not be waited. Therefore, in RMC plants, the wet system is more common than the dry system. In the wet system, all of raw

materials stored in different places are weighed separately and put into the mixing drum of the plant by means of the automation system. Since over-mixing will lead to segregation in the fresh concrete, the mixing process is continued for a specific duration in mixing drums, and then, the mixed concrete is poured into truck mixers where the mixing process will continue until it arrives to the construction site [9]. Finally, in construction sites, the fresh concrete transported by truck mixers is poured into formworks by concrete pumps, and residual concrete is transported back to RMC plants.

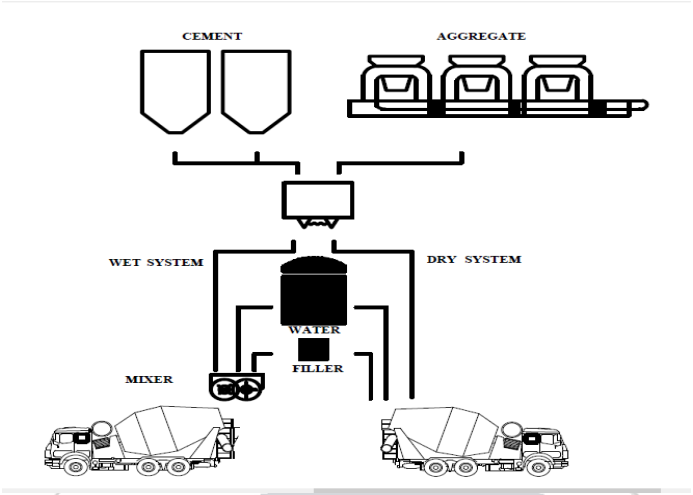

Figure 3. The operation schema of RMC plants

3. SOURCES OF FRESH CONCRETE WASTES

In order to identify the sources of fresh concrete wastes, three different RMC plants operating in different cities in Turkey were investigated as a part of an on-going research project. Each RMC plant was visited once a week for 12 months. After detailed observations, four sources for fresh concrete wastes were identified as follows.

3.1. During the Filling Process of Truck Mixers

Since the hopper of a truck mixer is at the back side, truck mixers have to draw close backwards to the mixing drum's discharging part. In this situation, depending on drivers' abilities, sometimes the hopper and discharging parts do not match exactly, and as a result, some fresh concrete is unintentionally poured outside of the truck mixer. In addition, if the production stops for a while or the concrete class changes, then the mixing drums should be washed up. In this process, some fresh concrete waste is generated. Although the amount of waste generated by each filling or washing up effort seems to be negligible, the sum of this waste in RMC plants with high production amounts becomes remarkable. For example, the waste amount shown in Figure 4 was produced within two hours in an RMC plant with an average daily concrete production of 750 m^3. However, it is very difficult to measure the amount of this waste due to the intensive vehicle traffic. In practice, when the production stops, this waste is collected and stored by loaders in the debris area.

3.2. Quality Control Laboratory

In RMC plants, besides the quality control of raw materials, the quality of the fresh concrete has to be controlled. In practice, for this purpose, some fresh concrete from each production is taken and filled up into cube formworks in the laboratory of the RMC plant. In general, this exceeds the needed amount, and hence, some fresh concrete waste is also generated in this process.

3.3. The Adhesive Concrete in a Truck Mixer's Drum

Although truck mixers try to pour all of the fresh concrete content in construction sites, there always remains some adhesive concrete in their drums. Therefore, after truck mixers return to RMC plants, their drums are washed up by adding about 200-300 liter water. In the context of the ongoing research project, in each visit of RMC plants, 10 truck mixers were washed and the waste content was measured. The preliminary statistical analysis revealed that approximately 500 kg aggregate comes out as waste in the 100 m^3 fresh concrete production.

Figure 4. The waste generation during the filling process

3.4. The Over-Order Concrete

In construction projects, wastes are inevitable. Therefore, the planned material amount rarely matches with the actual material need. Especially in concreting works, this difference can be observed more clearly due to some reasons such as the content of filler blocks and reinforcement and poor workmanship. In order to overcome this problem, many planning engineers have the tendency of over-ordering materials. For this purpose, they determine a coefficient based on their own personal experience and multiply it with the planned amount [[12], [7], [4]). Nevertheless, since these coefficients are based on experience and are not exact values, almost in every order the residual fresh concrete occurs because of over ordering. However, in practice, this residual concrete is not stored in the debris area. Instead, if the transport duration does not exceed two hours, it is mixed with lower class concrete of another order and used in other projects. For example, if the residual concrete class is C30, it is mixed with C25. Therefore, this type of wastes is mostly encountered at the end of the working day. Since this type of wastes is documented, the amount is measurable.

The aforementioned types of wastes are a part of the production and are inevitable. In addition to these waste sources, it was also observed that fresh concrete wastes are also generated from a problem in production, such as the breakdown of some machines. Although the amount of this waste can be huge when compared with other types of concrete wastes, it occurs rarely and randomly. For example, during on-plant observations, 3 m^3 fresh concrete was produced only once.

Similar to other enterprises, the aim of RMC plants is to make some profits. In this respect, many RMC plants neglect the environmental impact of fresh concrete wastes and do not strive to reduce or recycle these wastes. Interviews with plant managers revealed that the low cost and easy supply of raw materials are main obstacles for taking countermeasures.

4. CONCLUSIONS

In today's highly industrialized world, an enormous amount of wastes is originated from the construction industry. Since wastes are unused materials that do not have an economic value, they conversely affect both macro-economic conditions and the built environment of a country or a region. In this context, waste management becomes an important aspect of project management.

For an effective waste management procedure, it is important to determine which kinds of wastes can be reduced, reused, or recycled. In this regard, the first step of waste management should be the determination of waste sources. In this study, it was aimed to identify the sources of fresh concrete wastes in RMC plants. Toward this aim, three different RMC plants were observed in every week for a year. The results revealed that fresh concrete wastes are generated in four different sources in an RMC plant (i.e., during the filling process of truck mixers, quality control laboratory, the adhesive concrete in the truck mixer's drum, and overordering). Because of the operation process of the batching plants, only adhesive concrete in the truck mixer's drum and the over-order concrete are quantifiable.

ACKNOWLEDGMENT

The authors gratefully acknowledge the managers and employees of the batching plants for their generous collaboration and contributions. The authors also thank the financial supports provided by Committees on Research Grants of Akdeniz University and Bulent Ecevit University. This study is based on an on-going research project which is financially supported by the Scientific and Technological Research Council of Turkey (TUBITAK) under the grant number MAG-113M428.

REFERENCES

[1]. Y. H. Cho and S. H. Yeo, "Application of recycled waste aggregate to lean concrete subbase in highway pavement," *Canadian Journal of Civil Engineering*, vol. 31, pp. 1101–1108, 2004.
[2]. R. Herrador, P. Perez, L. Garach, and J. Ordonez, "Use of recycled construction and demolition waste aggregate for road course surfacing," *Journal of Transportation Engineering*, vol. 138, pp. 182-190, 2012.
[3]. A. Kazaz, S. Ulubeyli, and F. Turker, "The quality perspective of the ready-mixed concrete industry in Turkey," *Building and Environment*, vol. 39, pp. 1349-1357, 2004.
[4]. H. Kerzner, *Project Management: A Systems Approach to Planning, Scheduling and Controlling*, 10th ed., New Jersey, USA: John Wiley and Sons, 2009.
[5]. C. J. Kibert, "Deconstruction as an essential component of sustainable construction," in *Second Southern African Conference on Sustainable Development in the Built Environment, Pretoria*, 2000, p. 1-5.
[6]. S. Kou, B. Zhan, and C. Poon, "Feasibility study of using recycled fresh concrete waste as coarse aggregates in concrete," *Construction and Building Materials*, vol. 28, pp. 549-556, 2012.
[7]. J. P. Lewis, *Project Planning, Scheduling, and Control: A Hands-On Guide to Bringing Projects in on Time and on Budget*, 3rd ed., New York, USA: McGraw-Hill, 2001.
[8]. M. Osmani, J. Glass, and A. D. F. Price, "Architects' perspectives on construction waste reduction by design," *Waste Management*, vol. 28, pp. 1147-1158, 2008.
[9]. L. S. Pheng, *Theory and Practice of Construction Export Marketing*, Burlington, USA: Ashgate Publishing Company, 1996.
[10]. C. S. Poon, "Reducing construction waste," *Waste Management*, vol. 27, pp. 1715-1716, 2007.
[11]. A. Rao, K. N. Jha, and S. Misra, "Use of aggregates from recycled construction and demolition waste in concrete," *Resources, Conservation and Recycling*, vol. 50, pp. 71-81, 2007.
[12]. G. J. Ritz, *Total Construction Project Management*, New York, USA: McGraw-Hill, 1994.
[13]. R. V. Silva, J. de Brito, and N. Saikia, "Influence of curing conditions on the durability-related performance of concrete made with selected plastic waste aggregates," *Cement and Concrete Composites*, vol. 35, pp. 23-31, 2013.
[14]. M. A. Sobhan, S. A. Mofiz, and H. M. Rasel, "Effect of gradation and compactive effort on the properties of bituminous mixes with waste concrete aggregates," *International Journal of Civil and Environmental Engineering*, vol. 11, pp. 18-21, 2011.
[15]. M. S. Sobri, S. H. Hamzah, and A. R. M. Ridzuan, "Ultimate strength of steel fabric reinforced concrete short wall panel using crushed concrete waste aggregate (CCwA)," *International Journal of Civil and Environmental Engineering*, vol. 11, pp. 64-80, 2011.
[16]. M. J. Stokoe, P. Y. Kwong, and M. M. Lau, "Waste reduction: a tool for sustainable waste management for Hong Kong," in *R'99 World Congress, Geneva*, 1999, p. 165-170.
[17]. M. Şimşek, *Construction Materials – 1*, İstanbul, Turkey: Seçkin Publisher, 2013.
[18]. (2014) TRMCA (Turkish Ready Mixed Concrete Association) statistics. [Online]. Available: http://www.THBB.ORG/EN/INDUSTRY
[19]. T. Tuy, Y. Cheny, and L. Hwang, "Properties of HPC with recycled aggregates," *Cement and Concrete Research*, vol. 36, pp. 943–950, 2006.
[20]. G. Winkler, *Recycling Construction and Demolition Waste*, New York, USA: McGraw-Hill, 2010.
[21]. C. J. Zega and A. A. D. Maio, "Recycled concretes made with waste ready-mix concrete as coarse aggregate," *Journal of Materials in Civil Engineering*, vol. 23, pp. 281–286, 2011.

ISSN: 2458-8156

Journal Home page : http://dergipark.ulakbim.gov.tr/ejens * E-mail : editor@cnrgroup.eu

hosted by Turkish JournalPark ACADEMIC

EJENS

European Journal of Engineering and Natural Sciences CODEN: EJENS

The Effects of Irrigation with Treated Wastewater on Crops and Human Populations – A Review

Romanos - Vasileios Araviadis[1]*

[1] *Araviadis Romanos – Vasileios Technical and Construction Office , 53100, Florina, Greece*

**Corresponding Author email: romanosar@yahoo.gr*

Publication Info

Paper received:
10 December 2015

Revised received:
15 December 2015

Accepted:
18 December 2015

Abstract

The use of treated urban wastewater as a resource for irrigation water is a practice widely employed in arid and semi-arid regions of the world but also one that is expected to become more diffuse due to the reduction of water resources and the climax in the competition for water. Researchers' interests are, thus, focused on investigating the effects of the method under question on the crops on which it is applied. This review presents the main research findings on the topic with a specific focus on research carried out in Greece. The general conclusion of the present review is that the use of treated urban wastewater in irrigation can have beneficial effects on most crop yields, provided that quality characteristics of both treated wastewater and crops are sufficiently monitored

Key words

Agriculture, Contaminants, Greece, Treated wastewater,Water reuse

1. INTRODUCTION

The Mediterranean Sea basin contains just 2% of the global water reserves, while the population in the area corresponds to about 7% of the world population. The aforementioned water reserves are distributed unevenly and are found concentrated primarily in northern countries. As a result, water scarcity is a limiting factor for a variety of activities and especially for crop cultivation, which is the basic consumer of fresh water resources worldwide [1], [2]. Due to the uneven spatial distribution which characterizes the availability and the quantity of the water reserves, but also due to the intensive use that water resources are under, the reuse of treated water, over the last decades, has become an attractive proposal towards the reduction of the quantity of water that is abstracted from natural reserves. The use of treated wastewater in crop irrigation could cover part of the demand for fresh water, especially in Mediterranean countries and other arid and semi-arid regions that face an increasing water scarcity [3], [4], [5].

Both wastewater treatment and the use of treated wastewater in crop irrigation differ among Mediterranean countries. Northern countries process about 90 % of their wastewater but use only a small percentage of the treated wastewater for irrigation. Southern countries, on the other hand, which have lower water reserves, process a small percentage of their wastewater but tend to use a large percentage of fully but also minimally treated wastewater for crop irrigation [6].

Technological progress has enabled the treatment of wastewater to such a level, that most qualitative requirements are satisfied and the treated wastewater is suitable for various uses, such as the irrigation of crops and parks [3].

In technologically developed countries, on the other hand, like Israel, full-scale programs for the reuse of wastewater have created a framework for the reuse of 65% of wastewater for irrigation [7]. Water reuse is also used in other technologically advanced countries, such as the USA, France, Spain, Great Britain, Belgium and Cyprus [8]. In California, USA about 894 million tons of recycled water were used in 2009, a quantity that is estimated to rise to

1.540 million tons in 2015 and 1.880 million tons in 2020 [9]. The corresponding numbers for Beijing were about 680 million tons in 2010, a quantity that corresponds to 20% of the city's water needs. Furthermore, it was estimated that in 2015 the reuse of water in Beijing will exceed 1.000 million tons [10].

It is also important to point out that the use of treated wastewater can be successfully combined both with conventional treatment methods and with natural-system treatment methods, such as with the method of constructed wetlands [11].

This review aims to present and synthesize the findings of studies and publications on the effects that the use of treated urban wastewater in crop irrigation and other areas has on the qualitative characteristics of crops, on soil properties, on the environment and on the human population. It is one of only a few papers of this kind on this particular subject and one of very few which focus on case studies in Greece.

The scope of the present paper is, precisely, the investigation of the impact of the use of treated wastewater on crops and human population, since it constitutes a method that is widely diffuse in many parts of the world and which can contribute in the rational use of water resources in regions where they are limited.

After the present introduction, this paper presents the conditions necessary for the use of treated urban wastewater on crops, its advantages, its potential negative aspects, its implementation in Greece and ends with conclusions and proposals for further research on the subject.

2. CONDITIONS FOR THE USE OF TREATED URBAN WASTEWATER ON AGRICULTURE

There are official documents in various countries around the world which specify the qualitative characteristics that treated wastewater destined for irrigation should have.

In Greece, Ministerial Decision 145116/2011 (Government Gazette 354/B/03.08.2011)[12] specifies the required qualitative characteristics of treated wastewater that is destined for irrigation, the crops on which it can be applied and the type of irrigation that is allowed to be used. On the same document, a distinction is made between two types of irrigation, on the basis of the kind of crops irrigated, the irrigation system and the accessibility of the irrigated area to the public. The two types of irrigation distinguished are: a) limited irrigation, concerning exclusively crops whose products are destined either for industrial use, post-processing consumption, or that are not destined for human consumption at all, and b) unlimited irrigation, concerning crops whose products are destined for raw consumption and floricultural crops.

Water's suitability or unsuitability for application to each crop can be determined from the determination of a series of chemical and microbiological parameters, always taking into account the requirements and the resistance of the crop under question to specific environmental factors. Indicatively, some of the parameters required to assess the suitability of a water sample for irrigation are: its electrical conductivity (EC), the total dissolved solids (TDS), valuable anions and cations such as calcium (Ca^{2+}), magnesium (Mg^{2+}), sodium (Na^{+}), the pH, the sodium absorption ratio (SAR) and the concentration of heavy metals.

3. ADVANTAGES OF USING TREATED URBAN WASTEWATER IN CROP IRRIGATION

The use of treated urban wastewater for the irrigation of agricultural crops, green areas and recreation spaces presents several advantages such as water saving, the protection of the environment and economic benefits.

Firstly, the reuse of treated wastewater, particularly in agricultural applications is a practical solution to the problem of limited water resources [13], [14], [15].

Additionally, reuse of treated wastewater protects aquatic ecosystems, as the channeling of untreated sewage waters in aquatic ecosystems would cause eutrophication and algae growth [14].

As far as the cost of urban wastewater treatment is concerned, that depends on the processing method applied. However, in any case, urban wastewater treatment is economically more advantageous than other treatment methods employed for the production of water, like desalting, for instance [16].

The use of treated wastewater for agricultural crop irrigation has also been found to be advantageous for soil structure and fertility. According to Kiziloglu et al. (2007) [17] , treated wastewater has a high nutrient content, condition that can act beneficially for plant growth, reduce the need for the use of fertilizers and increase crop yield on poor soils. Various studies show that irrigation with treated urban wastewater increases the soil's concentration in elements associated with plant growth, such as nitrogen (N), phosphorus (P), iron (Fe), manganese (Mn), potassium (K), calcium (Ca), magnesium (Mg), zinc (Zn), boron (B), molybdenum (Mo) and other elements [18], [6], [13], [19], [20], [17], [21], [22], [23], [24], [25].

Cirelli et al. (2012) [26] report a yield increase of about 20% in tomato cultivations irrigated with treated urban wastewater, while Akponikpè et al. (2011) [18] report higher yield in eggplant cultivations on an average of 40%.

Rusan et al. (2007) [27] report significantly higher biomass production after irrigating fodder plant crops with treated urban wastewater, while Zema et al. (2012) [28] report increased biomass production in the cultivation of energy plants.

The total nitrogen content in the outflow of secondary wastewater treatment is usually 10 to 20 mg L^{-1} [18], [21], [4], while the ratio of ammonium ions, nitrates and organic nitrogen depends on the degree of treatment. Nitrogen compounds are usually not removed during the treatment of wastewater, so the treated effluent supplies plants with a significant amount of nutrients and reduces requirements in fertilizer. Furthermore, most of the nitrogen and phosphorus quantity is found in forms easily assimilable by plants [30]. Yi et al. (2011) [29] report that in 2010 30 million tons of treated wastewater were used for crop irrigation in Beijing, resulting in saving 4000 tons of nitrogen, 500 tons of phosphorus and in decreasing fertilizer needs by a percentage of 10-50%.

In case, however, that the treated wastewater is intended for other uses, such as industrial cooling, an additional treatment stage should intervene for the removal of nutrients that can lead to microbial growth and damage to equipment [16].

Irrigation with treated urban wastewater appears to increase the organic soil matter [13], [31], [17], [22]. In addition, it provides the soil with useful microorganisms [18], [13].

Irrigation with recycled water can contribute to the sustainability of the soil, especially in cases of poor urban lands [32]. The use of recycled water in California and Beijing improved the biological activity of the irrigated soils. On account of the nutrients present in the treated wastewater used for irrigation, enzymatic activity of soils improves, including the recycling of nutrients and of the microbial biomass of the soil [21], [33], [34].

Comparing areas irrigated with treated and fresh water, soil microbial biomass increased by 60.14% and 14.21% in urban green areas and farming fields, respectively. Furthermore, an enhancement in the activity of five soil enzymes (urease, alkaline phosphatase, invertase, dehydrogenase and catalase) was observed in the surface soil layer (0-20 cm) in percentages of 36.73% and 7.40% higher, in urban green areas and fields respectively [34]. Similar experiments in five different areas of Southern California, irrigated with treated urban wastewater for a long period, showed a doubling or tripling of the activity of 17 soil enzymes associated with the cycles of carbon, nitrogen, phosphorus and sulfur [33].

Regarding the use of recycled water for the irrigation of green areas, it is reported that through it there are economic advantages as well as an enrichment of the soil with high quantities of nitrogen, phosphorus and several trace elements [30], [35].

It becomes obvious, then, that the use of treated wastewater in agriculture is a practice with a high number of advantages, which, with the adherence to certain rules, guidelines and quality standards can assist in the establishment of safe and sustainable food cultivations [13].

4. NEGATIVE EFFECTS OF USING TREATED URBAN WASTEWATER ON CROPS

The use of treated wastewater for crop irrigation contains potentially negative effects on the environment and on public health.

One such risk to human health is the increase of the resistance of soil bacteria to antibiotics. Gatica and Cytryn (2013) [32], after reviewing numerous relevant studies, concluded that the use of treated wastewater for crop irrigation does not seem to have an effect on soil microflora, but further research should be carried out in order to investigate the horizontal gene transfer from antibiotic-resistant bacteria found in treated effluent to soil bacteria, so that a definitive conclusion on the topic can be made.

In regard to the environmental impacts, the degradation of soil quality, due to the increase in salinity and soil acidification (reduction of soil pH) [6], [17], [36], as well as the increase of soil hydrophobicity are reported [37], [38].

The use of treated wastewater on crops also contains some risks to public health, on account of the presence of pathogenic microorganisms, heavy metals and other potentially harmful substances in it. For example, the presence of viruses, protozoa and pathogenic bacteria could cause gastroenteritis, dysentery or typhoid fever, respectively [39].

An analysis of the main risk factors is made next:

Salts: The salinity level in treated urban wastewater is usually 1.5 to 2 times higher in comparison to drinking water. Furthermore, higher counts on the rates of sodium ions (Na+), chloride (Cl-) and bicarbonate (HCO3-) have been observed, condition which may pose danger to plants and the soil [16]. The irrigation of particular crops, such as maize, rice and industrial tomato, with high salinity water may, also, result in a yield reduction, that can approach 25% for corn [40].

Many studies demonstrate the effect of increased salinity on soil quality and on the development of cultivated plants. Generally, irrigation with recycled water can lead to intolerable salinity levels for most green-area and crop plants, especially in heavy soils [41].

Additionally, irrigation with treated urban wastewater can lead to serious problems in soil infiltration, due to the high sodium concentrations in comparison to the calcium and magnesium ion concentrations, which result in an increase of the Sodium Adsorption Relation (SAR) parameter [42]. It is reported, for example, that golf courses in the USA that were irrigated with recycled water showed higher electric conductivity values of the saturation extract (ECe) of about 187% and higher SAR values of about 481% [23].

The deposition of salts in the soil is influenced by many factors, such as the quality of the reused water, the irrigation method, the soil's properties and the plant's characteristics [41], [23]. Therefore, the risk of soil salinization varies depending on the characteristics of the reused water. Moreover, in some sensitive species, the contact of the foliage with chlorine and sodium ions may have toxic effects if the spray irrigation method is used.

Heavy metals: Heavy metals such as the arsenic (As), cadmium (Cd), copper (Cu), chromium (Cr), nickel (Ni), lead (Pb) and zinc (Zn) can be found in urban waste, but they can be removed to a large extent during sewage treatment. As a result, the concentrations of these elements in treated wastewater are insignificant and similar to those of fresh water [16].

Several studies have proved, however, the accumulation of heavy metals, like cadmium, nickel, chromium and lead in the soil and plants, when they are irrigated with treated urban wastewater [43], [44]. According to Gupta et al. (2010) [43], the presence of cadmium and chromium should raise even greater concern, as they accumulate in plant tissues, thus exposing consumers to risk. Kalavrouziotis and Drakatos studied the ability of some Mediterranean forest species to accumulate heavy metals from treated urban wastewater in their tissues and concluded that the tolerance of forest species in heavy metals from treated wastewater varies depending on the type of plant and this variable should, also, be taken into consideration during irrigation with treated wastewater so that toxicity is avoided [45].

Nutrients: The presence of high amounts of specific nutrients can cause a nutrient imbalance (such as the lack of phosphorus or potassium, for example) and a contamination of the groundwater with nitrates [13]. For example, the presence of high amounts of nitrogen in reused irrigation water renders it unsuitable for rice irrigation. In addition, excessive amounts of nitrogen result in extended vegetative growth at the expense of fruit yield maturation [46].

Contaminants: Many organic contaminants have been detected in soils irrigated with treated urban wastewater, such as polycyclic aromatic hydrocarbons, polychlorinated biphenyls and organochlorinated insecticides [11]. In addition, a cause for concern has also been the presence of pollutants, such as chemical substances that affect the endocrine system, pharmaceuticals and personal care products (PPCPs) which originate from drugs, veterinary drugs, fragrances and cosmetics. Many researchers believe that the presence of these substances will have an impact on soil and on human health [33]. Additionally, there is the risk of the potential impact of the aforementioned substances on ecosystems, with the increase of the environment's resistance to antibiotics being the most important risk of all [32].

Pathogens: Several studies have reported large populations of Total Coliforms (TC) and coliforms of intestinal origin in crop cultures that have been irrigated with treated urban wastewater [18], [26], [25], while other researchers have, also, detected pathogens of the genera Salmonella, Streptococci, Clostridium, Shigell, and Vibrio spp. [22]. Moreover, the presence of viruses, protozoa and helminthes, all of which are pathogenic for humans, has also been reported [53]. Mavridou et al., (2015) [39] reviewed the hazards of wastewater used for crop irrigation, based on bacterial indices, viruses and protozoa, and concluded that the hazard of wastewater is a function of its initial load, while its reduction extent varies depending on the treatment they undergo and on the number and type of the initial microbial load. Disinfection of wastewater by chlorination, ozonation or ultraviolet radiation has proved to have satisfactory results against microbial agents [48].

The evidence so far indicates that the spread of diseases due to irrigation with treated urban wastewater is rare, but has not been eliminated yet. In fact, it has been found to depend on various factors, beyond the microbiological quality of the treated wastewater, such as the type of plant in question, the irrigation method and the harvesting practices applied as well as a series of environmental factors (such as moisture and temperature) [16].

5. THE USE OF TREATED URBAN WASTEWATER FOR IRRIGATION OF CROPS IN GREECE

Greece is characterized by areas with a high water demand and limited water availability. Crop irrigation accounts for 86% of the total water demand and is followed by 11% for urban use, 2% for energy use and 1% for industrial use. Irrigation is predominant in the region of Thessaly, which presents a lack of water resources and in eastern Central Greece, while urban water use is predominant in Attica [8]. Reused water could significantly contribute to the irrigation of Thessaly and other regions of the country, it could cover the industrial needs in Western Macedonia as well as the firefighting needs throughout the country in summer months. Furthermore, studies on the qualitative

characteristics of treated urban wastewater conducted in the country have showed that its use to cover part of the irrigation needs is, indeed, possible [49], [40], [50].

Panoras et al. (2006b) [40] estimated the organic and inorganic load of the treated water effluent produced in the metropolitan area of Thessaloniki in order to investigate its use for crop irrigation in the Chalastra – Kalohori area, where crop cultures primarily include rice, and secondarily corn, cotton, sugar beet, alfalfa and industrial tomato, and concluded that the parameters determined render it appropriate for irrigation purposes. However, the high electrical conductivity value that was measured, which is directly related to the total concentration of salts in the water, urges for a rational use of the effluent as an irrigation resource [51].

Tsangarakis et al. (2004) [50] in a research on pilot wastewater treatment units in Crete observed that the treated effluent contained low concentrations of heavy metals, a characteristic they attributed to the absence of industrial units and the small population in the installation areas, and, also, relatively low electrical conductivity and total dissolved solids values.

Other Greek researchers have examined the effects of irrigation with treated urban wastewater on the characteristics of the growth of Mediterranean forest species [52] and other crops [40].

Successful small-scale water-reuse programs in Greece have been implemented in the past in Thessaloniki, Halkida, Crete and other areas[8]. For example, in the Chalastra – Kalohori region, 160,000 cubic meters of wastewater were channeled from the Wastewater Treatment Plant (WWTP) of Thessaloniki to a 12,000-acre cultivation area, following the appropriate treatment.

National legislation defined the conditions for the disposal of treated wastewater for irrigation from the WWTP of Thessaloniki with J.M.D. 141937 (2005), whereas the qualitative characteristics of wastewater destined for irrigation, the crops which may be used and the type of irrigation that may be applied are defined by Ministerial Decision 145116/2011 (Government Gazette 354/B/03.08.2011) [12].

6. CONCLUSION

This review attempted to synthesize the research findings of studies and research papers relative to the effects (positive and negative) of crop irrigation with treated urban wastewater.

The majority of the studies included in the present review show that irrigation with treated urban wastewater can have particularly beneficial effects on crops and especially on the increase of production (mainly through the increase in product yield).

However, specific limit values must be designated for the quality parameters of both wastewater and cultivated species – mainly in countries where there are no similar regulations- and actions should be taken so that the regular monitoring of the applied wastewater is ensured, something that will help to avoid the accumulation of pathogens and other substances in the soil and in crops.

It would be important for researchers to further investigate the maximum limits of the concentration values of heavy metals and other toxic substances that can be accumulated in soils and crops, so that the irrigation with treated urban wastewater can be planned in the long term for each crop and soil type.

In any cases, the effects of irrigation water produced through urban wastewater treatment are closely related to its qualitative characteristics prior to the application on a crop, or, in other words, the treatment it was subjected to previously. In addition, wastewater treatment does not always ensure the successful removal of all biological and chemical contaminants, which results in the transfer of organic matter and active substances in the soil environment (plants and soil), thus affecting, in various ways, both the soil's qualities and the ecosystem.

Therefore, it is important that wastewater be treated in equipped wastewater treatment plants, especially as far as non-technologically advanced countries are concerned, in order to reduce the harmful effects that irrigation with untreated urban wastewater can cause.

ACKNOWLEDGMENTS

The present research was carried out in the framework of the scholarship program "IKY FELLOWSHIPS OF EXCELLENCE FOR POSTGRADUATE STUDIES IN GREECE – SIEMENS PROGRAM" of the Greek Institute of State Scholarships (IKY), which I wish to sincerely thank for its support over the course of my post-graduate studies.

The present paper is the result of the development of a small segment of my Master's thesis, decided in collaboration with my supervising professor, Mrs. Kolokytha Elpida, Associate Professor in the Division of Hydraulics and Environmental Engineering of the Department of Civil Engineering, Faculty of Engineering of the Aristotle University of Thessaloniki, whom I wish to wholeheartedly thank for her overall contribution in the formation of this review.

REFERENCES

[1] FAO, *Crops and Drops: Making the Best Use for Agriculture*, 2002, FAO, Rome, Italy.
[2] Guardiola-Claramonte, M., Sato, T., Choukr-Allah, R., &Qadir, M., 2012, "Wastewater production, treatment and reuse around the Mediterranean region: current status and main drivers", In: *Integrated Water Resources Management in the Mediterranean Region* (pp. 139-174), Springer Netherlands.
[3] Levine, A.D. and Asano, T., 2004, "Recovering sustainable water from wastewater". Environmental Science and Technology, vol. 38, pp. 201A–208A.
[4] Pedrero, F., Kalavrouziotis, I., Alarcon, J.J., Koukoulakis, P. and Asano, T., 2010, "Use of treated municipal wastewater in irrigated agriculture—Review of some practices in Spain and Greece", Agricultural Water Management, vol. 97, pp.1233–1241.
[5] Pereira, B.F.F., He, Z.L., Silva, M.S., Herpin, U., Nogueira, S.F., Montes, C.R. and Melfi, A.J., 2011, "Reclaimed wastewater: impact on soil-plant system under tropical conditions", Journal of Hazardous materials, vol. 192, pp. 54–61
[6] Angin, I., Yaganoglu, P., and Turan, M., 2005, "Effects of long-term wastewater irrigation on soil properties", Journal of Sustainable Agriculture, vol. 26, pp. 31–42.
[7] Capra, A. and Scicolone, B., 2004, "Emitter and filter tests for wastewater reuse by drip irrigation", Agricultural Water Management, vol. 68, pp. 135–149.
[8] Koumartsiotou M., 2009, "Needs and water reuse in Greece", Postgraduate thesis, Interdisciplinary-Interdepartmental Postgraduate Studies (IPPS) "Environment and Development", NTUA
[9] California Water Planning, 2009, Department of Water Resources, State of California, 2009. Available at: http://www.waterplan.water.ca.gov/cwpu2009/index.cfm, Accesed: 29/11/2015
[10] Chang, D.H. and Ma, Z., 2012, "Wastewater reclamation and reuse in Beijing: influence factors and policy implications", Desalination, vol. 297, pp. 72–78.
[11] Cirelli, G.L., Consoli, S., Licciardello, F., Aiello, R., Giuffrida, F. and Leonardi, C., 2012, "Treated municipal wastewater reuse in vegetable production", Agricultural Water Management, vol. 104, pp. 163– 170.
[12] M.D. 145116/(2011) - Establishment of measures, conditions and procedures for the reuse of treated wastewater and other provisions (Government Gazette 354 / B / 03.08.2011).
[13] Candela, L., Fabregat, S., Josa, A., Suriol, J., Vigues, N. and Mas, J., 2007, "Assessment of soil and groundwater impacts by treated urban wastewater reuse. A case study: Application in a golf course (Girona, Spain)", Science of the Total Environment, vol. 374, pp. 26-35.
[14] Toze, S., 2006, "Reuse of effluent water—benefits and risks", Agricultural Water Management, vol. 80, pp. 140–159.
[15] Zhang, L. and Liu, Z., 1989, "A methodological research on environmental impact assessment of sewage irrigation region", Chinese Environmental Science, vol. 9, pp. 298–303
[16] Chen, W., Lu, S., Jiao, W., Wang, M., Chang, A.C., 2013, "Reclaimed water: A safe irrigation water source?", Environmental Development, vol. 8, pp. 74–83
[17] Kiziloglu, F., Tuean, M., Sahin, U., Angin, I., Anapali, O., and Okuroglu, M., 2007, "Effects of wastewater irrigation on soil and cabbage-plant (Brassica olereacea var. capitate cv. Yavola-1) chemical properties", Journal of Plant Nutrition and Soil Science, vol. 170, pp. 166–172.
[18] Akponikpe, P.B.I., Wima, K., Yacouba, H. and Mermoud, A., 2011, "Reuse of domestic wastewater treated in macrophyte ponds to irrigate tomato and eggplant in semi-arid West-Africa: benefits and risks", Agricultural Water Management, vol. 98, pp. 834–840
[19] Gwenzi, W., and Munondo, R., 2008, "Long-term impacts of pasture irrigation with treated sewage effluent on nutrient status of a sandy soil in Zimbabwe", Nutrient Cycling in Agroecosystems, vol. 82, pp. 197–207
[20] Kim, S., Park, S., Lee, J., Benham, B., and Kim, H., 2007, "Modeling and assessing the impact of reclaimed wastewater irrigation on the nutrition loads from an agricultural watershed containing rice paddy fields", Journal of Environmental Science and Health, Part A, vol. 42, pp. 305–315.
[21] Lubello, C., Gori, R., Nicese, F.P. and Ferrini, F., 2004, "Municipal-treated wastewater reuse for plant nurseries irrigation", Water Research, vol. 38, pp.2939–2947.
[22] Mañas, P., Castro, E., Heras J De las, 2009, "Irrigation with treated wastewater: effects on soil, lettuce (Lactuca sativa) crop and dynamics of microorganisms", Journal of Environmental Science and Health, Part A, vol. 44, pp. 1261–1273.
[23] Qian, Y.L. and Mecham, B., 2005, "Long-term effects of recycled wastewater irrigation on soil chemical properties on golf course fairways", Agronomy Journal, vol. 97, pp. 717–721
[24] Rezapour, S., and Samadi, A., 2011, " Soil quality response to long-term wastewater irrigation in inceptisols from a semi-arid environment", Nutrient Cycling in Agroecosystems, vol. 91, pp. 269–280
[25] Sacks, M., and Bernstein, N., 2011, "Utilization of reclaimed wastewater for irrigation of field-grown melons by surface and subsurface drip irrigation", Israel Journal of Plant Sciences, vol. 59, pp. 159–169.
[26] Cirelli, G.L., Consoli, S., Licciardello, F., Aiello, R., Giuffrida, F. and Leonardi, C., 2012, "Treated municipal wastewater reuse in vegetable production", Agricultural Water Management, vol. 104, pp.163– 170.

[27] Rusan, M. J. M., Sami, H. and Rousan, L., 2007, "Long term effect of wastewater irrigation of forage cropson soil and plant quality parameters", Desalination, vol. 215, pp. 143-152.
[28] Zema, D.A., Bombino, G, Andiloro, S. and Zimbone, S.M., 2012, "Irrigation of energy crops with urban wastewater: Effects on biomass yields, soils and heating values", Agricultural Water Management, vol. 115, pp. 55-65.
[29] Yi, L. L., Jiao, W. T., Chen, X. N., Chen, W. P., 2011, "An overview of reclaimed water reuse in China", Journal of Environmental Sciences, vol. 23(10), pp. 1585–1593
[30] Duncan, R.R., Carrow, R.N., Huck, M.T., 2009, Turfgrass and Landscape Irrigation Water Quality: Assessment and Management, CRC Press, Boca Raton, FL, USA.
[31] Jueschke, E., Marschner, B., Tarchitzky, J., Chen, Y., 2008, "Effects of treated wastewater irrigation on the dissolved and soil organic carbon in Israeli soils", Water Science Technology, vol. 57, pp. 727–733.
[32] Gatica, J., and Cytryn, E., 2013, "Impact of treated wastewater irrigation on antibiotic resistance in the soil microbiome", Environmental Science and Pollution Research International, vol. 20(6), pp. 3529–3538.
[33] Chen, W.P., Wu, L.S., Frankenberger, W.T.J. and Chang A.C., 2008, "Soil enzyme activities of long-term reclaimed wastewater irrigated soils", Journal of Environmental Quality, vol. 37, pp. 36–42
[34] Pan, N., Hou, Z.A., Chen, W.P., Jiao, W.T., Peng, C., and Liu W., 2012, "Study on soil enzyme activities and microbial biomass carbon in greenland irrigation with reclaimed water", Environmental Science, vol. 33, pp. 4081–4087.
[35] Martinez S, Perez-Parra J, Suay R., 2011, "Use of ozone in wastewater treatment to produce water suitable for irrigation", Water Resources Management, vol. 25, 2109–2124.
[36] Mohammad, M., and Mazahreh N., 2003, "Changes in soil fertility parameters in response to irrigation of forage crops with secondary treated wastewater", Communications in Soil Science and Plant Analysis, vol. 34, pp. 181–1294.
[37] Graber, E, Ben-Arie, O, and Wallach, R., 2006, "Effect of simple disturbance on soil water repellency determination in sandy soils", Geoderma, vol. 136, pp. 11–19.
[38] Tarchitzky, J., Lerner, O., Shani, U., Arye, G., Lowengart-Aycicegi, A., Brener, A., and Chen Y., 2007, "Water distribution pattern in treated wastewater irrigated soils: hydrophobicity effect", European Journal of Soil Science, vol. 58, pp. 573–588.
[39] Mavridou, A., Vantarakis, A., Smeti, E., Christopoulou, A.-M., Mplougoura, A., Schiejven, J., 2015, "Qualitative microbiological risk assessment for wastewater reuse for irrigation in Greece", e-Journal of Science & Technology, vol. 10(2).
[40] Panoras, C., Paraskevas, II., And Panoras, A., 2006b, "Investigation in the availability of Thermaikos Bay and reuse in agriculture of treated wastewater urban area of Thessaloniki". Hydrotechnica, E.Y.E., vol. 16, pp. 61-72.
[41] Palacios-Díaz, M.P. Mendoza-Grimón, V. Fernández-Vera, J.R. Rodríguez-Rodríguez, F. Tejedor-Junco, M.T. and Hernández-Moreno, J.M., 2009, "Subsurface drip irrigation and reclaimed water quality effects on phosphorus and salinity distribution and forage production", Agricultural Water Management, vol. 96, pp. 1659–1666
[42] Morugán-Coronado, A. García-Orenes, F. Mataix-Solera, J. Arcenegui, V. Mataix-Beneyto J., 2011, "Short-term effects of treated wastewater irrigation on Mediterranean calcareous soil", Soil and Tillage Research, vol. 112, pp. 18–26
[43] Gupta S, Satpati S, Nayek S, Garai D., 2010, "Effect of wastewater irrigation on vegetables in relation to bioaccumulation of heavy metals and biochemical changes", Environmental Monitoring and Assessment, vol. 165, pp. 169–177.
[44] Wang, Q., Cui, Y., Liu, X., Dong, Y., and Christie, P., 2006, "Soil contamination and plant uptake of heavy metals at polluted sites in China". Journal of Environmental Science and Health Part A, vol. 38, pp. 823–838.
[45] Kalavrouziotis, I.K. and Drakatos, P.A., 2002, "Irrigation of certain Mediterranean plants with heavy metals", International Journal of Environment and Pollution, vol. 18(3), pp. 294–300
[46] Shahalam A., Abu Zahra B.M. and Jeradat A., 1998, "Wastewater irrigation effect on soil, crop and environment: A pilot scale study at Irbid, Jordan", Water, Air, and Soil Pollution, vol. 106, pp. 425-445.
[47] Chen F, Ying G, Kong L, Wang L, Zhao J, Zhou L, Zhang L., 2011, "Distribution and accumulation of endocrine-disrupting chemicals and pharmaceuticals in wastewater irrigated soils in Hebei, China", Environmental Pollution, vol. 159, pp. 1490–1498.
[48] Hey G, Ledin A, la Cour JJ, Andersen H., 2012, "Removal of pharmaceuticals in biologically treated wastewater by chlorine dioxide or peracetic acid", Environmental Technology, vol. 33, pp. 1041–1047.
[49] Panoras, A., Eugenides, C., Bladenopoulou, S., Mellidou, B., Doitsinis, A., Samaras, I., Zdragkas, A., Panoras, C., 2006a, "Reuse of treated sewage for irrigation of maize", Hydrotechnica, E.Y.E., vol. 16, pp. 21-32.
[50] Tsagarakis, K.P., Dialynas, G.E. and Angelakis, A.N., 2004, "Water resources management in Crete (Greece) including water recycling and reuse and proposed quality criteria", Agricultural water management, vol. 66 (1), pp. 35-47.
[51] Panoras, A., Elias, A., 1999, Irrigation with treated urban waste water, Ed. Giachoudi - Giapoulis, Thessaloniki, 190 p.

[52] Mavrogianopoulos, G. and Kyritsis, S., 1995, Use of municipal wastewater for biomass production. Project report of Agricultural University of Athens.
[53] Qadir, M., Wichelns, D., Raschid-Sally, L., McCornick, P., Drechsel,P. Bahri, A. and Minhasf, P., 2010, "The challenges of wastewater irrigation in developing countries", Agricultural Water Management, vol. 97, pp. 561-568.

ISSN: 2458-8156

Journal Home page : http://dergipark.ulakbim.gov.tr/ejens * E-mail : editor@cnrgroup.eu

hosted by Turkish JournalPark ACADEMIC

EJENS

European Journal of Engineering and Natural Sciences CODEN: EJENS

Determination of the Effects of Operating Parameters on the Residual Turbidity of Quartz Suspensions by Design of Experiments

Adem Tasdemir[1]*, Tuba Tasdemir[1]*

[1]*Eskişehir OSmangazi University, Department of Mining Engineering, Division of Mineral Processing, 26480, Bati Meselik/Eskişehir Turkey.*

**Corresponding Author email: atasdem@ogu.edu.tr, tubat@ogu.edu.tr*

Publication Info

Paper received:
10 December 2015

Revised received:
15 December 2015

Accepted:
18 December 2015

Abstract

This research represents the results of flocculation of quartz particles in suspensions with an anionic flocculant by applying response surface method (RSM). The experiments were designed and carried out according to the Bohn-Behnken Design (BBD) which is a type of RSM. A BBD with five independent parameters at three levels was applied to jar test studies to investigate the effect of variables examined on quartz flocculation process. Flocculant dosage, rapid mixing time, rapid mixing rate, solid ratio and settling time were tested to evaluate the main and interaction effects of these factors on residual turbidity. An empirical quadratic model with a high correlation coefficient was obtained for the estimation of residual turbidity within the investigated ranges of parameters.

Key words

Quartz suspension, Flocculation, Response surface method, Box-Behnken Design

1. INTRODUCTION

Dewatering is a process identified as a part of solid/liquid separation and is an important process in most mineral processing operations. Generally, dewatering is accomplished by sedimentation or filtration ([1], [2]). Aggregation of fine particles in mineral suspensions can be carried out by applying methods such as coagulation, flocculation or agglomeration methods [3]. Knowledge of detailed information while applying an aggregation method on a special material are necessary to understand the mechanisms and to use less possible amount of reagents during the processes.

Flocculation is usually a necessary pretreatment step in many dewatering streams containing significant quantity of very fine particles. The purpose of flocculation is to form aggregates or flocs from finely dispersed particles with the help of long chain polymers which are referred to as flocculants. Flocculation of suspended particles by polymeric flocculants is a multistep process. A classical coagulation/flocculation process consists of three separate steps: i) Rapid or flash mixing: the suitable chemicals (coagulants/flocculants and if required pH adjusters) are added to the wastewater stream, which is intensively mixed at high speed. ii) Slow mixing (coagulation and flocculation): the wastewater is only moderately stirred in order to form large flocs, which are easily settled out. iii) Sedimentation: the floc formed during flocculation is allowed to settle out and is separated from the effluent stream ([4], [5]).

In a flocculation process applied, finding the optimum flocculation conditions is a very important entity. The flocculation of fine particle suspensions is a complex process and the effectiveness of the process depends not only on the usage of appropriate chemical reagents (coagulants, flocculants, etc.) but also on how they are applied. Flocculation is affected by the complex interactions between a numbers of factors. These factors may

include slurry properties such as particle size and surface charge of particles, solution chemistry, pH and physical variables such as mixing intensity (rate), mixing time and settling time. Each of them determines the flocculation rate and efficiency in term of settling rate, supernatant turbidity and sediment volume ([6], [7]). Therefore, determination of the flocculation behavior of the suspensions is important for an efficient solid/liquid separation. Jar test is one of the most efficient and commonly used methods to determine optimum flocculation conditions.

Classical jar test experiments are usually carried out by systematically chancing the level of one factor at a time (OFAT). In OFAT jar test experiments, optimum flocculation conditions are determined by varying a single factor while holding the level of the other factors constant [8]. The level of the factor that results in the best response (e.g. lowest residual turbidity) is then selected and used in subsequent tests which continue in the same manner for other factors [9]. But it is time consuming and does not fully explore the whole experimental space to find the best factors' conditions. Also, it is incapable of identifying the interaction effects resulting from the factors being considered. The classical jar test experiments of OFAT and studying the effect of the variable on the response is a complicated technique, particularly in a multivariate system as in the case of flocculation or if more than one response are of importance. Design of experiments (DOE) is statistical techniques which can be used for optimizing such multivariable systems. For these reasons, DOE has been proposed for the jar tests to overcome the shortcomings and to determine the influences of individual factors and their interactive influences.

The response surface methodology (RSM) which is a combination of experimental, regression analysis and statistical inferences is one of the DOE approach. It is useful for modeling and analyzing problems in which responses of interest are influenced by several factors or variables and in which objective is to optimize the responses. The RSM not only reduces the cost and time, but also provides required information about the interaction effects with minimum number of experiments [10].

There are many scientific works investigating effect of slurry properties such as flocculant dosage, pH on flocculation in the literature ([11]-[21]). However, fewer researches exist about the mixing conditions on flocculation ([4], [21]-[26]). The effect of mixing conditions under constant slurry properties on residual turbidity for the flocculation of quartz sample with anionic flocculant used in this work have been investigated recently by us [25]. Results of this study showed that the effect of rapid mixing rate and time are more important factors compared to slow mixing rate, slow mixing time and settling time. We have also previously examined the effect of slurry properties (flocculant dosage, pH and solid ratio) at constant mixing and settling conditions on residual turbidity for the same material [13]. According to this research, the efficiency of quartz flocculation was dependent to a large extent pH of the suspensions and the excellent results were obtained at alkaline media. However, the results at natural pH were not good compared to acidic or alkaline suspensions. Interaction between solid ratio and flocculant dosages on residual turbidity of suspensions were found to be significant in all pH values tested.

In this study, the effects of five independent variables which include the slurry and mixing conditions of flocculation process namely, flocculant dosage, rapid mixing rate, rapid mixing time, solid ratio and settling time on the flocculation behavior of quartz suspensions were investigated at natural pH of the suspensions. Since numerous numbers of experiments are needed to research the effects of five variables tested, the efficiency of flocculation under tested conditions was determined to examine the main and interaction effects between these variables by the application of five parameter Box-Benhken design (BBD).

2. EXPERIMENTAL

2.1 Materials and Method

A pure quartz sample from Çine region of Turkey was obtained and used in the experiments. The particle size of the sample was less than 20 μm sieve aperture. According to the particle size distribution determined by Malvern Mastersizer 2000, d_{90}, d_{50} and d_{10} diameters were obtained as 15.7 μm, 2.2 μm and 0.6 μm respectively. According to the XRD results all the peaks belonged to quartz and the sample contains more than 95.6 % SiO_2 content indicating that the sample is pure enough. The quartz sample which may causes pollution was chosen as a pollutant material since it is considered as one of the common components present in soils and clays [27].

SPP 508 (supplied from Superkim, Turkey) polymer was used for the flocculation of synthetically prepared fine quartz suspensions. Medium anionic SPP 508 is a high molecular weight (15-22x10^6 g/mol) polyacrylamide with 28% degree of ionization. A solution of polymer (0.01%) was prepared using distilled water. The pH of the solutions was not changed during the experiments and held constant at its natural pH. The neutral pH of samples was determined as 7.95 for all solid ratios by a pH-meter (Orion 5 Star).

A jar test apparatus (Velp Scientifica FC6S) was used in order to determine the effectiveness of flocculant in the experimental conditions tested. It consists of a set of six beakers, which can be stirred simultaneously at

specified speed. The flocculation tests consisted of three stages. First, the flocculant was added to the suspension and a rapid mixing was initiated. The objective is to obtain complete mixing of the flocculant with the suspension to maximize the effectiveness of destabilization of colloidal particles and initiate flocculation. Critical parameters for this stage are the rapid mixing time (duration) and the rapid mixing rate (intensity). Second, the suspension was slowly stirred to increase contact between flocculating particles and to facilitate the development of large flocs. In each experiment, a 10 minute slow mixing at 30 rpm was applied. Finally, mixing was terminated. The flocs are allowed to settle at predetermined settling times and then the turbidity of the supernatants was measured.

The turbidimeter (HF Scientific) was used to measure the residual turbidity. The turbidity is expressed in NTU (Nephelometric turbidity units). The initial turbidity of the samples were determined as 306 NTU for 0.1% solid ratio sample, 2496 NTU for 0.55% solid ratio sample and 4400 NTU for 1.0% solid ratio sample.

2.1 Design of Experiments

The surface response method RSM, using the Box-Behnken experimental design, yielded correlations between the residual turbidity of quartz suspensions and the five independent factors. The RSM involves an empirical model to evaluate the relationship between a set of controllable experimental factors and observed results. Factors considered included the flocculant dosage (mg/l), rapid mixing time (min), rapid mixing rate (rpm), solid ratio (%) and settling time (min). They are represented by *A* to *E*, respectively. The low, middle and high levels of each variable were designated as -1, 0 and +1 respectively, as listed in Table 1.

Table 1. Factors and levels for experimental design using BBD

Variables	**Ranges and coded levels**		
	-1	**0**	**+1**
A: Flocculant dosage (mg/l)	0.02	0.41	0.80
B: Rapid mixing time (min)	1	3	5
C: Rapid mixing rate (rpm)	100	200	300
D: Solid ratio (%)	0.1	0.55	1.0
E: Settling time (min)	5	15	25

The experiments were carried out according to the BBD which is given in Table 2. The independent variables and the mathematical relationship between the response Y and these variables can be approximated by a quadratic polynomial equation (1):

$$Y = b_0 + b_1A + b_2A + b_3A + b_4A + b_5A + b_{12}AB + b_{13}AC + b_{14}AD + b_{15}AE + b_{23}BC + b_{24}BD + b_{25}BE + b_{34}CD + b_{35}CE + b_{45}DE + b_{11}A^2 + b_{11}B^2 + b_{33}C^2 + b_{44}D^2 + b_{55}E^2 \quad (1)$$

Where; Y is the predicted response variable (turbidity), b_0 is the model constant, $b_1 - b_5$ linear coefficients, b_{12}, b_{13}, b_{14}, b_{15}, b_{23}, b_{24}, b_{25}, b_{34}, b_{35}, and b_{45} are the cross product coefficients and b_{11}, b_{22}, b_{33}, b_{44} and b_{55} are the quadratic coefficients [28]. Factors and levels and Box-Behnken design of five experimental variables in coded units are given in Table 1 and Table 2 respectively.

Table 2. Box-Behnken design of five experimental variables in coded units

Run	**Factors**					**Run**	**Factors**				
	A	**B**	**C**	**D**	**E**		**A**	**B**	**C**	**D**	**E**
1	-1	-1	0	0	0	24	0	-1	-1	0	0
2	1	-1	0	0	0	25	0	1	-1	0	0
3	-1	1	0	0	0	26	0	-1	1	0	0
4	1	1	0	0	0	27	0	1	1	0	0
5	0	0	-1	-1	0	28	-1	0	0	-1	0
6	0	0	1	-1	0	29	1	0	0	-1	0
7	0	0	-1	1	0	30	-1	0	0	1	0

8	0	0	1	1	0	31	1	0	0	1	0
9	0	-1	0	0	-1	32	0	0	-1	0	-1
10	0	1	0	0	-1	33	0	0	1	0	-1
11	0	-1	0	0	1	34	0	0	-1	0	1
12	0	1	0	0	1	35	0	0	1	0	1
13	-1	0	-1	0	0	36	-1	0	0	0	-1
14	1	0	-1	0	0	37	1	0	0	0	-1
15	-1	0	1	0	0	38	-1	0	0	0	1
16	1	0	1	0	0	39	1	0	0	0	1
17	0	0	0	-1	-1	40	0	-1	0	-1	0
18	0	0	0	1	-1	41	0	1	0	-1	0
19	0	0	0	-1	1	42	0	-1	0	1	0
20	0	0	0	1	1	43	0	1	0	1	0
21	0	0	0	0	0	44	0	0	0	0	0
22	0	0	0	0	0	45	0	0	0	0	0
23	0	0	0	0	0	46	0	0	0	0	0

3. RESULTS AND DISCUSSIONS

3.1 Model Fitting

The residual turbidity values obtained and predicted by the BBD model in each experiment are presented in Table 3. Analysis of the Box-Cox plots showed that residuals could be reduced significantly by a log transformation since the residual turbidity values has broad range of response from 3.3 to 62 NTU.

The Box-Cox plot provides a guideline for selecting the correct power law transformation ($y' = y^{\lambda}$). For this reason, the dependent variable produced after transformation transformation was named as Ln (Turbidity).

Table 3. Response results and predicted turbidities in supernatants

	Turbidity		**Ln of Turbidity**			**Turbidity**		**Ln of Turbidity**	
Run	**Obs.**	**Pre.**	**Obs.**	**Pre.**	**Run**	**Obs.**	**Pre.**	**Obs.**	**Pre.**
1	57	48.13	4.04	3.84	24	19.2	25.79	2.95	3.12
2	38	26.15	3.64	3.34	25	7.5	6.31	2.01	1.86
3	27	32.90	3.3	3.27	26	3.5	10.42	1.25	1.83
4	11	13.93	2.4	2.28	27	3.3	2.44	1.19	1.45
5	14	16.76	2.64	2.86	28	9.3	22.97	2.23	3.06
6	19.8	13.79	2.99	2.54	29	21.7	36.04	3.08	3.81
7	15	20.71	2.71	2.93	30	62	53.82	4.13	4.10
8	7.5	4.44	2.01	1.56	31	7.3	-0.21	1.99	1.86
9	16	19.63	2.77	2.71	32	18.5	13.86	2.92	2.56
10	5	5.66	1.61	1.91	33	3.8	3.30	1.34	1.62
11	15	19.38	2.71	2.75	34	17	12.92	2.83	2.49

12	4.5	5.91	1.5	1.91	35	4.2	4.23	1.44	1.73
13	53	47.39	3.97	3.98	36	34	35.95	3.53	3.41
14	19	19.46	2.94	3.18	37	16.3	14.47	2.79	2.63
15	31.6	30.31	3.45	3.08	38	32.5	34.94	3.48	3.39
16	12.5	17.29	2.53	2.39	39	16.8	15.47	2.82	2.69
17	17.2	15.18	2.84	2.84	40	32	24.55	3.47	3.00
18	7.9	10.68	2.07	2.20	41	16	4.52	2.77	2.07
19	17.2	13.38	2.84	2.68	42	8.9	15.55	2.18	2.44
20	11.5	12.48	2.44	2.42	43	5.5	8.13	1.7	1.73
21	4.6	6.69	1.52	1.78	44	7	4.29	1.95	1.59
22	4.6	6.69	1.53	1.78	45	7.2	4.29	1.97	1.59
23	4.8	6.69	1.57	1.78	46	4.8	4.29	1.57	1.59

After evaluation of experimental results, a quadratic function for the residual turbidity in terms of coded factors was obtained with a determination coefficient of 0.84 (R^2) and hence correlation coefficient of 0.9165 (R) as:

$$Ln(Turbidity) = 1.68 - 0.37A - 0.41B - 0.42C - 0.23D + 0.012E - 0.12AB + 0.03AC - 0.75AD + 0.02AE + 0.22BC + 0.05BD - 0.01BE - 0.26CD + 0.04CE + 0.09DE + 1.15A^2 + 0.25B^2 + 0.23C^2 + 0.47D^2 + 0.29E^2 \quad (2)$$

According to this result, the 84 % of the variance can be explained by Eq. 2 and 16% of the variance could not be defined by the model.

3.2 Main Effects of Parameters

The main effect of individual variables of *A, B, C, D* and *E* and the perturbation plot which shows the comparison of all factors are plotted in Fig. 2 (a-e) and Fig. 2(f) respectively. In Fig. 2 (a-f), the log transformed residual turbidity is plotted by changing only one factor over its range while the others held constant at their center points. Therefore, both individual and perturbation plots show the main effects of these parameters on residual turbidity at center points of parameters. All individual variables were found to have their own important effect of residual turbidity.

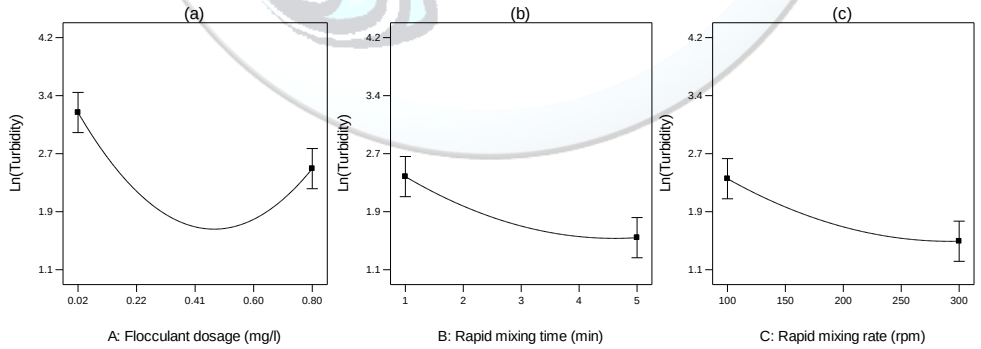

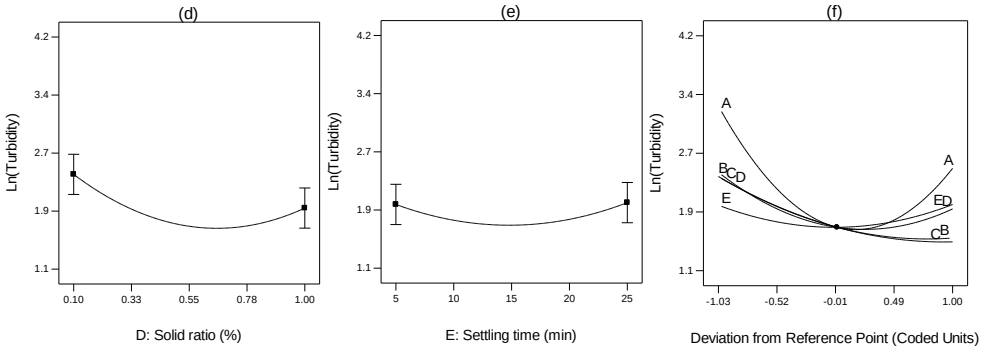

Figure 2. Main effects of flocculation variables (a-e) and perturbation plot for the response (f). For each factor, the remaining factors have held at their middle levels.

It is seen that variables have a curvature effect indicating that the turbidity removal by quartz flocculation within the investigated ranges of variables could be adequately explained by a second order model used in this study. Since the flocculation is considered as a second order rate process, the quadratic model by BBD can adequately describe the flocculation of quartz suspensions within the ranges of variables tested. According to the main effects plots in Fig. 2, the flocculant dosage, *A*, was the most effective parameter (Fig. 2.a). Initially, the residual turbidity decreases as the increasing of *A* and thereafter again increases. Altered rapid mixing time (*B*) and rapid mixing rate (*C*) affect the residual turbidity. An increase in these operating variables results in an improvement supernatant turbidity as seen in Fig 2 (b-c). While keeping the all parameters at their middle values, solid ratio had a quadratic effect on residual turbidity as shown in Fig. 2(d). Settling time (*E*) had less a little curvature effect on the response (Fig. 2.e). However, it is not very significant statistically in the investigated range.

3.3 Interactions Between Factors

Figure 3 (a-i) shows the second order interactions among the factors and curvature effects as predicted by the second order model. The log transformed residual turbidity is plotted by changing only one factor over its range while the others held constant at their center points in Fig. 3 (a-i). It should be noted that the response variable values plotted as a function of one operating parameter over a range of values and the other parameter at two levels indicate the parameter interaction effects. In other words, lines in parallel indicate no parameter interaction effects between the two variables considered. Fig. 3 shows that there are no significant interactions between the variables represented on these plots. The most efficient interaction was found between flocculant dosage (*A*) and solid ratio (*D*) and it is given in Fig. 4. However, we can see that altered the process variables from their low values to high values affect the responses significantly (Figs. 3.a, 3.b, 3.d, 3.e and 3.g). On the other hand, changing settling time from 5 min. to 25 min. did not affect the responses considerably since the flocs quickly settle out within the first 5 minute (Figs. 3.c, 3.f, 3.h and 3.i).

In the interaction plots presented in Fig. 3, we can see the effect of rapid mixing rate and time on the residual turbidity of quartz suspensions achieved. In Fig. 3(a, b, d, e, f, g and h) it can be seen clearly that increasing rapid mixing rate from 100 to 300 rpm and increasing the rapid mixing time from 1 to 5 minutes reduces the supernatant turbidities of quartz suspensions. These plots indicate that higher turbidity removal can be achieved by keeping the rapid mixing time and rate at their maximum values when the other variables held constant at their middle values. The first stage of flocculation process is to add the flocculant to the suspension and then a rapid and high intensity mixing is initiated. Reference [7] states that the initial mixing intensity and the mixing time are the most important parameters in the determining the size of the flocs formed and rapid mixing conditions can have major effects on the flocculation process [7]. The flocculants are usually added as fairly concentrated and viscous solutions during the flocculation process. Therefore, intense mixing is needed to achieve rapid and uniform distribution of the polymer molecules throughout the suspension [29]. The objective is to obtain complete mixing of the flocculant with the suspension to maximize the effectiveness of destabilization of suspended particles. The effects of fast stirring rate on flocculation process are well known and some detailed studies have been carried out ([22]-[26]). Reference [7] showed that the poor performance of a flocculation process in the many applications could be attributed to inadequate mixing [6]. If the fast mixing rate is not enough, the flocs are hardly grow and longer flocculation time is required. Insufficient mixing can also

lead to local overdosing and restabilization of some particles, which is responsible for the residual haze in suspensions ([22]-[24]). On the contrary, too high intensity of mixing rate and long mixing time may cause breakup of flocculated flocs and this may cause detrimental effects on flocculation [30]. According to Fig. 3d, at constant solid ratio, flocculant dosage and settling time, more stirring time is required at low stirring rate of 100 rpm to achieve the same turbidity in the supernatant solution. However, at highest stirring rate of 300 rpm, residual turbidity remains almost constant after 3 min fast mixing time.

The effects of fast mixing rate/time and solid ratio on residual turbidity are shown in Fig. 3e and 3g when the other variables held constant at their midpoints. As seen in these plots, there are no clear interactions between rapid mixing rate-solid ratio and rapid mixing time-solid ratio parameters. Increasing rapid mixing time decreases the residual turbidity for all solid ratios but it has a more pronounced effect for the higher solid ratio at constant mixing rate of 200 rpm, flocculant dosage of 0.41 mg/l and settling time of 15 minutes (Fig. 3e). In addition, higher turbidity removal was achieved with increasing rapid mixing time from 1 min. to 5 min. Confirming these findings, it was shown that the effects of mixing conditions are much more apparent for suspensions with higher solid concentrations ([22], [23],[26]). Also, these findings confirmed that flocculation is a second order rate process and flocculation rate depends on the square of particle concentration [29]. These may due to the higher collision probability which causes adsorption of flocculant molecules onto particle surfaces and flocculation of particles for the higher particle concentrations. It is possible to achieve the same turbidity values at rapid mixing rate of 100 rpm for all solid concentrations but less turbidity are accomplished by increasing the mixing rate for the solid ratio of 1.0% while the residual turbidity values remain almost constant for the solid ratio of 0.1% (Fig. 3g).These results may be attributed to the increase in collision probability between the quartz particles and flocculant at higher solid concentrations [30].

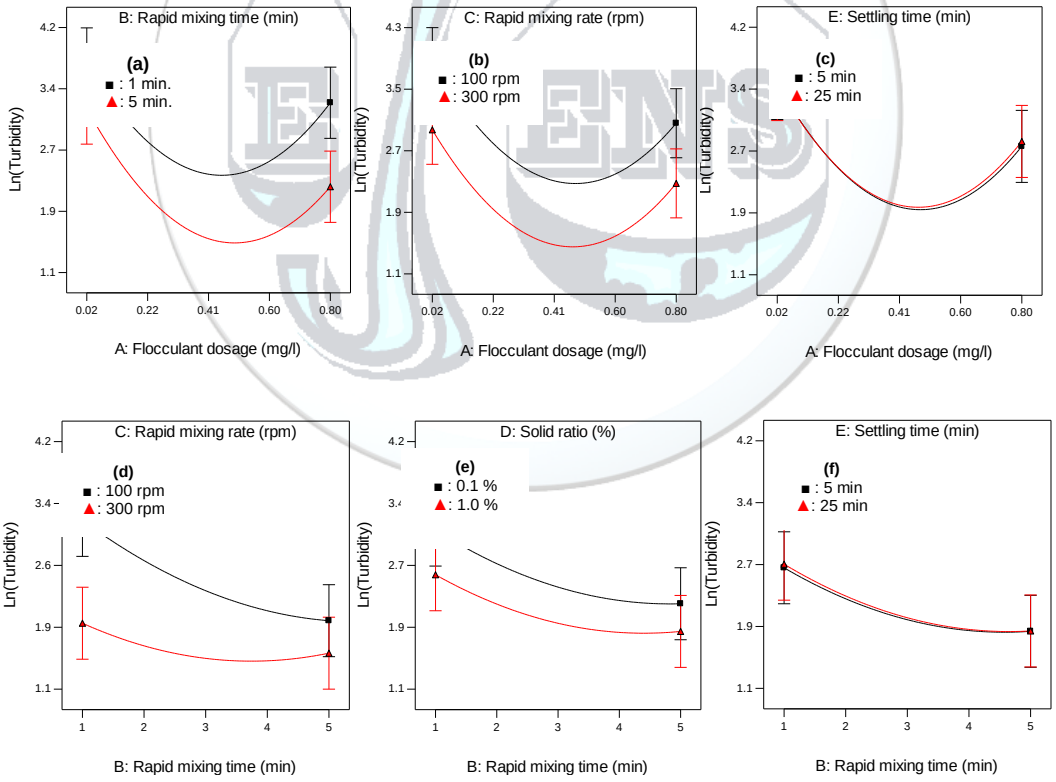

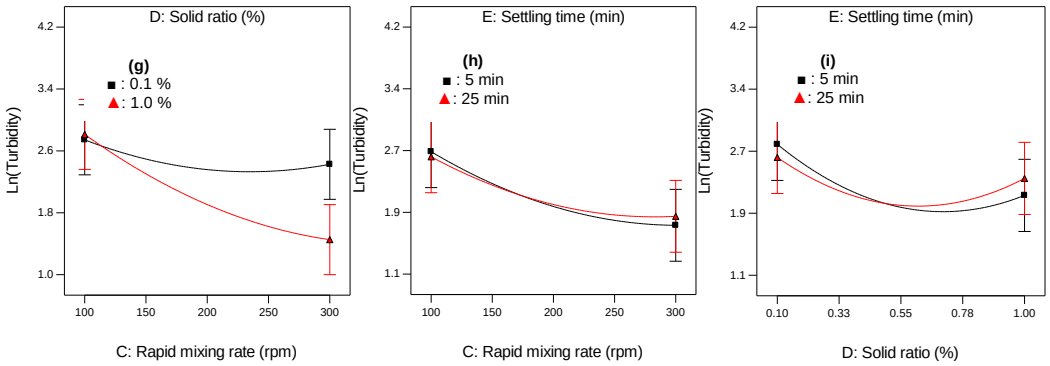

Figure 3. Interaction plots showing effects of flocculation parameters on residual turbidity. For each pair of factors, the remaining factors have held at their midpoint values.

The effects of flocculant dosage and solid ratio on residual turbidity while keeping the other variables at their midpoint levels are shown on the interaction and contour plots in Fig. 4.

As seen from these plots, there is an important interaction between the solid ratio and flocculant dosages. The residual turbidity is decreased with increasing flocculant dosages then increases again after a critical flocculant dosage for the both low and high solid ratio. As seen, less amount of flocculant is sufficient for the solid content of 0.1%. It is well known from the literature that, the optimum polymer dosage generally increases proportionally when particle concentration increases [29]. These critical flocculant dosages indicate the half surface coverage point described by References [2] and [31]. Excess amount of flocculant higher than optimum dosages starts to reverse effect on the residual turbidity for all solid concentrations. In Fig. 3a and 3b, we can see similar effect of flocculant dosage with rapid mixing speed and time and on the supernatant turbidity at constant solid ratio of 0.55% and settling time of 15 minutes. In these figures, residual turbidity decreases with increasing of flocculant dosage up to an optimum dosage and then increase again with over dosage of flocculant.

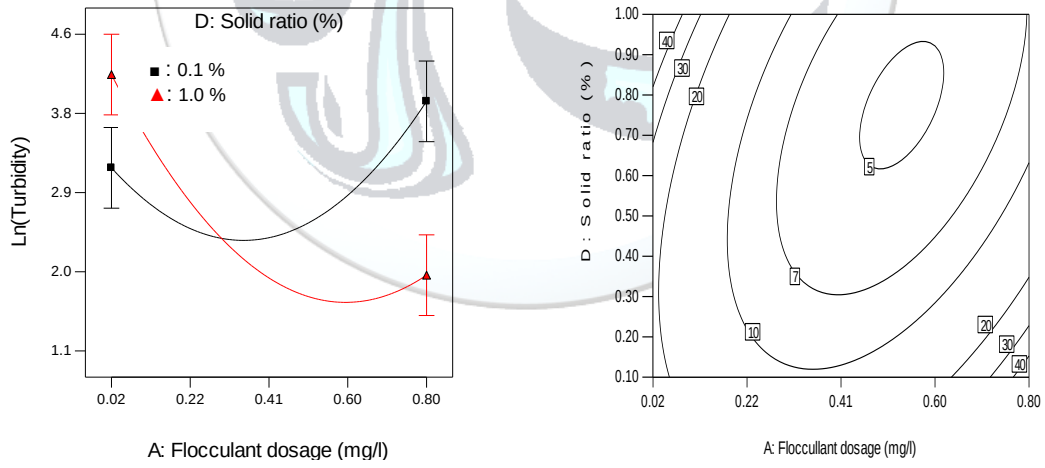

Figure 4. Interaction graph (left) and contour plot (right) of residual turbidity showing effect of solid ratio and flocculant dosage. The other variables are held constant at their midpoint levels.

3.4 Simplified Model for Residual Turbidity

Since some terms of the model in Eq. (2) do not statistically significant at 95% significance level, removal of them did not chance the R^2 significantly and a simpler model containing less parameter was obtained for estimating the residual turbidity. The other model terms in Eq. 3 were obtained after removing the insignificant terms (Prob >F more than 0.1) in Eq. 2 for the model improvement by applying backward elimination procedure.. Final second order equation in terms of coded factors for the supernatant turbidity estimation was obtained as:

$$Ln(Turbidity) = 1.68 - 0.37A - 0.41B - 0.42C - 0.23D + 0.012E - 0.75AD + +1.15A^2 + 0.25B^2 + 0.23C^2 + 0.47D^2 + 0.29E^2 \quad (3)$$

According to the interaction effect analysis, flocculant dosage and solid ratio (*AD*) on supernatant turbidity were found statistically significant compared to other interactions between variables. The determination coefficient, R^2, hence correlation coefficient, *R*, were calculated to be 0.82 and 0.9055 respectively.

4. CONCLUSIONS

Flocculation is defined as a second order rate process. This study confirmed the quadratic effects of investigated parameters on the residual turbidity of quartz suspensions resulted from jar test of flocculation process and showed that the mixing conditions (rapid mixing rate and time) and flocculant dosage had a great influence on the flocculation process. The second order equation obtained from the BBD method can be used to determine the optimum flocculation conditions of quartz suspensions within the investigated ranges of variables.

The second order effect of flocculant dosage (A^2) was found to be the most significant factor to have the largest effect on supernatant turbidity and this was followed by the linear effect of rapid mixing rate (*C*), linear effect of rapid mixing time (*B*), the two level interactions between flocculant dosage and solid ratio (*AD*), the linear effect of flocculant dosage (*A*), the second order effect of solid ratio (D^2). Moreover the main effect of solid ratio (*D*), the second order effect of settling time (E^2), the second order of rapid mixing time (B^2) and the second order of rapid mixing time (C^2) were determined to affect the residual turbidity of suspensions. It should be realized that this order of significance is valid strictly within the range of parameter values tested in this study.

ACKNOWLEDGEMENT

This study presents preliminary results of a project supported by Scientific Research Projects Committee of Eskişehir Osmangazi University (Project No: 200815020).

REFERENCES

[1]. R. Hogg, "Flocculation and dewatering," *International Journal Mineral Processing*, vol. 58, pp. 223-236, 2000.

[2]. T. Tripathy and De, B. Ranjan, "Flocculation : A New Way to Treat the Waste Water," *Journal of Physical Sciences*, vol. 10, pp. 93-127, 2006.

[3]. A. Özkan, H. Uçbeyiay, and S. Düzyol, "Comparison of stages in oil agglomeration process of quartz with sodium oleate in the presence of Ca (II) and Mg(II) ions," *Journal of Colloid and Interface Science*, vol. 329, pp. 81-89, 2009.

[4]. J. M. Ebeling, P. L. Sibrell, S. R. Ogden and S. T. Summerfelt, "Evaluation of chemical coagulation-flocculation aids for the removal of suspended solids and phosphorus from intensive recirculating aquaculture effluent discharge," *Aquacultural Engineering*, vol. 29, pp. 23-42, 2003.

[5]. M. Rossini, J. Garrido and M. Garcia Galluzzo, "Optimization of the coagulation-flocculation treatment influence of rapid mix parameters," *Water Research*, vol. 33(8), pp. 1817–1826, 1999.

[6]. Ü. İpekoğlu, *Dewatering and Methods*, İzmir, Turkey: Dokuz Eylül University, Mining Faculty Impress, No: 179, 1997.

[7]. J. Gregory, *Particles in Water: Properties and Process*, London, United Kingdom: University College, 2005.

[8]. T. K. Trinh, and L. S. Kang, "Application of response surface method as an experimental design to optimize coagulation tests," *Environmental Engineering Research*, vol. 15(2), pp. 63-70, 2010.

[9]. M. Zainal-Abideen, A. Aris, F. Yusof, Z. Abdul-Majid, A. Selamat, and S. I. Omar, "Optimizing the Coagulation Process in A Drinking Water Treatment Plant-Comparison Between Traditional and Statistical Experimental Design Jar Tests," *Water Science & Technology*, pp. 496-503, 2012.

[10]. J. P. Wang, Y. Z.Chen, X. W. Ge, H. Q. Yu, "Optimization of coagulation-flocculation process for a paper-recycling wastewater treatment using response surface methodology," *Colloids and Surfaces A: Physicochem. Eng. Aspects*, vol. 302, pp. 204-210, 2007.

[11]. T. Taşdemir, and H. Kurama, "Fine Particle Removal from Natural Stone Processing Effluent by Flocculation," *Environmental Progress&Sustainable Energy*, vol. 32(2), pp. 317-324, 2013.

[12]. E. Sabah, and C. Açıksöz, "Flocculation Performance of Fine Particles in Travertine Slime Suspension," *Physicochemical Problems of Mineral Processing*, vol. 48(2), pp. 555-566, 2012.

[13]. A. Taşdemir, T. Taşdemir, and H. Kılıç, "Usage of Box-Behnken Experimental Design for The Flocculation of Quartz Suspensions," in *Proc. The 14th Balkan Mineral Processing Congress*, 2011, pp. 250-256.

[14]. E. Sabah, and Z. E. Erkan, "Interaction mechanism of flocculants with coal waste slurry," *Fuel*, vol. 85, pp. 350-359, 2006.

[15]. A. Sworska, J. S. Laskowski, G. Cymerman, "Flocculation of the Syncrude fine tailings Part I. Effect of pH, polymer dosage and Mg^{2+} and Ca^{2+} cations," *International Journal of Mineral Processing*, vol. 60, pp. 143–152, 2000.

[16]. P. Somasundaran, and S. Krishnakumar, "Adsorption of surfactants and polymers at the solid-liquid interface," *Colloids Surfaces A: Physicochemical and Engineering Aspects*, pp. 491-513, 1997.

[17]. M.L. Taylor, G.E. Morrıs, P.G. Self, and R.St.C. Smart, "Kinetics of Adsorption of High Molecular Weight Anionic Polyacrylamide onto Kaolinite: The Flocculation Process," *Journal of Colloid and Interface Science*, vol. 250, pp. 28–36, 2002.

[18]. J.M. Henderson, and A.D.Wheatley, "Factors Affecting the efficient flocculation of tailings by polacrylamides," *Coal Preparation*, vol. 1987(4), pp. 1-49, 2007.

[19]. X. Yu, and P. Somasundaran, "Role of Polymer Conformation in Interparticle-Bridging Dominated Flocculation," *Journal of Colloid and Interface Science*, vol. 177, pp. 283-287, 1996.

[20]. L. Besra, D. K. Sengupta, S. K. Roy, and P. Ay, "Influence of polymer adsorption and conformation on flocculation and dewatering of kaolin suspension," *Separation and Purification Technology*, vol. 37, pp. 231-246, 2004.

[21]. B. Ersoy, "Effect of pH and polymer charge density on settling rate and turbidity of natural stone suspensions," *International Journal of Mineral Processing*, vol. 75, pp. 207 – 216, 2005.

[22]. J. Gregory, and L. Guibai, "Effects of dosing and mixing conditions on polymer flocculation of concentrated suspensions," *Chemical Engineering Communications*, vol. 108, pp. 3-21, 1991.

[23]. M.M. Nourouzi, T.G. Chuah, and T.S.Y. Choong, "Optimization of flocculation process for cut-stone wastewater Effect of rapid mix parameters," *Desalination and Water Treatment*, vol. 22, pp. 127-132, 2010.

[24]. M. A. Yukselen, and J. Gregory, "The effect of rapid mixing on the break-up and re-formation of flocs," *Journal of Chemical Technology and Biotechnology*, vol. 79, pp. 782–788, 2004.

[25]. T. Taşdemir, and A. Taşdemir, "Effect of Mixing Conditions on Flocculation" in *Proceedings of XIIIth International Mineral Processing Symposium*, 2012, pp. 831-837.

[26]. A. Sworska, J. S. Laskowskı, and G. Cymerman, "Flocculation of the Syncrude fine tailings Part II. Effect of hydrodynamic conditions," Int. J. Miner. Process., vol. 60, pp. 153–161, 2000.

[27]. M.G. Kılıç, Ç. Hoşten, and Ş. Demirci, "A Parametric Comparative Study of Electrocoagulation and Coagulation Using Ultrafine Quartz Suspensions," *Journal of Hazardous Materials*, vol. 171, pp. 247-252, 2009.

[28]. D. C. Montgomery, *Design and Analysis of Experiments*. 5th Edition, Hoboken, New Jersey: John Wiley & Sons, Inc., 2001.

[29]. B. Boltoa, and J. Gregory, "Organic polyelectrolytes in water treatment," *Water Research*, vol. 41, pp. 2301-2324, 2007.

[30]. K. Miyanami, K. Tojo, M. Yokota, Y. Fujiwara, and T. Aratani, "Effect of Mixing on Flocculation," *Ind. Eng. Chem. Fundam.*, vol. 21, pp. 132-135, 1982.

[31]. S. Biggs, M. Habgood, G. J. Jameson, and Y. Yan Y, "Aggregate structures formed via a bridging flocculation mechanism," *Chemical Engineering Journal*, vol. 80, pp. 13–22, 2000.

ISSN: 2458-8156

Journal Home page : http://dergipark.ulakbim.gov.tr/ejens * E-mail : editor@cnrgroup.eu

hosted by Turkish JournalPark ACADEMIC

EJENS

European Journal of Engineering and Natural Sciences CODEN: EJENS

Application of Digital Image Correlation in Uniaxial Tensile Test

Murat Aydin[1]*, Xin Wu[2], Kerim Cetinkaya[1], Ibrahim Kadi[1], Mustafa Yasar[1]

[1]*Karabuk University, Department of Industrial Design Engineering, 78050, Merkez/Karabuk, Turkey.*

[2]*Wayne State University, Department of Mechnaical Engineering, 48202, Detroit/Michigan, USA.*

**Corresponding Author email: murataydin@karabuk.edu.tr*

Publication Info

Paper received:
10 December 2015

Revised received:
15 December 2015

Accepted:
18 December 2015

Abstract

Application fields of non-contact measurement techniques have been recently increasing by means of optics and technological development in measurement applications. Digital image correlation (DIC) is the one and powerful non-contact measurement method that can be used to obtain elongation and strain as well. It is versatile and flexible measurement method can be adopted to many traditional test experiments such as tensile, compression, and bending in order to calculate mechanical properties of materials. In this study, DP600, DP800 and DP980 steel materials were performed to uniaxial tensile test and DIC technique was used to determine local strains in terms of comparison in different regions at the fracture area. While performing experiments, commercial DSLR camera was installed to capture videos under the white led lighting which is needed to decrease visual blurring and keep contrast as constant. Recorded videos were analyzed with VIC-2D software in an effort to calculate strain data. As a result, it was showed that the strains at the fracture area that were measured with DIC were higher than those measured which out of the fractured area and concluded that DIC method was appropriate and efficient technique to measure local strains in traditional uniaxial tensile test.

Key words

Digital Image Correlation, Optical Measurement, Sheet Metal, Strain Measurement, Tensile Test.

1. INTRODUCTION

Rapid development of technology and improvements of optic instruments has caused widely usage of non-contact measurement techniques both in industry and private applications. Image based measurement methods has recently been popular not only traditional methods can not satisfy customer requirements but also specific instruments are very expensive and adapted hardly. To give an easy, low cost, and flexible solution for those problems, digital image correlation (DIC) method is developed and has been used in many fields such as automotive industry, material testing, and medical applications.

DIC technique is mainly based on the photogrammetry field which is a science of making measurements from photographs, especially for recovering the exact positions of surface points. Roots of image based measurements techniques dates back to Leonardo da Vinci writings about the perspective and imagery in 1480 and 1492 as pointed out by Doyle [1] and Gruner [2]. Photogrammetry and its mathematical improvements has been enhanced by means of development of optic tools and imaging technology, especially digital photogrammetry in 1985 up to present [3]. Hobrough [4] used digital image correlation so as to get position information. He

purposed a tool that can be used to correlate high-resolution reconnaissance photography with high precision survey photography for calculating ground conditions. Yamaguchi [5] used laser speckles that are scanned by a linear image sensor in the diffraction field and made cross correlation function of the signal.

Ultrasonic approach was the prior studies in two dimensional measurement with digital image correlation. Peters [6] and Ranson [6] developed an approach. In their study, the ultrasonic waves were sent to the reference and deformed images and compared digital images of small areas as known subsets before and after process in order to calculate deformation measurements in material systems. They suggested to use continuum mechanics concept for measuring small areas in matching process to determine locating positions of all subsets. Sutton et all [7] improved some numerical algorithms based on earlier study and applied to experiments to record images with optical instruments and this is known today as 2D DIC. In the last decade, digital image correlation has been applied material testing experiments such as tensile, compression, bending and forming limit curves on the purpose of calculating mechanical properties of the sheet materials. One of the crack propagation study was accomplished by McCormick [8] and Lord [8]. They demonstrated the calculation of crack opening measurement using concrete specimens under compression and they suggested that output of DIC gives local deformation map which shows the cracks not visible to the human eye.

DIC measurement technique generally is adopted to material test experiments such as tensile, compression, and forming limit curves. Zhu et al [9] suggested the two cameras DIC system to measure true stress-strain curves of low carbon steel under uniaxial tension. They used dog bone specimen with 10mm circular cross section area. They calculated the true strain stress curves on the specimen using different local points along the length of the specimen and indicated that while region that enters the plastic zone provides axial plastic deformation because of decreasing cross sectional area, region that entered the plastic zone or not entered yet keeps constant deformed state. Dong et all [10] focused on an application of DIC under high temperature using micro scale pattern. They examined variety speckle patterns and sizes to get good correlation under the high temperature experiments and suggested that using a macro scale speckle patterns that is produced by ceramic based paint to micro scale caused the high number of errors of correlation when the subset size is too small. In addition, they found that fine-sprayed paint and abrasion of polished surface caused micro scale pattern stable under 1400 °C and errors were below 0.04 pixel.

2. EXPERIMENTAL

2.1. Materials

In this study, commercial automotive steels, DP600, DP800, and DP980 that consist of a ferrite matrix and a hard second phase, usually islands of martensite was used in order to calculate local strains using DIC method in uniaxial tensile test. The thicknesses of materials are 1.3mm and the tensile specimens were machined according to ASTM E8. Chemical compositions of these materials are given in Table 1.

Table 1. Chemical compositions of DP600, DP800, and DP980

DP800 [11]						
C % max	**Si % max**	**Mn % max**	**P % max**	**S % max**	**Cr % max**	**Al_{tot} % max**
0,160	0,250	1,90	0,020	0,004	0,500	0,015
DP980 [12]						
C % max	**Si % max**	**Mn % max**	**Mo % max**	**B % max**	**Cr % max**	**Al_{tot} % max**
0,135	0,05	2,1	0,35	0,007	0,15	0,45
DP600 [11]						
C % max	**Si % max**	**Mn % max**	**P % max**	**S % max**	**Cr % max**	**Al_{tot} % max**
0,120	0,300	1,660	0,020	0,004	0,500	0,020

2.2. Methods

All the mechanical tests were performed with 100 kN Instron 8801 uniaxial tensile machine. DIC is mainly used to calculate the displacement and strain over specified field in whole process. One of the crucial instruments in DIC measurement is the camera. The professional high resolution and high frame per second (fps) camera can increase the accuracy and precision of measure. In this study, Canon T3i DSLR with a 58mm diameter and 18-55mm (f/3.5-5.6) lens that has 1920x1080 resolution and 30fps was used, see Figure 1.

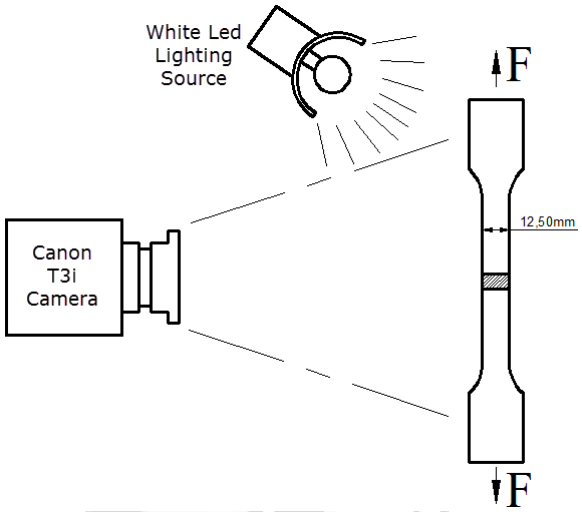

Figure 1. Schematic view of DIC setup

Creating random speckle pattern on the specimen surface is one of the important issues that can directly affect accuracy and precise of the correlation results. In order to obtain high and accurate correlation, the pattern size must be small. Experiments performed at room temperature, most of the water based paints can give proper correlation results to create speckle pattern. In this study, VHT FlameProof, a silicone ceramic based paint was used to create black speckles onto white background because of rapid drying time and high color contrast. As an example, DP600 painted specimen that consists of the calibration meter and dashed area of interest is shown in Figure 2. On the purpose of calculating local strains, five points were selected on horizontal alignment in the fracture area as seen in Figure 2(b). Point 1 is the nearest left edge of specimen and Point 3 is the middle of the fractured edge, and Point 5 is closed to the right edge of specimen out of fracture area. Lighting conditions is another important factor that is crucial for the correlation results. In this study, regular white led lighting source which was subjected to the specimen surface directly gives good correlation results.

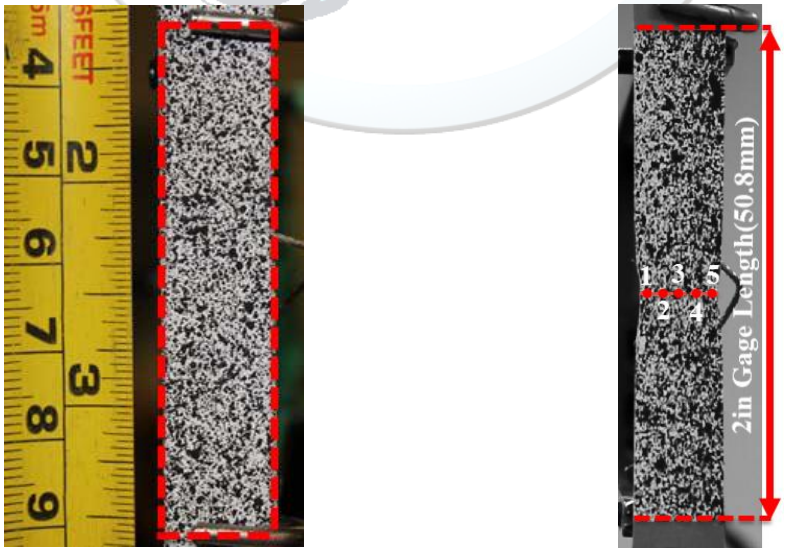

Figure 2. (a) Calibration meter and area of interest *(b) Virtual gage length and selected points*

3. RESULTS AND DISCUSSION

In conventional tensile tests, regular extensometer which has 2in (50.8mm) gage length has been used in order to measure the elongation and calculate strain. On the other hand, regular extensometer is not able to install some special experiments as hot tensile tests or hot forming limit tests due to high temperature of test environment and require special equipment like ceramic grips. Therefore, these special tools increase the measurement setup's cost. As an alternative method, DIC, can easily adopt to room and high temperature material mechanic tests. Elongation can be calculated by DIC as well as physical extensometer measurement.

Uniaxial tensile tests were performed with 0.1mm/s cross head speed for three materials. The frames were created from test movies after the whole recorded processes. In the case of non-contact measurement, the extension was obtained from the images using VIC-2D software. Two boundaries were defined that overlay with the two gage length edges, which were created by two Scott types that shielded the paint. After the paint was dried, the types were peeled out. Figure 2 shows the clear boundary of the tensile gage length.

Converting pixels to millimeter was established with common tape measure onto specimen surface at the beginning of the uniaxial tensile test. The camera was setup as 1920x1080 pixels resolution and 16:9 aspect ratio and 16 bit depth of color. The total test times were 35.457 seconds for DP600, 23.779 seconds for DP800, and 18.706 seconds for DP980. The recorded videos were edited with video editing software to obtain series of image sequences. The images were got as 30 frames per second. The images were converted into greyscale format as a TIF file type that has better quality rather than other image types after getting image sequences. Performing correlation the image sequences were imported into VIC-2D software.

The DIC technique is based on tracking and matching process for each unique pattern regions among images or different times. The unique pattern of each location can be defined using subset size and step size to track and calculate displacements. The subset size for room temperature tensile tests is 24x24 pixels and step size 2x2 pixels. Figure 3 shows the Von Misses strains of the fractured areas for DP600, DP800, and DP980. On the scale bar, red color shows the maximum Von Misses strains in the fracture zone before the failure of specimens. Maximum Von Misses strains were found as 0.562, 0.296375, and 0.164625 for DP600, DP800, and DP980, respectively.

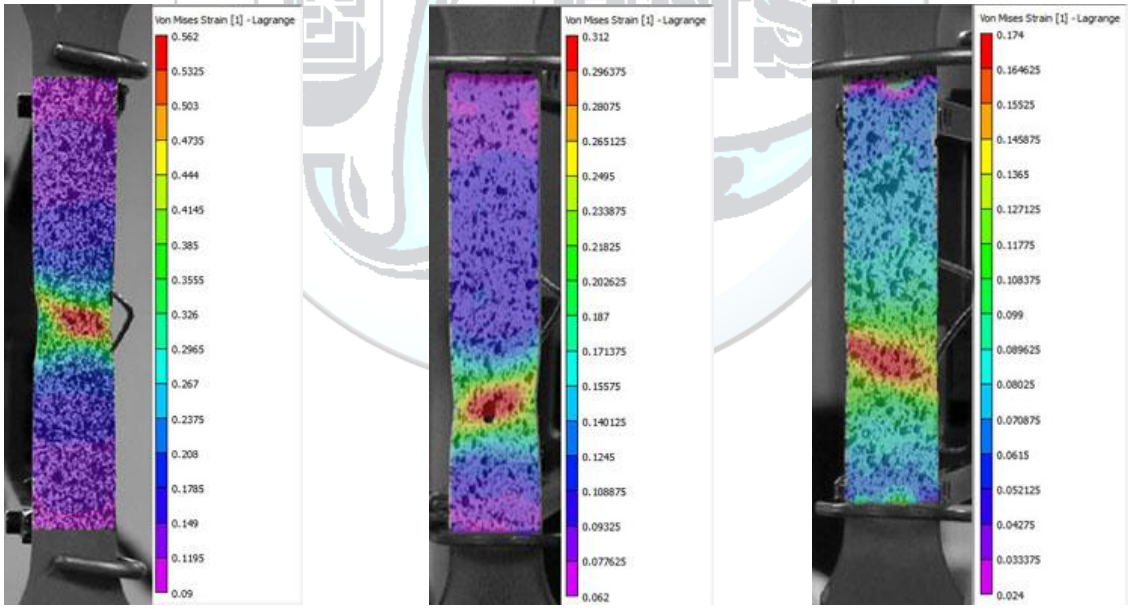

(a) *(b)* *(c)*

Figure 3. Von Misses strains before fracture. (a) DP600, (b) DP800, (c) DP980

Figure 4 shows the plot of the strains in y direction of five points that are shown in Figure 2(b). In Figure 4, Point 3 which is a middle point of the fracture area is always higher points that are slightly out of the fractured area.

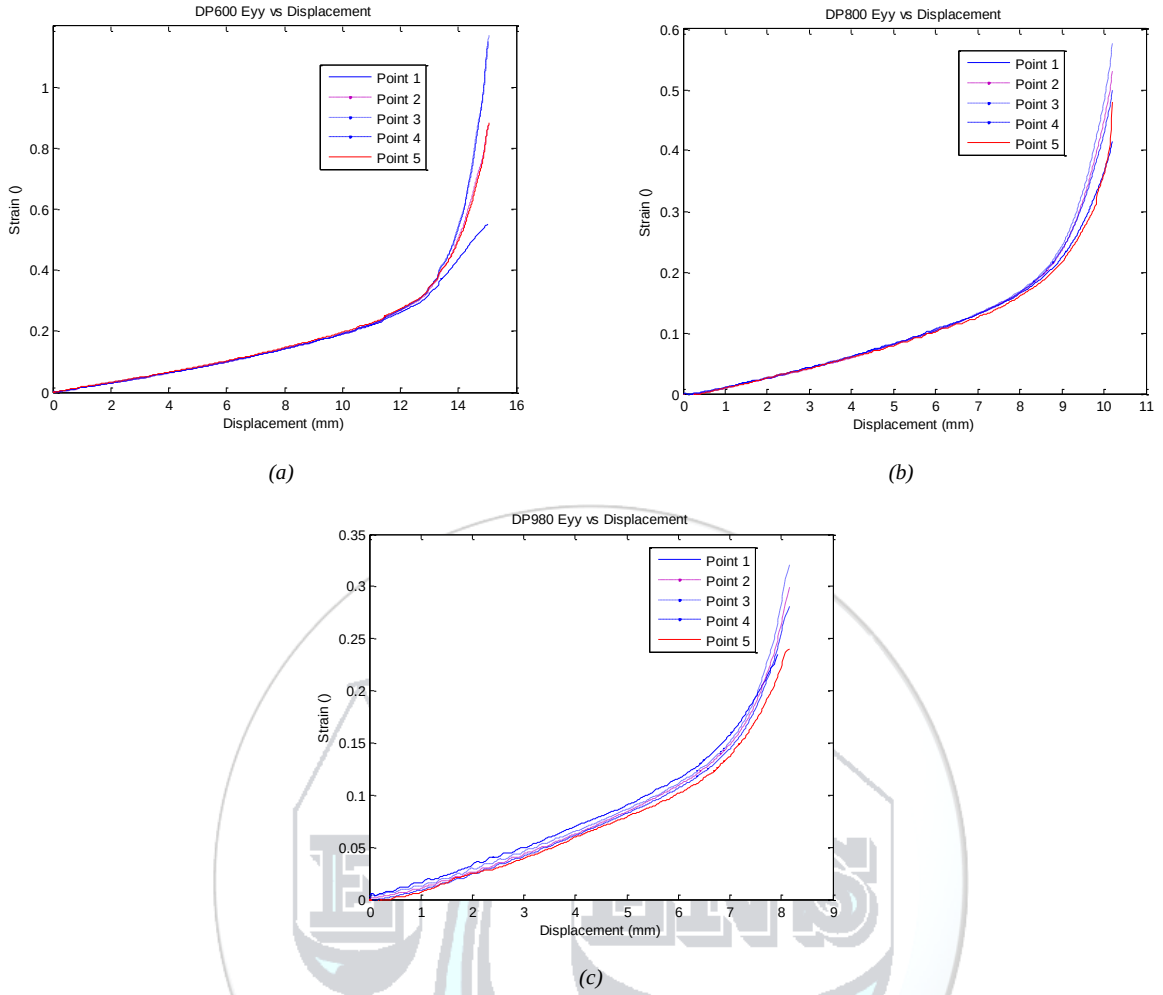

Figure 4. Strains in y direction of five points for (a) DP600, (b) DP800, and (c) DP980

4. CONCLUSIONS

In this study, DIC technique was performed to install uniaxial tensile test in order to get local strains. Three different material, DP600, DP800, and DP980, were used to calculate all points of strain curves versus displacement. Following conclusions can be made about the DIC method;

1) DIC can easily adapt to materials mechanical tests instead of traditional measurement methods.

2) A low cost, easy to setup and consumer camera system can be used for non-contact strain and displacement 2D measurements over flat specimens in uniaxial tensile test.

3) When the local strains take into account, the region (Point 3) which is the middle of the fracture area has always higher strains than the regions that are out of the fracture area for those materials.

4) The strains along the gage width are not homogenous. So, DIC method is an effective technique that can be used to determine local strain evolutions at the crack edge in notch specimens.

REFERENCES

[1]. Doyle F. J., The historical development of analytical photogrammetry, Photogrammetric Engineering, 1964, 259–265.
[2]. Gruner H., Hugershoff R., Photogrammetric Engineering, Vol. 37, No. 9, 1971, 939–947.
[3]. Sutton M.A., Orteu J.J., Schreier H.W., Image Correlation for Shape, Motion and Deformation Measurements, Springer, 2009, 1-2.
[4]. Hobrough A.G.L., The Photogrammetric Record, Vol. 18, No. 104, 2003, 337–340.

[5]. Yoneyama S., Ogawa T., Kobayashi Y., Evaluating mixed-mode stress intensity factors from full-field displacement fields obtained by optical methods, Engineering Fracture Mechanics, Vol. 74, No. 9, 2007, 1399–1412.
[6]. Peters W.H., Ranson W.F., Digital imaging techniques in experimental stress analysis, Optical Engineering, Vol. 21, No. 3, 1982, 427–431.
[7]. Sutton M.A., Wolters W.J., Peters W.H., Ranson W.F., and McNeill S.R., Determination of displacements using an improved digital correlation method. Image and Vision Computing, Vol. 1, No. 3, 1983, 133–139.
[8]. McCormick N., Lord J., Digital Image Correlation, Materials Today, Vol. 13, No. 12, 2010, 52-54.
[9]. Zhu F., Bai P., Zhang J., Lei D., and He X., Measurement of true stress-strain curves and evolution of plastic zone of low carbon steel under uniaxial tension using digital image correlation, Optics and Lasers in Engineering, Vol. 65, 2015, 81-88.
[10]. Dong Y., Kakisawa H., and Kagawa Y., Development of micro scale pattern for digital image correlation up to1400°C, Optics and Lasers in Engineering, Vol. 68, 2015, 7-15.
[11]. SSAB Swedish Steel, 07-10-11,
[12]. Sreenivasan S., Xia M., Lawson S., and Zhou Y., Effect of laser welding on formability of DP980 steel, Journal of Engineering Materials and Technology, Vol. 130, 2008, 1-9.

ISSN: 2458-8156

Journal Home page : http://dergipark.ulakbim.gov.tr/ejens * E-mail : editor@cnrgroup.eu

hosted by Turkish JournalPark ACADEMIC

EJENS

European Journal of Engineering and Natural Sciences CODEN: EJENS

The Effect of River Type Hydroelectric Power Plants on Aquatic Ecosystems: the Case Study of Göksu River-Eastern Mediterranean

Havva Ates[1], Selim Dogan[1]*, Ali Berktay[2]

[1]*Selcuk University, Department of Environmental Engineering, 42031, Selcuklu/Konya, Turkey.*

[2]*Usak University, Department Civil Engineering, 64100, Usak, Turkey.*

**Corresponding Author email: sdogan@selcuk.edu.tr*

Publication Info

Paper received:
10 December 2015

Revised received:
15 December 2015

Accepted:
18 December 2015

Abstract

The contribution of the hydropower energy potential to the reconstruction of the energy structure is very important in Turkey. In spite of numerous social and economic benefits experienced in the area in social and economic spheres due to the project, there is also a plurality of adverse impacts observed in the environment. In social and economic spheres, the land acquiring and resettlement of people are important issues. Large-scale irrigation causes salinization and leads to soil erosion; huge water reservoirs affect local climate and are a source of considerable amounts of pollution. The construction and operation of hydroelectric power plants is directly related to the flow of the river. Therefore, environmental flow is described as the quantity, timing, and quality of water flows required to sustain freshwater and estuarine ecosystems and the human livelihoods and well-being that depend on these ecosystems. Environmental flow estimation is considered as a safe guard for an aquatic ecosystem in the water basins with regulated flow regime. Environmental flow not only the self purification flow to fulfill the water quality demand, but also the flow demand for the existing aquatic lives. Natural flow regime is critically important in sustaining the natural biodiversity and ecosystem integrity in river basins.

Construction of dams and hydroelectric power plants development projects will likely continue. As a result, legal and policy frame works for protecting and restoring them also continue to develop, and various governmental agencies, community-based organizations, private-sector actors, and individuals are becoming involved with implementing and monitoring these flows.

This research estimates the environmental flow requirements in the Göksu River in Eastern Mediterranean and to understand the impact of hydroelectric power plant in maintaining the natural flow regime. The current operation policy can cause severe hydrological alteration in the natural flow regime so current status and calculated amount of flow are compared.

Key words

Dams, ecosystems, environmental flow, hydroelectric power

1. INTRODUCTION

The environmental damage caused by hydropower schemes has become increasingly apparent over the last decade or so. Changes to river flows are one of the key consequences of the construction of dams and/or hydroelectric power plants. Maximizing the electricity output of a hydropower plant according to demand can have serious consequences both for ecosystems and other users, as flow conditions downstream of the plants are altered. However, in many cases it is possible to adjust the operational regime of a dam to better meet a variety of needs. So called 'environmental flows' provide critical contributions to river health, economic development and poverty alleviation [1].

Total economic hydroelectric power potential of Turkey is 129.5 TWh/yr by the end of February 2007. 35.5% of this potential is in operation while 11.1% and 53.4% of this potential are under construction and in various design level, respectively [2].

Turkey is an energy-importing country. In order to be less dependent on other countries, Turkey needs to use its sustainable sources. From this point of view, hydropower is a very attractive choice, since it is economical, sustainable, and environmentally friendly and it is a publically familiar source of energy in Turkey [3].

Environmental flow is regulated in order to contribute to river basin planning. Environmental flows can include some restrictive and active management such as dams planning, reducing irrigation and water supply. This management can be applied in various situations such as low and high flow regime, particularly during dry periods. The EFA finds the optimal balance between ecosystem and the various utilizations such as water use and regulation of flow within a river, wetland or coastal zone. There are adverse effects of a time-varying flow regime over the ecosystem [4]. The influence of climate change, decreasing river flows, degradation of the river bed, flow regulations, agricultural and industrials activities and human use cause the change of deterioration of the natural conditions of the rivers. Aquatic organisms that are using river as habitat are affected by these negative effects. The EFA approach was developed to establish balance between ecological concerns in the context of the river ecosystems and sustainability and requirements of modern world. If the river flow has been greatly influenced by the human activity and natural, such as reservoirs, channels and urban diversion, erosion, these will limit the application of the hydrological methods. Because of the erosion, the shapes of the cross sections are changing continuously, especially in the lower reaches. The natural flow regime consists of flow magnitude, frequency, timing, duration and rate of change of flows. In order to protect the ecological functions it is important to maintain a semblance of the natural state of each component of the flow regime as each of these components contributes towards maintaining critical instream ecological functions [5]. The major problem in the management of rivers has not been protection and use balance over the water resources Management problems normally exacerbate during low-flow periods and with on-going water resources development resulting in gradual reduction of flow available for instream uses[6].

Instream flows are usually referred as environmental, minimum or maintenance flows that guarantee a sufficient level of protection for the aquatic environment in regulated rivers. Various types of environmental flow methodologies have been proposed in different region of the world to secure particular environmental needs. Flows that led to a enough level of protection for the aquatic environment in rivers are usually name as environmental, minimum or sustainable flows. During the last few decades numerous methodologies have been developed to establish environmental flows in regulated rivers. These methodologies can be grouped in four categories (Tharme 2003) described which could be differentiated into hydrological (Hydrological or historic flow methods [5]. They are based on the study of historical flow regime records, for instance, the Tennant (1976) method determines the environmental flow as a percentage of the mean annual flow.), hydraulic rating(These methods are based on the study of the hydraulic geometry of stream channels (cross-sections), habitat simulation and holistic methodologies. These methods have been used by many researchers and they highlighted that the one of the most common method is the Tennant method and modified Tenant method [7], 7Q10, Q95 [8, 9], wetted perimeter method which can use both hydrological and ecological data [10]. A comparison of the approaches for instream flow methods were explained in some detail [11]. Application of the hydrologic and hydraulically derived geometric parameters was evaluated to determine the minimum water requirements of ecological habitats [12]. All these methodologies, independently of the advantages and disadvantages they may have and their theoretical foundation, have a common characteristic that usually make them difficult to apply, which is the need of a large amount of data. Due to the small data requirement, hydraulic rating methods are widely applied. But the relationships are also concluded from natural rivers. It may fail to assess ecological base flow in regulated river using hydraulic rating methods. Long-term high-quality information on hydrological or hydraulic parameters, or habitat preference data, is rarely available. Hydraulic and habitat simulation methods demand intensive field work and sometimes long periods of time for their correct implementation [5, 13].

The objective of this study is to compare four commonly used hydrologically based instream flow assessment methods. Environmental flows is calculated in the hydroelectric power plant on the Göksu river to using five

hydrologically based methods. The recorded average daily flow data at the downstream point, Göksu river for 18 years (1995-2013) was analyzed in two periods from 1995 to 2010 as pre-hydropower plant construction and 2010-2013 as post-hydropower construction to obtain the flow alteration at the measuring station due to hydropower development in the river.

2. STUDY AREA

The Göksu river is located in Eastern Mediterranean basin (Turkey). The basin covers the provinces of Antalya, Konya, Karaman and Mersin.

The river is 260 km long and discharges into the Mediterranean Sea 16 km south east of Silifke (in Mersin province). Akgöl Lake and Paradeniz Lagoon are within the delta of the Göksu. The location of the study area in the basin are shown in Figure 1.

The recorded average daily flow data of 18 years (1995-2013) at the downstream point of Göksu river was analyzed in two periods from 1995 to 2010 as pre-hydropower plant construction and 2010-2013 as post-hydropower construction to obtain the flow alteration at the measuring station due to hydropower development in the river.

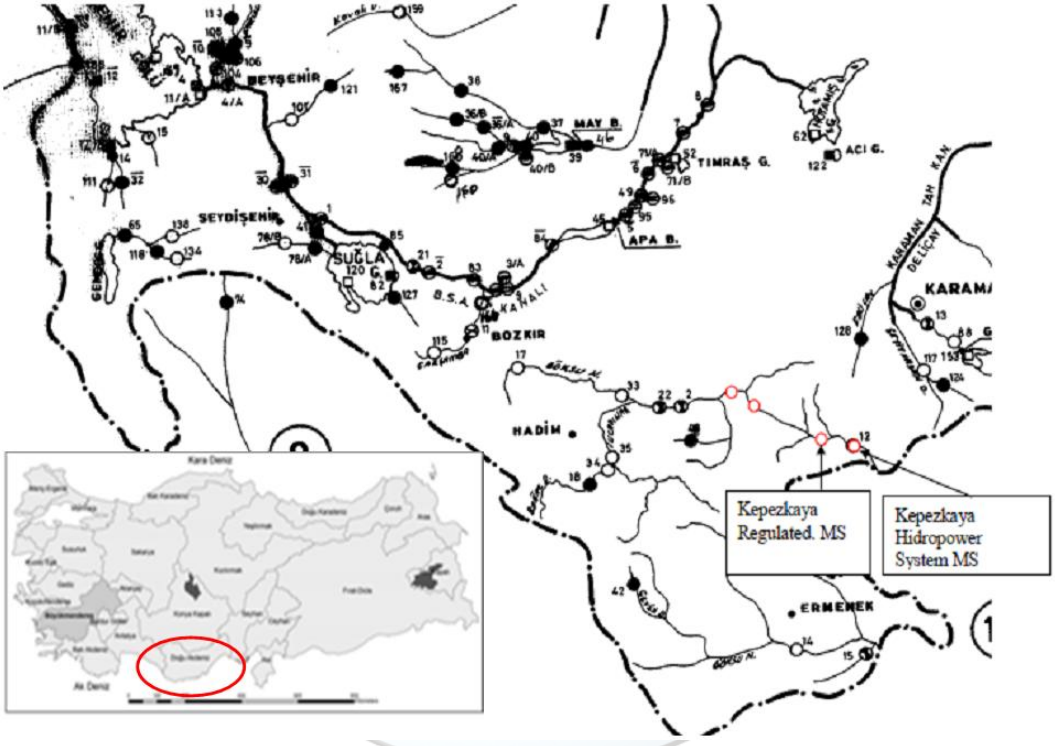

Figure 1. The location of study area

3. METHODS

Some methods, which are considered as hydrological and hydraulic methods, were examined to generate the environmental flow as explained above. These methods are 7Q10, Q95, the original Tennant method, modified Tennant method. These methods are summarized as the following.

3.1. 7Q10 Method

Daily river flows in the 7Q10 range are general indicators of prevalent drought conditions which normally cover large areas. The river flows that occurs over 7 consecutive days and has a 10-year recurrence interval period, or a 1 in 10 chance of occurring in any one year. 7Q10 values are also used by the U.S. for regulating water withdrawals and discharges into streams [9, 10, 14]. According to U.S. Fish and Wildlife Service the 7Q10 flow is a flow statistic used in identifying the volume for dilution to set permit limits for wastewater discharge so it does not cover the habitat alterations in rivers [14].

3.2. Q95 Method

The exceedance percentile Q95 can be interpreted as the flow discharge which can be expected to be exceeded 95% of the time. The index is sometimes described as one from Look-up table method that is using the flow duration curve of a river. Q95 index of natural low flow has been employed to define the environmental flow and the flow that is equaled or exceeded for 95% of the time. The Q95 index was determined solely by the hydrological data. However, the implementation of this method often requires the use of ecological information. Q95 index may be used to determine the dry periods such as the mean annual minimum flow [5, 11].

3.3. Original Tennant Method

It was developed by using historical data of 11 rivers in the states of Montana, Wyoming, and Nebraska in the USA to determine minimum flows to protect the aquatic life in rivers. Percentages of the mean annual flow are identified that provide different quality habitat for fish e.g. 10% for poor quality (survival), 30% for moderate habitat (satisfactory) and 60% for excellent habitat over two certain periods of the year for instance, October to March (6 mounts) as wet period and April to September (6 mounts) as dry period. This method can be used elsewhere, but there are some important issues about using this method in other areas. The method directly can be used for other areas if there are morphological similarities with other rivers. Otherwise application of this method directly is not recommended whereas the modification of this method is possible to simulate the aquatic life in other rivers [7,11].

3.4. Modified Tennant Methods

Modified Tennant method is different from original Tennant method that the selection of the periods may be different. The average flow of the river was determined by the means of 18-year data and 15% of the daily mean flow has been applied for wet period whereas 20% was for dry period [15].

4. RESULTS and DISCUSSION

For the station some statistics such as minimum, maximum and standard deviation of the daily mean flows is given in Table 1.

Table 1. Some statistics for the station

Month	Min	Max	STD	Mean
O	2.55	29.5	1.78	8.14
N	1.14	145	12.04	13.45
D	1.14	247	29.60	27.72
J	6.16	124	16.70	23.44
F	9.02	163	19.50	32.50
M	10.5	340	31.15	52.74
A	9.56	226	38.20	62.30
M	7.78	124	17.35	29.80
J	2.75	33.8	3.40	11.90
J	2.13	22.7	1.57	8.40
A	1.2	14.8	1.14	7.44
S	1.08	13.4	1.19	7.25

Daily average flow of the river is well illustrated in Figure 2. According to daily average flows data, 30 percent of 20-year daily flow data has exceeded the average flow and 50 percent of 20-year daily flow data has exceeded the median flow.

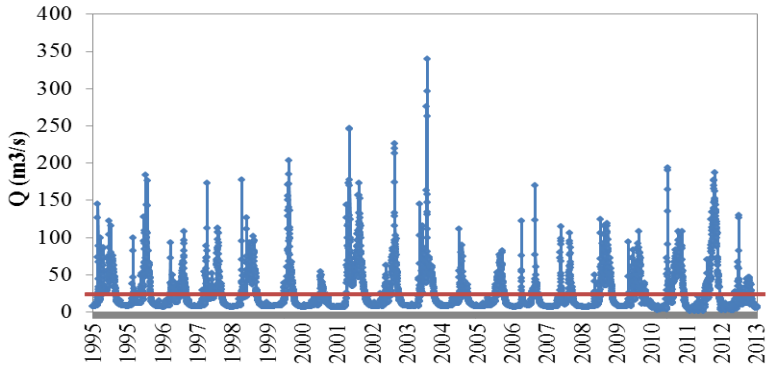

Figure 2. Flow time series

Figure 3 shows the flow duration curve of the river. The result of the Q95 method is derived from Figure 3 and calculated as to 7.22 m^3/s as the flow rate which is exceeded 95% of the time.

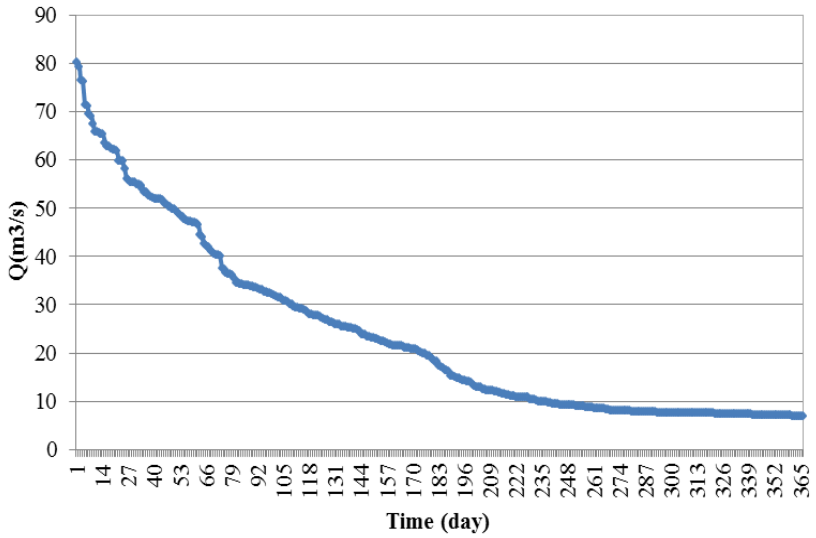

Figure 3. Flow Duration Curve

The monthly average flows are shown in Figure 4 Due to average and median flows are calculated for the estimating the environmental flow. In Figure 4 flow rate that plot above the average flow is accepted as wet period and below the average flow is dry period from which is indicated in the part of the modified Tennant method. Wet and dry periods, which set for each station, are provided in the Table 2.

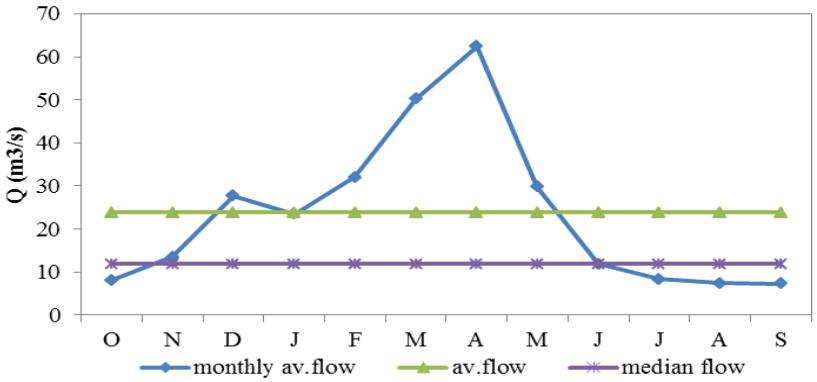

Figure 4. Monthly average flows

Table 2. Modified Tennant Method periods

Qaverage	From December to May (%15)	From June to November (%20)
Qmedian	From November to May (%15)	From June to October (%20)

The results of environmental flow with various methods are given in Table 3 where as the relationship between monthly incoming flows and release flows are given in Table 4 for the year of 2010-2013 periods. In order to compare them that must be in the same time period. For this, monthly incoming flows and release flows shown in Table 4 are the flows that exist in the river for the year of 2010-2013. Difference row of Table 4 shows the amount of water used for hydroelectric generation purposes.

Table 3. The results of environmental flow with various methods

	Flow rates by months (m^3/s)											
	O	N	D	J	F	M	A	M	J	J	A	S
Monthly Qav	8.14	13.45	27.72	23.44	32.5	52.74	62.32	29.8	11.9	8.4	7.44	7.25
Qav	23.8	23.8	23.8	23.8	23.8	23.8	23.8	23.8	23.8	23.8	23.8	23.8
Qmed	11.9	11.9	11.9	11.9	11.9	11.9	11.9	11.9	11.9	11.9	11.9	11.9
7Q10	4.23 (+)	4.23 (+)	4.23 (+)	4.23 (+)	4.23 (+)	4.23 (+)	4.23 (+)	4.23 (+)	4.23 (+)	4.23 (+)	4.23 (+)	4.23 (+)
Q_{95}	7.22 (+)	7.22 (+)	7.22 (+)	7.22 (+)	7.22 (+)	7.22 (+)	7.22 (+)	7.22 (+)	7.22 (+)	7.22 (+)	7.22 (+)	7.22 (+)
Original Tennant Method	3.9 (+)	3.9 (+)	3.9 (+)	3.9 (+)	3.9 (+)	3.9 (+)	4.23 (+)	4.23 (+)	4.23 (+)	4.23 (+)	4.23 (+)	4.23 (+)
Modified Tennant Method (by Qav)	1.88 (+)	1.88 (+)	5.64 (+)	5.64 (+)	5.64 (+)	5.64 (+)	5.64 (+)	5.64 (+)	1.88 (+)	1.88 (+)	1.88 (+)	1.88 (+)
Modified Tennant Method(byQmed)	1.72 (+)	5.12 (+)	5.12 (+)	5.12 (+)	5.12 (+)	5.12 (+)	5.12 (+)	5.12 (+)	1.72 (+)	1.72 (+)	1.72 (+)	1.72 (+)

(+) This amount of water is below baseflow, so, can be supplied by Monthly Qaverage

As it can be seen in Table 3, (+) indicates sufficient amount of water can be provided as environmental flow. When this situation is taken into consideration, all methods shows that environmental water flow exist in all months of the year. However for dry period, Modified Tennant methods have low values which cannot be assumed as environmental flow. Moreover the values which were calculated by Tennant methods were observed to be lower than the baseflow (7.25 m^3/s). In this case the flow amounts which remain lower than the base flow (which used to be evaluated as life water) are not suggested as environmental flow.

In the method which was suggested by Tennant in 1976 [7], water year was divided into two, as wet and dry periods. In modified Tennant method, if many factors such as hydrological and climatic properties of basin and river are taken into consideration it will not be meaningful to apply the original Tennant method directly to all rivers. When the flows that are supposed to exist in river system and the average flows in original Tennant method are checked, water deficiency is not observed in whichever months. In modified Tennant method according to average and median flow water deficiency is not observed. Environmental flow is calculated as 7.22 m^3/s using Q95 method. This value almost equals to baseflow. So, water deficiency can be observed especially in 2 months (Aug, Sep). Water should not be taken from river system in months that of water deficiency.

As it can be seen in Table 3, (+) indicates sufficient amount of water can be provided as environmental flow. When this situation is taken into consideration, all methods shows that environmental water flow exist in all months of the year. However for dry period, Modified Tennant methods have low values which cannot be assumed as environmental flow. Moreover the values which were calculated by Tennant methods were observed to be lower than the baseflow (7.25 m^3/s). In this case the flow amounts which remain lower than the base flow (which used to be evaluated as life water) are not suggested as environmental flow.

In the method which was suggested by Tennant in 1976 [7], water year was divided into two, as wet and dry periods. In modified Tennant method, if many factors such as hydrological and climatic properties of basin and river are taken into consideration it will not be meaningful to apply the original Tennant method directly to all rivers. When the flows that are supposed to exist in river system and the average flows in original Tennant method are checked, water deficiency is not observed in whichever months. In modified Tennant method according to average and median flow water deficiency is not observed. Environmental flow is calculated as 7.22

m^3/s using Q95 method. This value almost equals to baseflow. So, water deficiency can be observed especially in 2 months (Aug, Sep). Water should not be taken from river system in months that of water deficiency.

Table 4. Relationship between incoming flow and release flow (2010-2013)

	Flow rates by months (m^3/s)											
	O	N	D	J	F	M	A	M	J	J	A	S
Monthly Qav	6.73	7.16	31.6	21.56	28.32	57.66	79.41	47.33	12.52	7.47	6.2	5.83
Release flow	2.5	2.63	17.61	3.25	4.05	21.93	43.76	15.87	2.61	2.43	2.85	2.43
Difference (Monthly Qav-Release flow)	4.23	4.53	13.99	18.31	24.27	35.73	35.65	31.46	9.91	5.04	3.35	3.4

When current status and calculated amount of flows are compared to one and other, the Tennant Methods are not suitable for the river because of calculated values much lower than those of average and median flow value. In current conditions, released flow values are low for some months. Although, the released flows are seemed to be appropriate comparing to some methods used in this investigation, it might be suggested to increase release flow up to some value towards the average monthly flows of the river.

5. CONCLUSION

Hydropower potential is an attractive solution for energy need because of being a clean way of energy generation. Hydropower plants are the large-scale water management program aiming to increase the domestic electricity production and develop vast irrigation schemes for agriculture. There are 25 hydrological basins in Turkey, Turkey has great advantages from the view point of hydropower potential without storage and hydroelectric energy which is a clean and renewable energy source rise in importance day by day due to its domestic energy resource feature to meet Turkey's electricity energy need.

Many reasons such as limited water sources throughout the world or the decrease in usable water amount requires more attention for the management of the water sources. The necessity to maintain the sustainability of water in long term against increasing water demand placed integrated water source management to forefront.

In this case environmental flow evaluation studies constitute the base of integrated water sources management. The environmental flow evaluation studies aim to minimize the pressure and effects on a river while maintaining the balance between using and preserving thus ensuring the effective usage of water. Environmental flow evaluation may vary from country to country and even in different basins within the country. Therefore environmental flow evaluation should be made specific to each river in the basin.

ACKNOWLEDGMENT

Presentation of this research has been financially supported by the Scientific Research Project Fund (BAP) of Selcuk University, Konya-Turkey.

REFERENCES

[1]. M.Dyson, G.Berkamp, J. Scanlon(eds) "Flow – the Essentials of EnvironmentalFlows" IUCN, Glandand Cambridge,2003.
[2]. The Electrical Power Resources Survey and Development Administration (EİE).Hydro Electric Power Plant Projects Carried out by EİE. Ankara, Turkey, 2007.
[3]. Turkey Country Report. Prepared for the 3rd World Water Forum. Ankara, Turkey, 2003.
[4]. J.M.King, R.E.Tharme, M. De Villiers (eds). "Environmental flow assessments for rivers: Manual for the building block methodology" Water Research CommissionTechnology Transfer Report No.TT354/08; 2008. Water Research Commission: South Africa.

[5]. R.E.Tharme “A global perspective on environmental flow assessment: emerging trends in the development and application of environmental flow methodologies for rivers” River Research And Applications vol.19,2003, pp. 397-441.
[6]. V.U.Smakhtin, “Low flow hydrology: a review”, Journal of Hydrology, 2001, pp.147-186.
[7]. D.L. Tennant,“Instream flow regimens for fish, wildlife, recreation and related environmental resources”Fisheries,1:6, 1976.
[8]. V.U. Smakhtin, R.L.Shilpakar, D.A.Hughes,“Hydrology-based assessment of environmental flows: an example from Nepal” Hydrological Sciences Journal, 51(2), 2006, pp. 207–222.
[9]. R.S. Pyrce,“Considering baseflow as a low flow or instream flow” WSC Report No.04-2004 Appendix, Watershed Science Center, 2004, Peterborough, Ontario, 17.
[10]. A.Shokoohi, Y. Hong,“Using hydraulic and hydraulically derived geometric parameters of perennial rivers to determine minimum water requirements of ecological habitats (case study: Mazandaran Sea Basin - Iran)”, Hydrological Processes; vol.25, 2011, pp 3490-3498.
[11]. I.G.Jowett,“Instream flow methods: a comparison of approaches. Regulated Rivers” Research &Management 13, 1997, pp. 115–127.
[12]. B. Clausen and B.J.F.Biggs,“Flow variables for ecological studies in temperate streams: groupings based on covariance” Journal of Hydrology, 2000, vol. 237, pp. 184-197.
[13]. J.Alcâzar, A.Palau,C.Vega-Garcîa, ,“Neural net model for environmental flow estimation at the Ebro River Basin”, Journal of Hydrology, 349, 2008, pp. 45-55.
[14]. R.S.Pyrce,“Hydrological low flow indices and their uses” WSC Report No.04-2004.Watershed Science Centre, Peterborough, Ontario, 2004, pp.33.
[15]. H. Ates, S. Dogan and A.Berktay, “Assessment of environmental flows in rivers with the example of Great Menderes Basin”, the 3rd Biennial Symposium of the International Society for River Science Achieving Healthy and Viable Rivers, Beijing, China August 5-9, 2013.

ISSN: 2458-8156

Journal Home page : http://dergipark.ulakbim.gov.tr/ejens * E-mail : editor@cnrgroup.eu

hosted by Turkish JournalPark ACADEMIC

EJENS

European Journal of Engineering and Natural Sciences CODEN: EJENS

Thermal Change for Heat Exchanger Cooling System of PCM

Numan Yuksel[1]*

[1]*Bursa Technical University, Department of Mechatronics Engineering, 16330, Yıldırım/Bursa, Turkey.*

**Corresponding Author email: numan.yuksel@btu.edu.tr*

Publication Info

Paper received:
10 December 2015

Revised received:
15 December 2015

Accepted:
18 December 2015

Abstract

A current study is presented in which a real-size room at daytime is cooled by a heat charge and discharge in a latent-heat-storage unit of phase changed materials. The unit is designed as a shell-and-tube heat exchanger. The tubes are vertical and filled with a phase-change material. The PCM melts and the room air is cooled down to a comfortable level, which lasts as long as the PCM is melting. While the ambient temperature changes from 35◦C to 45◦C, the comfortable time and variations are analytically calculated. Some cases are considered: an insulated room, a room heated by the ambient. By using the averaged values defined for the phase changed materials, the obtained analytical calculations and solutions are carried out with the available data in the literature. It is shown that the present theoretical study results related to the cooling using ambient conditions and the different dimensions will have an effect on the time of cooling. In addition, it can be seen from the results that dimension has a dominant effect on the temperature of stored energy than conditions.

Key words

Cooling Time and Heat Exchanger , Phase Change, Energy Storage

1. INTRODUCTION

Many studies about the energy problems and solutions have been reported. The problems can be solved by using thermal energy storage. Several theoretical and experimental investigations were devoted to modelling the thermal performance of the storage units and phase changed materials (PCM) [1-6], the different phase change materials, investigation of new geometries, and new concepts/ for energy storage technology. In these studies, the effects of various working parameters, the storage time, the efficiency of system and phase changed materials were investigated.

Thermal storage units are used for domestic, waste, vehicle heating or cooling in systems characterized by different temperatures in the daytime and cool nights. During the day the PCM absorbs heat in it and melts, and then it releases its latent heat to the ambient while at night/different times. So, a PCM-based unit in air conditioner decreases considerable energy consumption and solves an energy problem in its operation.

Units of similar and different structure have been investigated in the literature. Farid and Kanzawa [7] theoretically investigated a shell-and-tube heat exchanger unit based on thermal storage. The air of system was flowing in the shell across the tubes filled with PCM. The performance of the unit improves by using different PCMs in the same unit. However, Lacroix [8] investigated numerically and experimentally the PCM stored in the shell and the heat-transfer fluid circulated inside the vertical tubes in a shell-and-tube unit. Turnpenny et al. [9,10] studied a unit utilized as a ventilation cooling system in buildings and used a heat pipe embedded in a

phase-change material. Mozhevelov et al. [11] studied thin vertical storage units installed parallel to walls in a room. In daytime heat was free-convected from the room air, while at night heat was released from the unit into the ambient by both free and forced convection. Mozhevelov [12] also investigated simulations of a portable storage unit with cooling elements of various shapes in a shell: vertical plates, horizontal plates, horizontal square tubes in in-line and staggered configurations, and vertical square tubes in an in-line configuration. Arye and Guedj [13] experimented with a shell-and-tube unit, in which the tubes were vertical and filled with paraffin wax. The room air convected by fans through the shell. While the ambient temperature at daytime was 30 ◦C to 35◦C and at night, 18 ◦C to 19◦C. Mosaffaa et al [14] presented a comparative study for solidification of the PCM in cylindrical shell and rectangular storages having the same volume and heat transfer surface area. Vakilaltojjar and Saman [15] investigated the effect of slab thickness on a rectangular storage unit performance by using a semi-analytical method for phase change for air conditioning applications. Akgun et al. [16] experimentally carried out PCM melting and solidification in a shell and tube heat exchanger. Hosseini et al [17] studied experimentally and numerically thermal behavior and heat transfer characteristics of Paraffin RT50 as a phase change material (PCM) during constrained melting and solidification processes inside a shell and tube heat exchanger. Hosseini et al [18] investigated the effect of inlet temperature of the heat transfer fluid on melting process in a shell and tube heat exchanger numerically and experimentally. Agyenim et al. [19-22] investigated melting and solidification on a paraffin in a shell and tube heat exchanger for various operating conditions and geometric parameters. Erek et al [23] carried out experimental and numerical investigation of thermal energy storage with a finned tube. In this type of heat exchanger, PCM fills the annular shell space around the finned tube while the heat transfer fluid flows within the tube.

Due to the relatively low thermal conductivity of PCMs, many studies have been performed to improve the heat transfer in a storage unit. Zhang and Faghri [24] investigated the heat transfer enhancement in a latent storage system using a finned tube. Sciacovelli et al [25] analysed the melting process in a single vertical shell-and-tube latent heat thermal energy storage, unit and directed at understanding the effect of nanoparticle enhancement of the system.

It can be seen from the studies above, to understand the effect of ambient and the problems faced with sizing the thermal energy storage system, a simplified heat exchanger can be a good contribution and practical both in design and also in operation. Therefore, a shell-and-tube heat exchanger based on the PCMs is presented in this paper. This uses basic mathematical calculations to estimate total time of charging and discharging processes under constant or mean entrance conditions. Furthermore, the calculations are carried out for a latent-heat-storage unit utilized for temperature moderation of an enclosed space. In the examined case, a real-size room is cooled down to a comfortable level, which continues as long as the PCM is melting. The design of the unit and its mode of operation temperature determine the thermal change of PCM and the rate of air cooling in the room.

2. HEAT EXCHANGER SYSTEM DESIGN

In this study, a shell and tube heat exchanger unit selected in order to investigate the change of storage time for a latent heat storage system. Fig. 1 illustrates a picture and a schematic diagram of the unit, which consist of airflow through tubes, and the heat exchanger section based on PCM. Because most engineering systems use cylindrical tubes and heat loss from the shell and tube system is minimal. The shell-and-tube heat exchanger as a portable cooler is operated in crossflow. The tubes are vertical and the room air is fan-driven through the shell. PCM in vertical tubes is unmixed, airflow in shell is mixed. The external dimensions of the heat exchanger section are 1.35 m length (L), 0.21 m width (W) and 0.80 m height (H) [26].

The fans are positioned vertically and the overall length of the fans is 1.55 m. Also a fan which is 0.20 m length has been located centrally and height and width are the same as in the heat exchanger. In the fans, the velocity u_∞ of air outside the tube array is changed from 1.2 m/s to 2 m/s [26].

The dimensions of tubes are diameter (d) of 0.01 m; height (H) of 0.80 m. They are vertical, thin, and circular and are made of aluminum [26]. The square in-line configuration of the tubes is $Sp = Sn = 1.5 \times d$, as shown in Fig.2, where Sn is the tube pitch normal to flow and Sp is the tube pitch parallel to flow. The location of the tubes in the exchanger are indicated in Fig. 2, detailing as $Sp = Sn = 1.5 \times d$.

The external size of the exchanger determines by reducing 25%, 50% and 75%, except for the current size of a conventional air conditioner cooler.

The dimensions of a real room has selected as the following: height 2.5 m, length 4.0 m, and width 4.0 m [27]. The initial temperatures of air in the room is $T_{r,i}$ =35 ◦C, 37 ◦C, 40 ◦C and 45 ◦C. The room temperature at any instant is uniform (the room air is mixed). Radiation inside the room is ignored.

For simplification of calculations, all the thermophysical properties are assumed independent of temperature. The PCM is homogeneous and isotropic as both a liquid and a solid. The phase change material is a paraffin wax

(RT-25 by Rubitherm). The thermophysical properties of the PCM are as follows: melting temperature Tm, 23◦C; specific enthalpy of melting hm, 206 kJ/kg; liquid density ρl, 750 kg/m3; solid density ρs, 800 kg/m3; thermal conductivity k, 0.2 W/m K; specific heat capacity cp, 2500 J/kg K [26].

In calculations, a real-size room is cooled at daytime by a unit in which the PCM melts at 23◦C, while the ambient temperature is changed from 35◦C to 45◦C. Then, the paraffin solidified at night, and thermal comfort is preserved in the room. The calculations are conducted analytically.

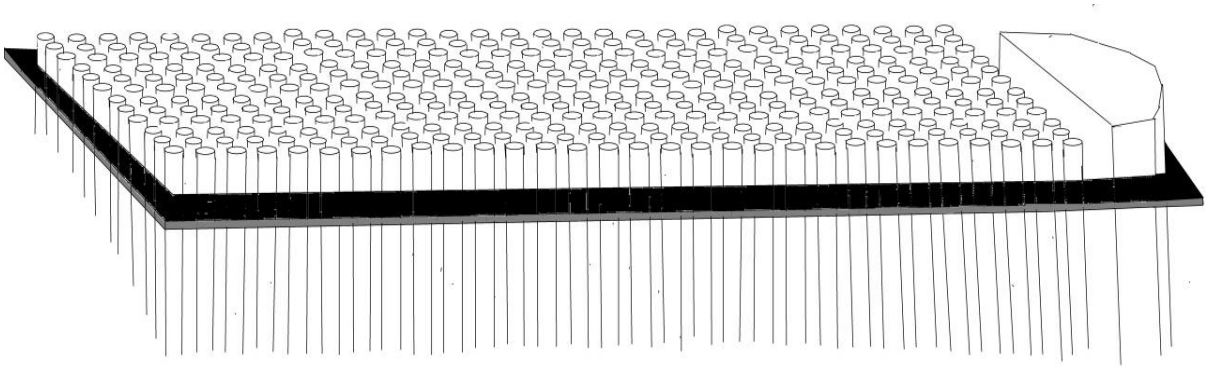

Figure.1 The structure of the heat exchanger system.

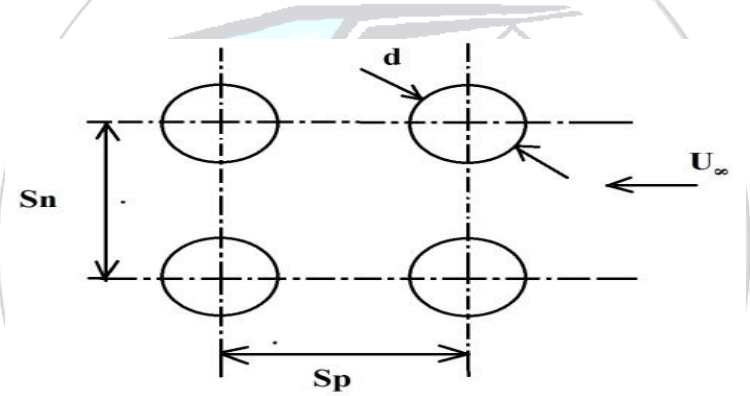

Figure.2 Square in-line configuration of tubes in the heat exchanger.

where N Total number of tubes. N_n and N_p is number of tubes in a row normal to flow and number of tubes in a row parallel to flow. The width and length of the configuration is as follows:

$$W = N_n.S_n = N_n.(1.5 \times d) \quad (1)$$

$$L = N_p.S_p = N_p.(1.5 \times d) \quad (2)$$

The total number of tubes in the exchanger is $N = N_n.\ N_p = 14 \times 90 = 1260$. The liquefied PCM mass in tubes fills each tube up to its top. The mass can be expressed [26]:

$$M_{PCM} = N.V_{tube}.\rho_l = N.\left(\left(\pi.d^2/4\right).H\right).\rho_l \quad (3)$$

For the crossflow of air, the convection heat transfer coefficient outside the tubes (h_o) is calculated by the Grimson correlation [27]:

$$\left[h_o.d/k_a\right] = C.\left(\left(U_{max}.d/\nu_a\right).H\right)^n.Pr^{1/3} \quad (4)$$

Where C, n are constants of relation. For an square in-line configuration, C = 0.278 and n = 0.620 according to the pitch-to-diameter ratio $S_n/d = S_p/d = 1.5$. The properties have been evaluated as air at atmospheric pressure and room temperature of 27◦C (300 K). The air density ρ_a= 1.177 kg/m^3, specific-heat capacity $c_{p,a}$ = 1006 J/kg K, thermal conductivity k_a =0.026 W/m K, kinematic viscosity ν_a= 15.7x10^{-6} m^2/s, and Prandtl number Pr = 0.708. In an square in-line arrangement, the air velocity at the minimum frontal area U_{max} is expressed [26]:

$$U_{max} = U_{\infty} \cdot \left({}^{S_n}/_{(S_n - d)} \right) \quad (5)$$

For S_n/d = 1.5, substituting above values in the equation changes the velocity versus U_{∞}. Thus, the air heat capacity rate is

$$C_a = \dot{m}_a . c_{p,a} \quad (6)$$

where the mass flow rate of air across the free cross-sectional area A_c is [26]:

$$\dot{m}_a = U_{\infty} . \rho_a . A_c \quad (7)$$

Where the area A_c for flow of air from the fans into the tube array is $A_c = W.H$. The area changes also according to reducing 25%, 50% and 75%. Mass of air in the room can be given [26]:

$$M_a = V_{room} . \rho_a \quad (8)$$

The shell dimensions of shell-and-tube heat exchanger are changed as rate of percent. Because of the thinness of the tube wall, the inside and outside surfaces are accepted as the same. The surface heat-transfer area of the tubes A can be given as [26]:

$$A = N.\pi.d.H \quad (9)$$

3. METHODS

The analysis of the PCM based heat exchanger unit is investigated for two conditions. In conditions, the exchanger operates for an insulated room and a room heated by the ambient. Each condition is to be analyzed in a way: An ideal performance of the exchanger. The wall temperature of all tubes is preserved at the constant temperature of melting Tm. This is an extreme condition. In the actual performance of the exchanger, the temperature of a tube wall varies with the melt fraction accumulated in the tube.

Both performances are compared with respect to the temperature achievable in the room, the range of operation of the ambient temperature and the design of the exchanger.

The melting of the PCM advances gradually from the first row to the last one. The wall temperature has risen above the melting point, while the tubes downstream are full of solid PCM and their wall is preserved at the melting temperature.

3.1. Room perfectly insulated

For ideal performance**,** the melting-point temperature is preserved throughout the whole operation at the wall of all the tubes in the exchanger: $T_w = T_m$. The lowest temperature achievable in the room could be $T_{r,min} = T_m$. In such a case, the heat absorbed from the room by the exchanger and the PCM mass to be melted would have to be [26]:

$$Q_a = \left(M.c_p\right)_a . \left(T_{r,o} - T_m\right) \quad (10)$$

$$\Delta Q_{PCM} = Q_a = (\Delta M.\Delta h)_{PCM} \quad (11)$$

At such a specific melt fraction most of the tubes remain fully solid and at a temperature T_m. The time required to reach any comfortable temperature is assessed from the heat balance over the air [26-29]:

$$-\left(M.c_p\right)_a {}^{dT}/_{dt} = \left(\dot{m}.c_p\right)_a (T_r - T_m) \quad (12)$$

$$\Delta t = -\left({}^{M}/_{\dot{m}}\right)_a \ln\left[(T_r - T_m)/(T_{r,o} - T_m)\right] \quad (13)$$

3.2. Room heated by the environment

Heat is transferred from the surroundings to the room through the walls and ceiling. The floor is adiabatic. An overall heat-transfer coefficient (U_r) is assigned to both the walls and the ceiling and 1.2 W/m^{2}K. The ambient room temperature during the whole operation of the exchanger cooling is changed from 35◦C to 45 ◦C. For ideal performance, the heat balance over the room is [26]:

$$\left(M.c_p\right)_a {}^{dT}/_{dt} = (A.U)_r (T_{\infty} - T_r) - \left(\dot{m}.c_p\right)_a (T_r - T_m) \quad (15)$$

where the inlet temperature of air to the exchanger is the room temperature, $T_{in} = T_r$ and its outlet temperature is $T_{out} = T_m$ in the very long heat exchanger. At steady state, the temperature could be given as [26]:

$$(A.U)_r(T_\infty - T_r)_{ss} = (\dot{m}.c_p)_a(T_r - T_m)_{ss} \quad (16)$$

$$T_{r,ss} = \left[\left((A.U)_r/(\dot{m}.c_p)_a\right).T_\infty + T_m\right]/\left[1 + (A.U)_r/(\dot{m}.c_p)_a\right] \quad (17)$$

$$NTU = {(A.h_o)}/{C_a} \quad (18)$$

where Ar = 4 × (4 × 2.5) + 4 × 4 = 56 m^2. At this temperature the rate of heat gains through the walls and ceiling amounts to [26]:

$$q_{amb} = (A.U)_r(T_\infty - T_{r,ss}) = (\dot{m}.c_p)_a(T_r - T_m)_{ss} \quad (19)$$

The duration of the exchanger operation in this mode can be estimated from the heat capacity of the PCM mass [26]:

$$\Delta t = {Q_{PCM}}/{q_{amb}} = {(M.\Delta h)_{PCM}}/{q_{amb}} \quad (20)$$

4. RESULTS AND DISCUSSION

In this calculation the time duration of the operation is determined, considering the initial ambient temperature of the room and the dimension change of the exchanger. All the figures given above relate to an ideal operation in which the tubes are maintained at the melting temperature. For actual performance, the full analysis of an actual performance is presented in literature.

However, if the equations described in the section are adopted to the insulated room and room heated by the environment, it would be obtained the evolution of the room temperature with time and the cooling time in operation. The room temperature versus time is plotted in Fig. 3, 4 and 5. As estimated above, while the different room temperature investigates from 35 ◦C to 45◦C, the temperature decreases from 35 ◦C to 23 ◦C (or 25◦C). Thus, the ideal and actual performances are the same.

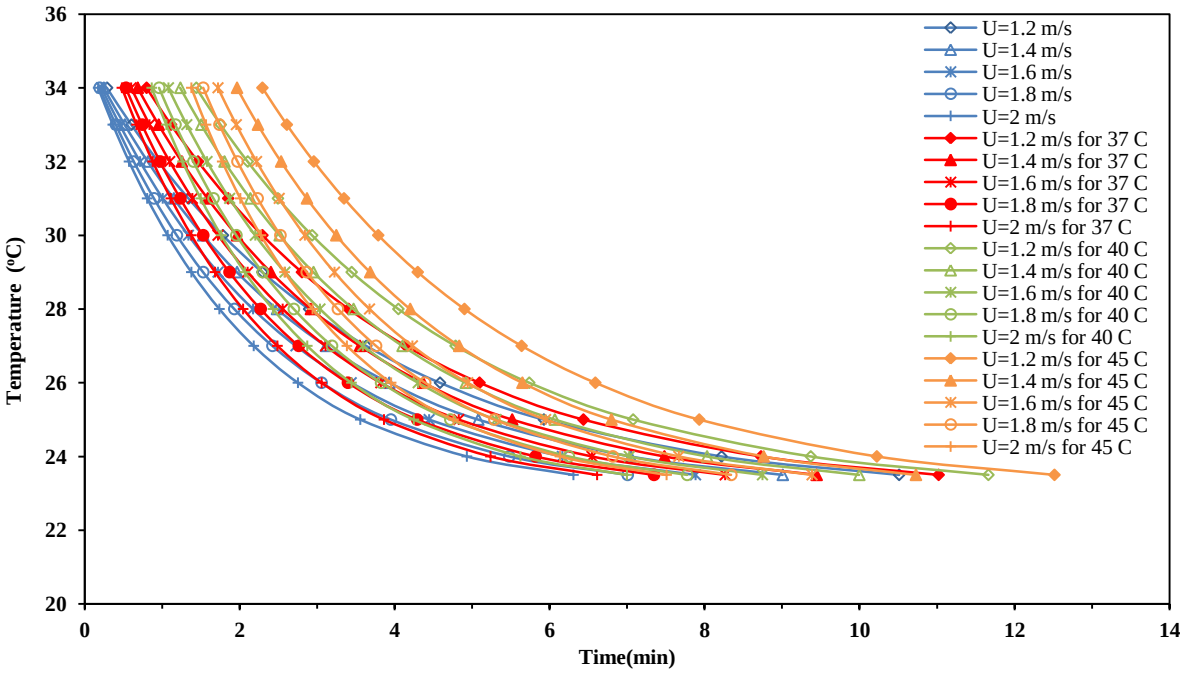

Figure.3 Cooling of an insulated room for different velocity and different ambient temperature: room temperature versus time for current exchanger dimensions.

Figure 3 displays the comparison between different velocity and different ambient temperature results and involves the change of the room temperature versus time. In this comparison, the inlet temperatures and the velocities for ambient are taken to be 35 °C, 37 °C, 40 °C, 45 °C and 1.2 m/s, 1.4 m/s, 1.6 m/s, 1.8 m/s, 2.0 m/s respectively. It is obvious from this figure that room temperature decreases as time go by. The amount of time for high ambient temperatures seems lower than the low temperatures. But when the velocity is decreased, the amount becomes larger than the others. This is expected due to the heat transfer factors on the current exchanger for lower ambient conditions.

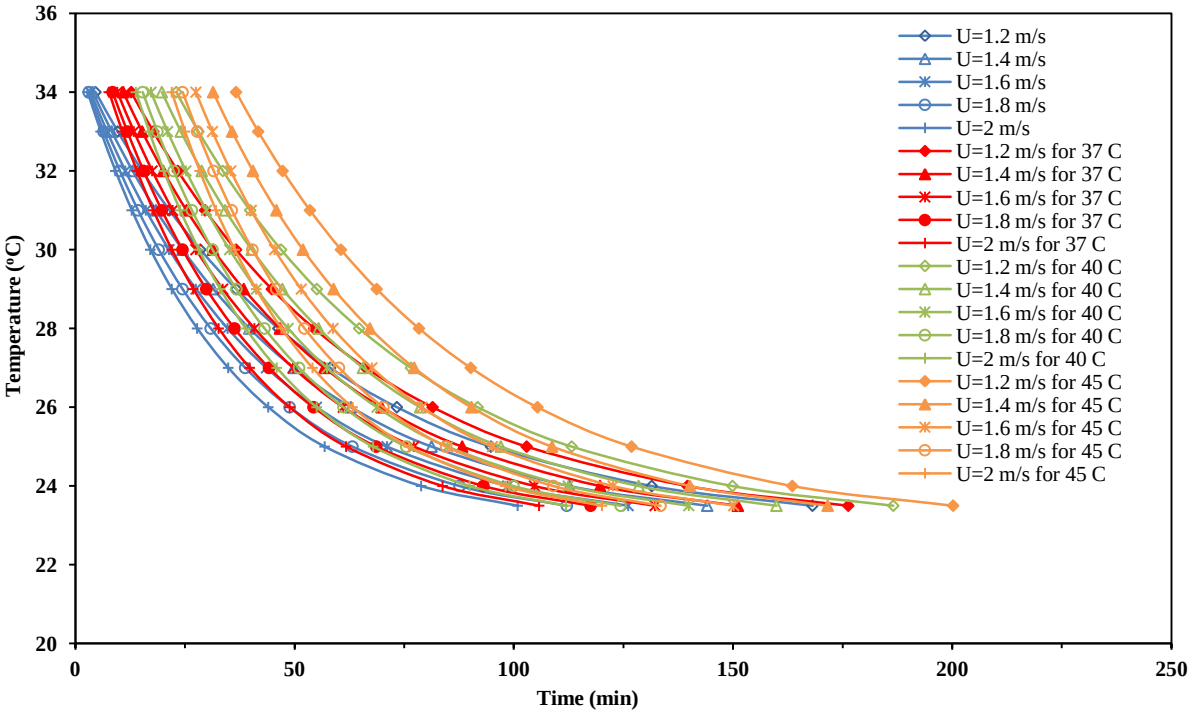

(a)

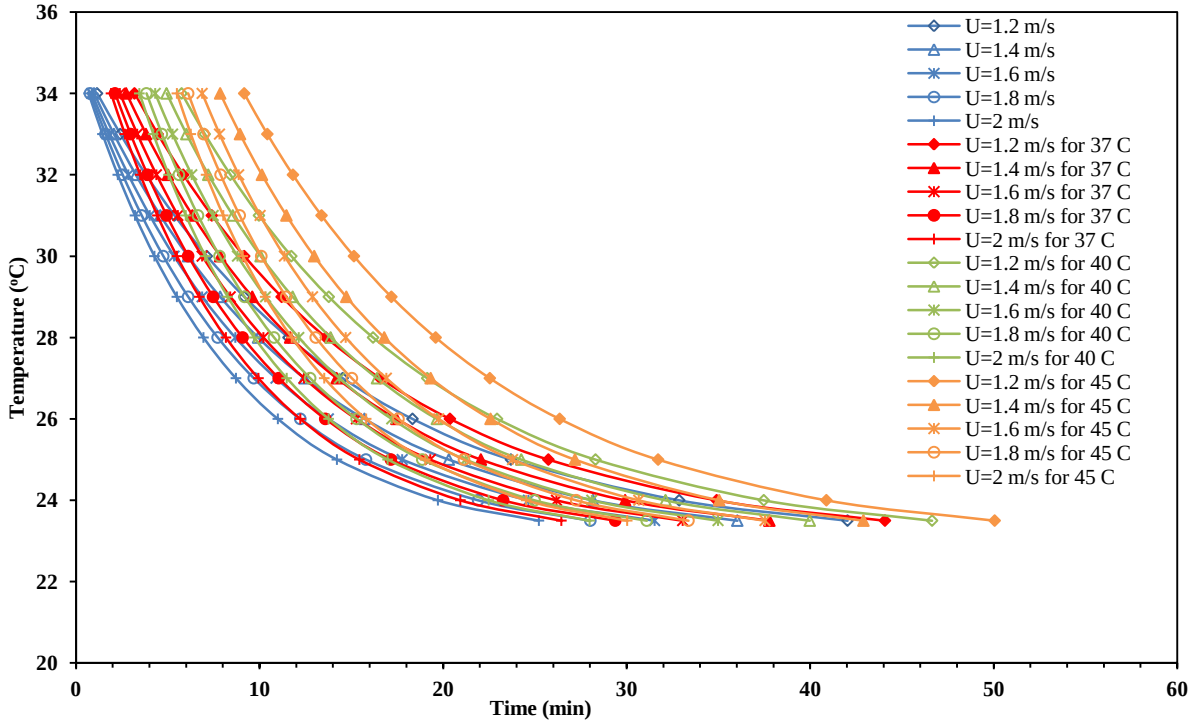

(b)

Figure.4 Cooling of an insulated room for different velocity and different ambient temperature: (a) room temperature versus time for current exchanger dimensions of 25 %; (b) room temperature versus time for exchanger dimensions of 50 %.

Figure 4, 5 shows the change of temperatures of thermal energy stored as a function of time for different heat exchanger dimensions (25%, 50% and %75). The time decreases increasing ambient velocity, decreasing ambient temperatures. In addition, it can be seen from the figures that dimension has a dominant effect on the temperature of stored energy than conditions. If the dimension is decreased 50% for the heat exchanger having same condition parameters, the amount of time is decreased from 100.8 min to 25.2 min, approximately. The effect of different dimension of 75% on the time is given on Figure 5. These results show that the increase in the ambient temperature increase the time rate, as expected. This rate also increases with the decreasing ambient velocity. The change of temperature in stored energy is dramatically decreased after the dimensions is passed from current to 75%.

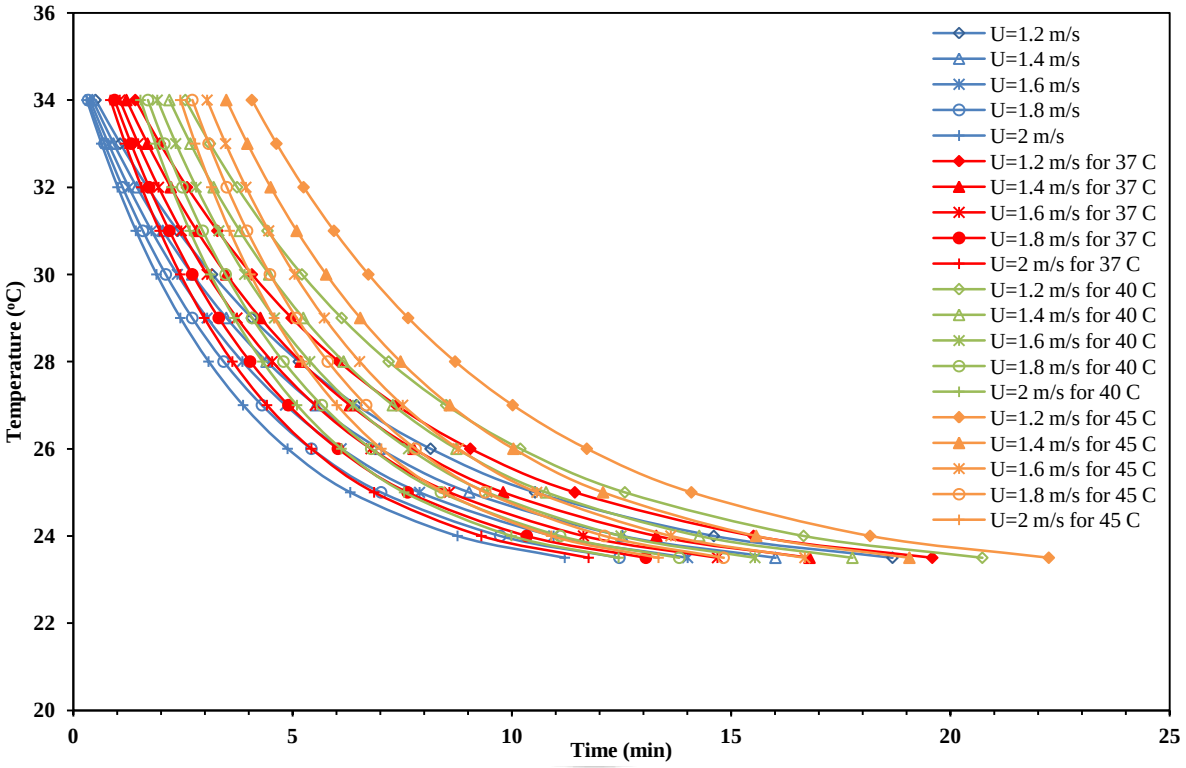

Figure.5 Cooling of an insulated room for different velocity and different ambient temperature: room temperature versus time for exchanger dimensions of 75 %.

Figure 6 shows the cooling time for the different ambient room temperatures reaching 23◦C. In the cooling time of a room heated by the environment, the variation of velocity with time is also shown in Fig. 6. These times remain at same level for different ambient room temperatures. It can be seen that the effect of velocity on the time is not very significant for the cooling time of a room heated by the environment. In the room guarded as thermal, the heat extraction decreases and the time passes as distribution temperature decreases.

It can be seen from these figures that the effects of dimensions on the decrease of time are excessive than ambient parameters. As the effect of ambient conditions, the change of time can be accelerated by decreasing the dimensions. The effect of ambient temperature on the times depends on the difference between the fluid inlet and melting temperatures, as shown in Figure. It seems that the effect of increasing ambient temperature is more significant than increasing the velocity.

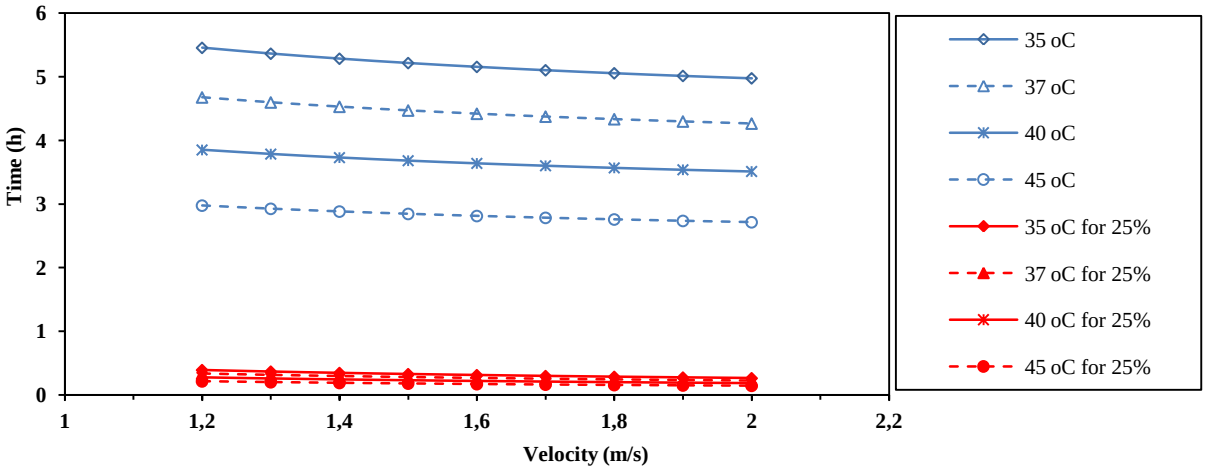

(a)

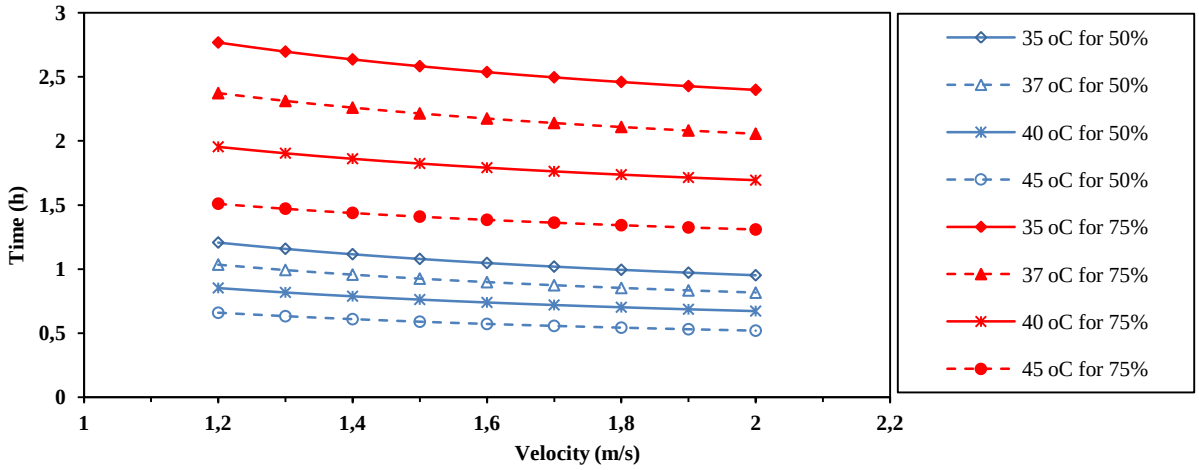

(b)

Figure.6 The cooling time of a room heated by the environment for different velocity and different ambient room temperatures: time versus velocity for exchanger dimensions of (a) current, 25 %, (b) 50 % and 75 %.

4. CONCLUSIONS

In all the calculations presented herein a few simplifying assumptions were involved. The density of liquid PCM was used for both liquid and solid. The room temperature was assumed uniform, as if the air were perfectly mixed. Air properties were considered constant. Radiation in the room was ignored. These simplifications affect the closeness of the results to a real situation, but enable the comparison of solutions. The analytical solution is the simplest, while the real solution is a heavily time-consuming procedure. Two cases were analyzed: cooling of an insulated room and a room heated by the ambient. Different cases were solved analytically, for an "ideal" performance. In all cases the analytical results were close to the literature [26] results and could have been used for estimates of the room temperature.

The analytical calculations related to exactly the different dimensions. The solution was also based on different ambient room temperatures. The results obtained by this method could have been the most accurate. However, in the present study the analytical method provides the cooling times of the PCM process.

Another issue of interest is the temperature distribution of the heat transfer fluid along the heat exchanger. It has been show that, during periods of the cooling time of a room heated by the environment, the HTF temperatures are dominated by the second case, but the change of dimension in the system is very significant than HTF temperature.

Finally, in relation between the cases and the conditions, data have shown that the amount of time by the HTF in the insulated room is negligible compared to the cooling time of a room heated by the environment.

REFERENCES

[1]. N. Yüksel, and A. Avcı, "The Modelling of Energy Storage System (in Turkish)", *Journal of Thermal Science and Technology*, 2, 23, 2003.

[2]. N. Yüksel, "The Modeling and Optimization of Energy Storage Systems (in Turkish)", *Master Thesis*, Natural and Applied Sciences, Uludağ University, Bursa, 130 pages, 2004.

[3]. N. Yüksel, A. Avci, and M. Kilic, "A Model for Latent Heat Energy Storage Systems", *Int. Journal of Energy Research*, 30, 14, 1146–1157, 2006.

[4]. N. Yüksel, and A. Avcı, "The Effect of Phase Change Material on Exhaust Waste Heat Recovery from Diesel Engine (in Turkish)", *VI. Automotive Technology Congress*, 04 - 05 June 2012, 160 pages, Bursa, Turkey.

[5]. N. Yüksel, and A. Avcı, "The Effect of Operating Parameters on Thermal Storage System with PCM (in Turkish)", *I. National Air Conditioning, Refrigeration Education Congress*, 05 – 07 September 2012, Balikesir, Turkey.

[6]. N.Yüksel, A. Avcı, and M. K. İşman, "The Effect of Phase Change Material on the Thermal Energy Storage System (in Turkish)", in *19th National Congress of Thermal Sciences and Technology*, 9-12 September 2013, Samsun, Turkey.

[7]. M. M. Farid, and A. Kanzawa, "Thermal Performance of a Heat Storage Module Using PCMs with Different Melting Temperatures: Mathematical Modeling," *Journal of Solar Energy Engineering*, 111, 152–157, 1989.

[8]. M. Lacroix, "Numerical Solution of a Shell-and-Tube Latent Heat Thermal Energy Storage Unit," *Solar Energy*, 50(4), 357–367, 1993.

[9]. J. R. Turnpenny, D.W. Etheridge, and D. A. Reay, "Novel Ventilation Cooling System for Reducing Air Conditioning in Buildings. I. Testing and Theoretical Modeling," *Applied Thermal Engineering*, 20, 1019–1038, 2000.

[10]. J. R. Turnpenny, D.W. Etheridge, and D. A. Reay, "Novel Ventilation Cooling System for Reducing Air Conditioning in Buildings. II. Testing of a Prototype," *Applied Thermal Engineering*, 21, 1203–1217, 2000.

[11]. S. Mozhevelov, G. Ziskind, and R. Letan, "Numerical Study of Temperature Moderation in a Real Size Room by PCM-Based Units", *Heat Transfer in Components and Systems for Sust. En. Tech.*, France, April 5–7, 2005.

[12]. S. Mozhevelov, "Cooling of Structures by a Phase-Change Material (PCM) in Natural and Forced Convection", *M.Sc. thesis*, Mechanical Engineering Department, Ben-Gurion University of the Negev, Beer-Sheva, Israel, 2004.

[13]. G. Arye, and R. Guedj, "A PCM-Based Conditioner", Heat Transfer Laboratory, Mechanical Engineering Department, Ben-Gurion University of the Negev, Beer-Sheva, Israel, final report 13-04, 2004.

[14]. A.H. Mosaffaa, F. Talati, H. Basirat Tabrizi, and M.A. Rosen, "Analytical modeling of PCM solidification in a shell and tube finned thermal storage for air conditioning systems", *Energy and Buildings* 49, 356–361, 2012.

[15]. S.M. Vakilaltojjar, and W. Saman, "Analysis and modelling of a phase change storage system for air conditioning applications", *Applied Thermal Engineering* 21, 249–263, 2001.

[16]. M. Akgun, O. Aydin, K. Kaygusuz, "Experimental study on melting/solidification characteristics of a paraffin as PCM", *Energy Conversion and Management* 48, 669–678, 2007.

[17]. M.J. Hosseini, A.A. Ranjbar, K. Sedighi, and M. Rahimi, "A combined experimental and computational study on the melting behavior of a medium temperature phase change storage material inside shell and tube heat exchanger", *Int. Commun. Heat and Mass Transfer* 9 (39), 1416–1424, 2012.

[18]. M.J. Hosseini, M. Rahimi, and R. Bahrampoury, "Experimental and computational evolution of a shell and tube heat exchanger as a PCM thermal storage system". *International Comm. in Heat and Mass Transfer* 50, 128–136, 2014.

[19]. F. Agyenim, P. Eames, and M. Smyth, "Heat transfer enhancement in medium temperature thermal energy storage system using a multitube heat transfer array", *Renew. Energy* 35, 198–207, 2010.

[20]. F. Agyenim, P. Eames, and M. Smyth, "Experimental study on the melting and solidification behaviour of a medium temperature phase change storage material (Erythritol) system augmented with fins to power a LiBr/H2O absorption cooling system", *Renew. Energy* 36, 108–117, 2011.

[21]. F. Agyenim, and N. Hewitt, "The development of a finned phase change material (PCM) storage system to take advantage of off-peak electricity tariff for improvement in cost of heat pump operation", *Energy Build.* 42, 1552–1560, 2010.

[22]. F. Agyenim, P. Eames, and M. Smyth, "A comparison of heat transfer enhancement in a medium temperature thermal energy storage heat exchanger using fins", *Sol. Energy* 83, 1509–1520, 2009.

[23]. A. Erek, Z. Ilken and M. A. Acar, "Experimental and numerical investigation of thermal energy storage with a finned tube", *Int. J. Energy Res.*, 29, 283–301, 2005.

[24]. Y. Zhang, and A. Faghri, "Heat transfer enhancement in latent heat thermal energy storage system by using an external radial finned tube", *Journal of Enhanced Heat Transfer* 3, 119–127, 1996.
[25]. A. Sciacovelli, F. Colella and V. Verda, "Melting of PCM in a thermal energy storage unit: Numerical investigation and effect of nanoparticle enhancement", *Int. J. Energy Res.* 37, 1610–1623, 2013.
[26]. M. Kutz, *Heat Transfer Calculations*, 1th ed., Chapter 39, McGraw-Hill, 768 pages, 2005
[27]. J. P. Holman, *Heat Transfer*, 8th ed., McGraw-Hill, New York, New York, 1997.
[28]. Arabacigil B., Yüksel N., Avcı A., "The use of paraffin wax in a box-type solar cooker having inner and outer reflectors", *Thermal Science*, Vol. 19, No. 5, pp. 1663-1671, 2015.
[29]. Yüksel N., Arabacigil B., Avcı A., "The thermal analysis of paraffin wax used in a box-type solar cooker", *Journal of Renewable and Sustainable Energy*, 4 (6), 433-441, 2012.

ISSN: 2458-8156

Journal Home page : http://dergipark.ulakbim.gov.tr/ejens * E-mail : editor@cnrgroup.eu

hosted by Turkish JournalPark ACADEMIC

EJENS

European Journal of Engineering and Natural Sciences CODEN: EJENS

A Statistical Model for Predicting Yarn Evenness of Cotton Sirospun Yarns

Tuba Bedez Ute[1]*, Huseyin Kadoglu[1]

[1]*Ege University, Department of Textile Engineering, 35100, Bornova/İzmir, Turkey.*

**Corresponding Author email: tuba.bedez@ege.edu.tr*

Publication Info

Paper received:
10 December 2015

Revised received:
15 December 2015

Accepted:
18 December 2015

Abstract

Raw material costs constitute the majority of the yarn production costs, therefore it is critically important to select the suitable cotton blend and to know required fibre characteristics for spinning. This article is a part of a comprehensive work including the experimental research and the modeling of the physical and mechanical properties of the cotton sirospun yarns. In this paper, a model for estimating sirospun yarn evenness from cotton fibre properties was investigated. For this purpose, different cotton blends were selected from different spinning mills in Turkey and their properties were measured with AFIS (Advanced Fibre Information System). Besides some yarn production parameters were also selected as independent variable (predictor) due to their significant effect. Sirospun yarns were produced at Ege University Textile Engineering Department's spinning mill under the same conditions. Linear multiple regression method were performed and statistical evaluation showed that generated equations for predicting yarn evenness had a large R2 and adjusted R2 values.

Key words

AFIS, Estimation, Multiple regression analysis, Prediction, Sirospun, Yarn evenness

1. INTRODUCTION

Yarn production is a sequence of processes that convert fibres into yarn, which will be used in various end products. Basic interest of every spinner is to reduce costs and to optimize the spinning process as well as to reach the desirable yarn quality. Raw material costs are more than half of the total manufacturing costs in a spinning mill, therefore knowing and monitoring the quality characteristics of the fibers, with the purpose of reducing costs and optimizing the spinning process, have great importance for the spinners.

For many years, the spinning machinery manufacturers enhanced the spinning process and reduced the mass variation of yarns, rovings and slivers thanks to precise measurement. This improvement provides an opportunity to increase productivity and to reduce considerably the raw material costs [1].

As much as spinners would like to produce an absolutely regular yarn, it is unachievable because of cross sectional fibre variation and the mechanical constraints. Accordingly, there are limits to achievable yarn evenness. According to Martindale, in the best possible conditions, the following evenness limit could be achieved for ring-spun yarns:

$$U_{lim}\frac{80}{\sqrt{n}} \times \sqrt{1+0,0004{CV_D}^2} \quad \text{or} \quad CV_{lim}\frac{100}{\sqrt{n}} \times \sqrt{1+0,0004{CV_D}^2} \qquad (1)$$

n is the number of fibers in the yarn cross section

CV_D is the coefficient of variation of the fiber diameter

Since the variation of the fibre diameter is small enough to be ignored in industrial use, the equations reduce to:

$$U_{lim}\frac{80}{\sqrt{n}} \quad \text{or} \quad CV_{lim}\frac{100}{\sqrt{n}} \tag{2}$$

This can be expressed approximately as CV~= 1.25U. In the evaluation of the achieved evenness, the unevenness index I is commonly used which is defined as [2]:

$$I = \frac{CV_{actual}}{CV_{lim}} \tag{3}$$

In recent years, prediction of the yarn quality characteristics from process parameters and fibre properties is one of the favorite research subjects for the engineers. Consequently researchers have been developed various mathematical, statistical and empirical models which are considerably important for the spinners in terms of raw material selection [3-9].Especially, Hunter [8] and Ethridge et. al. [9] has investigated models for predicting yarn irregularity by using fibre parameters. Most of the researchers are focused on modeling of ring spun and rotor spun yarn properties but there is a few study on modeling sirospun yarn characteristics.

It is authenticated that, yarn properties are particularly influenced from fibre properties and this effect becomes more influential in the case of finer yarns. This paper is a part of a work concerning the experimental research and determination of the equations and models for estimating the sirospun yarn quality characteristics from the yarn production parameters and cotton fiber properties which are measured by the HVI and AFIS systems. As a result, equations were derived for the prediction of yarn tenacity, breaking elongation, unevenness and hairiness by using fiber and yarn properties. Some of the results are given in previous papers [10-13]. Regressional estimation of cotton sirospun yarn properties from fibre properties measured with HVI [11], regressional estimation of yarn hairiness of cotton sirospun yarns from AFIS fiber properties [12] and the prediction of yarn strength of cotton sirospun yarns from AFIS fiber properties by using linear regression analysis [13] were investigated previously.

2. EXPERIMENTAL

2.1. Materials

As the raw material represents about 50-75% of the manufacturing cost of a short-staple yarn and it has a significant effect on productivity and quality, yarn producers focus on the suitable blend [14].

In order to investigate the effect of fibre properties, various cotton blends were supplied from spinning mills in different regions of Turkey. Cotton fibres properties were analyzed with Advanced Fibre Information System (AFIS) which is developed for the measurement of individual fibres. The features provided with the USTER are given in Table 1 [15].

Table 1. Fibre properties that can be measured with AFIS.

Nep Classification:	Fiber and seed coat nep count per gram and size (m) distribution.
Length:	Fiber length by number and by weight distributions; short fiber content by number and by weight (%).
Maturity:	Maturity, immature fiber content (%) and fineness (mtex) distribution.
Trash:	Dust and trash count per gram and size (m) distribution; visible foreign matter content (%).

AFIS can be used for blend composition, analysis of changes in fibre properties during processing, optimization of the process parameters and predicting the produced yarn quality [16]. Different blends are coded from B1 to B11 and fibre properties measured with AFIS are given in Table 2.

Table 2. Fibre properties of different blends measured with AFIS.

Fibre properties	Abbreviation	B1	B2	B3	B4	B5	B6	B7	B8	B9	B10	B11

Fiber nep count per gram	Nep Cnt/g	4	19	24	8	5	7	152	12	19	25	17
Mean length by weight	L(W) (mm)	29,5	28,1	25	30,3	26,8	27	24,8	26,1	26,3	28	25,5
Upper Quartile Length by weight	UQL (w)	35,2	33,9	30,7	36,6	32	32,6	30,9	31	31,2	33,9	30,6
Short fibre content by weight	SFC (w) %	2,3	3,7	6,2	2,4	3,8	4,6	9,9	3,7	4,6	3,9	5,1
Mean length by number	L(n) (mm)	25,8	24,2	21,5	26,4	23	23,3	20,2	22,9	22,7	24,3	22,2
Length variation by number	L(n) %cv	37,6	40,3	40,3	38,9	38,4	40	48,5	37,8	39,6	39,2	38,7
Short fibre content by number	SFC (n) %	8,5	11,6	15,1	9	11,3	13,2	25,5	11	12,8	11,4	14,2
5% Length by number	5.0% (mm)	40,9	39,9	36,7	42,4	37,3	38,2	35,6	36,1	36,9	39,1	35
Total trash count per gram*	Total Cnt/g	8	11	14	7	29	16	84	5	14	9	9
Trash count per gram	Trash Cnt/g	0	0	0	0	0	0	11	0	2	0	2

* dust particles included

Upper quartile length by weight and 5% length by number values of the different blends are given in Figure 1. B4 blend has the highest values, whereas B11 has the lowest length values.

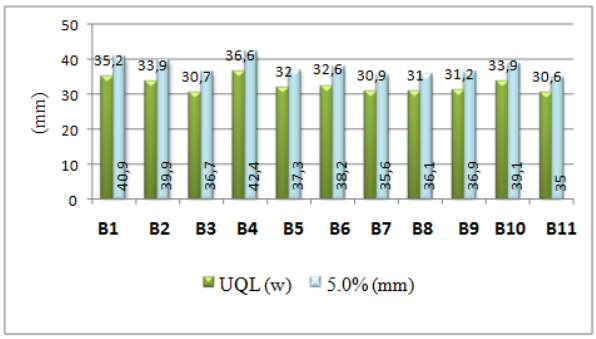

Figure 1. UQL (w) and 5.0% (mm) values of the different blends

Short fibre content by number and by weight values of the different blends are given in Figure 2. B1 and B4 blends have the lowest short fibre content while B3 and B7 blends have the highest ratios.

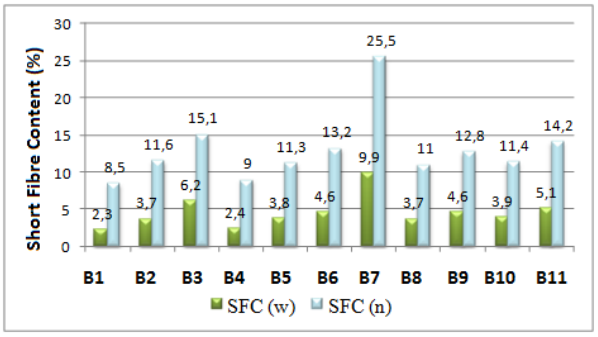

Figure 2. Short fibre content by weight and short fibre content by number values of the different blends

2.2. Methods

Yarn production parameters, as is known, have significant effect on yarn properties. Accordingly, yarn count, twist coefficient and strand spacing, which is defined as the distance between the two parallel roving strands fed

through the drafting system, were also selected as predictors. As the sirospun yarns are produced with two rovings, spinners have to produce finer rovings and increase the creel capacity of the spinning frame. Besides, a double roving sirospun guides and condensers must be used in siro-spinning, which is mounted on the rail and disconnected from the traverse mechanism.

According to experimental design, it is planned to spun in four yarn counts (11.81, 14.77, 19.69 and 29.53 tex), at three twist coefficients and three strand spacing values, for each blend. More clearly, each linear density was spun at 3, 6 and 9 mm strand spacing, and at three different twist multipliers (α_{Tt} 3831, α_{Tt} 4310 and α_{Tt} 4789). Cotton sirospun yarns were produced on a Rieter Model G30 ring spinning machine by keeping the spinning conditions constant. Some samples cannot be produced because of the raw material quality and drafting limits of the machine. For each yarn type, ten samples were produced and tested. Comparison was made between the yarns of different linear density, different twist factor and strand spacing. Experimental plan for each blend and yarn codes are given in Figure 3 and Table 3, respectively.

Subsequently yarn quality characteristics was measured and Uster Tester 5 was used for determining of the yarn unevenness, number of thin places, number of thick places, number of nep.

Final step is determining the equations and models for estimating the sirospun yarn uneveness from the yarn production parameters and cotton fiber properties which are measured by AFIS instrument. For this purpose, multivariate linear regression methods were performed. Statistical analyses were performed using Gretl (GNU Regression, Econometrics and Time-series Library) software.

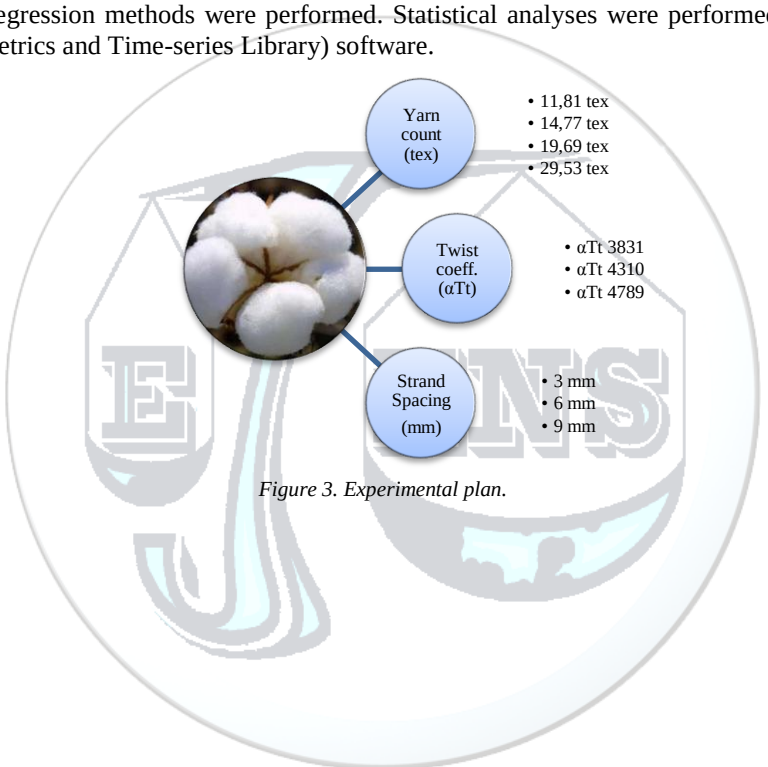

Figure 3. Experimental plan.

Table 3. Yarn code matris.

Twist coeff.	Strand spacing	Yarn count			
		11,81 tex	14,77 tex	19,69 tex	29,53 tex
	3 mm	**28**	**1**	**10**	**19**
α_{Tt} 3831	6 mm	**29**	**2**	**11**	**20**
	9 mm	**30**	**3**	**12**	**21**
	3 mm	**31**	**4**	**13**	**22**
α_{Tt} 4310	6 mm	**32**	**5**	**14**	**23**
	9 mm	**33**	**6**	**15**	**24**
	3 mm	**34**	**7**	**16**	**25**
α_{Tt} 4789	6 mm	**35**	**8**	**17**	**26**
	9 mm	**36**	**9**	**18**	**27**

3. RESULTS AND DISCUSSION

Yarn unevenness, number of thin places, number of thick places, number of nep were measured with Uster Tester 5. According to the Figure 4, it is found that yarn unevenness is higher for finer yarns and increases with the increasing of the twist coefficient and strand spacing. For some blends, some yarn types cannot be produced because of poor spinning stability depending on the fibre quality, strand spacing and yarn count.

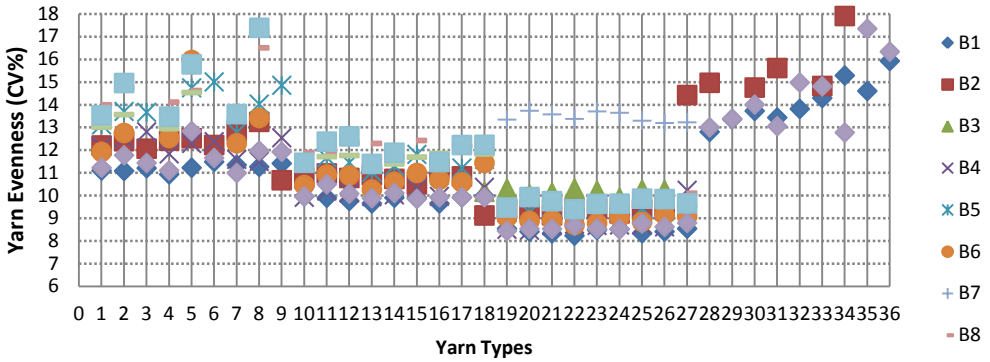

Figure 4. Yarn uneveness values (CV%).

Regression analysis is used for the investigation of relationships between two groups of variables. The obtained model can be used to describe the relationship between dependent and independent variables and to predict new values. As the yarn characteristics are influenced by fibre properties, production parameters, the spinning conditions, etc. the multiple regression analysis and ordinary least-squares methods were selected. The types of relationship between selected parameters and yarn properties were checked by curve estimation and correlation analysis. Based on statistical analysis, a nearly linear relationship between fibre properties measured with AFIS and yarn properties was found, therefore, the linear multiple regression analysis method was chosen for this study [7].

Table 4. Pearson correlation coefficients between fibre properties measured with AFIS.

	Nep	**L_w**	**SFC_w**	**UQL_w**	**L_n**	**SFC_n**	**$\%5L_n$**	**Total**	**Trash**
Nep	1	-0,366**	0,788**	-0,256**	-0,493**	0,838**	-0,283**	0,778**	0,901**
L_w	-0,366**	1	-0,804**	0,986**	0,986**	-0,739**	0,973**	-0,386**	-0,451**
SFC_w	0,788**	-0,804**	1	-0,709**	-0,885**	0,989**	-0,706**	0,706**	0,786**
UQL_w	-0,256**	0,986**	-0,709**	1	0,953**	-0,640**	0,985**	-0,309**	-0,383**
L_n	-0,493**	0,986**	-0,885**	0,953**	1	-0,833**	0,935**	-0,489**	-0,556**
SFC_n	0,838**	-0,739**	0,989**	-0,640**	-0,833**	1	-0,645**	0,754**	0,843**
$\%5 L_n$	-0,283**	0,973**	-0,706**	0,985**	0,935**	-0,645**	1	-0,314**	-0,420**
Total	0,778**	-0,386**	0,706**	-0,309**	-0,489**	0,754**	-0,314**	1	0,783**
Trash	0,901**	-0,451**	0,786**	-0,383**	-0,556**	0,843**	-0,420**	0,783**	1

***Correlation is significant at 0.01 level (two-tailed).*

According to Pearson correlation coefficients, there is high correlation between number based and weight based measurements (r>0,98). Besides, correlation between fibre length measurements ($UQL_{(w)}$-$L_{(w)}$) were also high (Table 4). As a result, for regression analysis, fibre properties that have a higher correlation with yarn unevenness were used: nep /gr, $L_{(w)}$, $SFC_{(w)}$, Total cnt, Trash cnt. Besides these, yarn count, twist coefficient and strand spacing were also chosen as independent variables.

A polynomial relation was found between short fibre content and yarn unevenness, due to curve estimation. Apart from that, there is a linear relationship between fibre properties and yarn properties. Following the curve estimation and collinearity tests, Best Subsets Regression method was used for determining which independent variables should be included in the model. To analyze the model in details, Stepwise regression was used. Models with higher adjusted R2, but lower Akaike and Schwarz values were determined. Finally,

heteroskedasticiy is tested with White test, it is found and a new model was established. Otherwise, it can invalidate statistical tests of significance that assume that the modelling errors are uncorrelated and normally distributed and that their variances do not vary with the effects being modelled.

Regression coefficients of variables, t-values and significance level of each variable of the final model are given in Table 5. Regression coefficients, which are constants, represent the rate of change of the yarn unevenness as a function of changes in the fibre properties and yarn parameters. Signs (+ or -) of regression coefficients of variables indicate the direction of influence P-value indicate the statistically significance. If the p-value is less than the significance level α, the null hypothesis is rejected and the result is statistically significant.

Table 5. Regression coefficients, t-values and significance level of t-values of linear regression model for yarn unevenness.

	Coefficient	**Std. error**	**t-ratio**	**p-value**
Constant	19.977	0.505	39.556	<0.00001***
Strand spacing (mm)	0.028	0.004	7.932	<0.00001***
Yarn count (Ne)	0.181	0.001	151.054	<0.00001***
Twist coefficient (α_e)	0.058	0.019	3.036	0.00242**
L_w	-0.529	0.013	-39.271	<0.00001***
SFC_w	0.378	0.117	3.228	0.00126***
SFC_w^2	-0.191	0.021	-8.964	<0.00001***
SFC_w^3	0.018	0.001	15.025	<0.00001***
Trash cnt	0.023	0.011	2.084	0.0373**
R^2	**0.9272**	**Adjusted R^2**	**0.9269**	

Yarn unevenness (CV%) = 19,977 + 0,028 F.A.M. + 0,181 Yarn count (Ne) + 0,058 (α_e) – 0,529 L_w+ 0,378 SFC_w -0,191 SFC_w^2 + 0,018 SFC_w^3 + 0.023 Trash cnt

** *is significant for α=0.05.*
*** *is significant for α=0,01.*

All of the regression coefficients in the model are statistically significant. According to the equation, yarn unevenness increases with the increase of yarn fineness, twist coefficient and strand spacing. Among fibre properties, fibre length and short fibre content have greater influence on yarn evenness. As fibre length increases and trash count decreases, yarn unevenness decreases. Short fibre content has a polynomial relation, yarn uneveness increase with the increase of short fibre content, up to a limit, after that decrease and increase again.

Figure 5 shows the scatter plot of predicted yarn unevenness values versus actual yarn unevenness values and regression line of the models. A high correlation (r=0,95) was found between actual and predicted values.

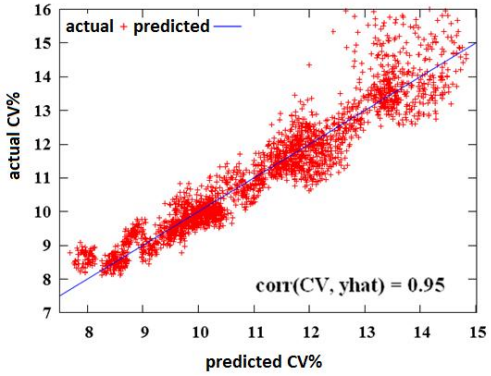

Figure 5. Predicted versus actual values of yarn evenness.

4. CONCLUSION

As the raw material costs are more than half of the total manufacturing costs in a short staple spinning mill, therefore knowing and monitoring the quality characteristics of the fibers, have great importance for the spinners. In this paper, a model for estimating sirospun yarn evenness from cotton fibre properties was investigated. This article is a part of a comprehensive work and some of the results are given in previous papers. Cotton fibre properties, measured with AFIS and some yarn production parameters such as yarn count, twist coefficient and strand spacing were selected as predictors. Linear multiple regression method were performed and statistical evaluation showed that generated equations for predicting yarn evenness had a large R2 and adjusted R2 values. Prediction ability of our model is very high as shown in Figure 5. Yarn unevenness increases with the increase of yarn fineness, twist coefficient and strand spacing. Fibre length and short fibre content are most important fibre properties for yarn unevenness. As fibre length increases and trash count decreases, yarn unevenness decreases.

ACKNOWLEDGMENT

The authors express their thanks to the **Republic of Turkey, Ministry of Science, Industry and Technology** and **SÖKTAŞ**, which is a designer and producer of cotton and cotton blended fabrics, for supporting this research.

REFERENCES

[1]. Rupp, J., 2008, *Efficient Yarn Production*, September-October, 2008, *http://www.textileworld.com*, http://www.textileworld.com/Issues/2008/September-October/Features/Efficient_Yarn_Production

[2]. The Unevenness Limit, www.rieter.com, http://www.rieter.com/cz/rikipedia/articles/technology-ofshort-staple-spinning/reducing-the-unevenness-of-yarn-mass/unevenness-of-yarn-mass/the-unevenness-limit/ (Date Accessed: April 2015)

[3]. El Mogahzy Y., Broughton R. M., Lynch W. K.; Statistical Approach for Determining the Technological Value of Cotton Using HVI Fiber Properties, Textile Res. J. Vol. 60 (1990) pp. 495-500.

[4]. Majumdar P. K., Majumdar A.; Predicting the Breaking Elongation of Ring Spun Cotton Yarns Using Mathematical, Statistical, and Artificial Neural Network Models, Textile Res. J., Vol. 74 (2004) pp. 652-655.

[5]. Frydrych I. and MatusakM., 2002, Predicting the Nep Number in Cotton Yarn Determining the Critical Nep Size, Textile Research Journal, 72: 917-923.

[6]. Majumdar A., Majumdar P. K. and Sarkar B., 2005, Application of linear regression, artificial neural network and neuro-fuzzy algorithms to predict the breaking elongation of rotor-spun yarns, Indian Journal of Fibre&Texile Research, 30: 19-25.

[7]. Üreyen M.E. and Kadoğlu H, Interactions Between AFIS Fibre Properties and Ring Cotton Yarn Properties, Tekstil ve Konfeksiyon, 18 (1), p.8-14., 2008.

[8]. Hunter L., 2004, Predicting cotton yarn properties from fibre properties in practice, 27th International Cotton Conference, Bremen, Germany, 62-70.

[9]. Ethridge M. D., Zhu R.; Prediction of Rotor Spun Cotton Yarn Quality: A Comparison of Neural Network and Regression Algorithms, Proceedings of the Beltwide Cotton Conference Vol. 2, 1996, pp.1314-1317.

[10]. Bedez Ute T., Research On Spinning of Short Staple Fibres by Sirospun System, Ege University Graduate School of Natural and Applied Sciences, Master of Science Thesis, 2007.

[11]. Bedez Üte T., Kadoğlu H., 2014, Regressional estimation of Cotton Sirospun Yarn Properties From Fibre Properties, AUTEX Research Journal, Vol. 14, No:3, September 2014, p.161-167.

[12]. Bedez Ute T., Kadoglu H., 2012, Regressional Estimation of Yarn Hairiness of Cotton Sirospun Yarns From Afis Fiber Properties, 6th International Textile, Clothing & Design Conference - Magic World of Textiles, October 07-10, Dubrovnik, Croatia.

[13]. Bedez Ute T., Kadoglu H., 2012, The Prediction of Yarn Strength of Cotton Sirospun Yarns From AFIS Fiber Properties By Using Linear Regression Analysis, The Inter-Regional Research Network On Cotton For The Mediterranean& Middle East Regions, November 05-07, Antalya.

[14]. Characteristics of the Raw Material, www.rieter.com, http://www.rieter.com/tr/rikipedia/articles/technology-ofshort-staple-spinning/raw-material-as-a-factor-influencing-spinning/characteristics-of-the-raw-material/, (Date Accessed: April 2015)

[15]. Uster AFIS Pro Brochures, www.uster.com, Uster Technlogies, http://www.uster.com/en/ instruments/fiber-testing/uster-afis-pro/(Date Accessed: 27 Temmuz 2012)

[16]. Frydrych I. and Matusiak M., 2002, Trends of AFIS Application in Research and Industry, FIBRES & TEXTILES in Eastern Europe, July/September,: 35-39.

[17]. Ureyen M.E. & Kadoğlu H, 2006, Regressional Estimation of Ring Cotton Yarn Properties from HVI Fiber Properties, Textile Research Journal, Vol 76, 2006, p360.